Theses and Dissertations

2016

Renewable Bio-Based Intermediates, Monomers And Polymeric Materials From Plant Oils

Liang Yuan
University of South Carolina

Follow this and additional works at: https://scholarcommons.sc.edu/etd

Part of the Chemistry Commons

RENEWABLE BIO-BASED INTERMEDIATES, MONOMERS AND POLYMERIC
MATERIALS FROM PLANT OILS

by

Liang Yuan

Bachelor of Science
Nankai University, 2009

Master of Science
Nankai University, 2012

Submitted in Partial Fulfillment of the Requirements

For the Degree of Doctor of Philosophy in

Chemistry

College of Arts and Sciences

University of South Carolina

2016

Accepted by:

Chuanbing Tang, Major Professor

Brian C. Benicewicz, Committee Member

Caryn E. Outten, Committee Member

Peisheng Xu, Committee Member

Cheryl L. Addy, Vice Provost and Dean of the Graduate School

DEDICATION

To my parents, my wife, my whole family and all my friends, without their support and encouragement, none of my accomplishments would be possible.

ACKNOWLEDGEMENTS

First I would like to show my deepest appreciation to my advisor, Dr. Chuanbing Tang, who gave me the opportunity to work in his research group and offered me tremendous guidance and support on my research projects. I feel very fortunate to have worked under his guidance for the past four and a half years. His enthusiasm for polymer science influenced me a lot and I am grateful for all I have learned from Dr. Tang and hope to learn more from him in the future.

Then I would like to thank Dr. Brian Benicewicz, Dr. Caryn E. Outten and Dr. Peisheng Xu for being my committee members and providing me valuable suggestions for my research as well as this dissertation. Also I want to express my gratitude to all my department colleagues, especially the members in Dr. Tang's research group, Dr. Zhongkai Wang, Dr. Yali Qiao, Dr. Yi Yan, Dr. Xiaodong Ying, Dr. Yanming Han, Dr. Yuzhi Xu, Dr. Jifu Wang, Dr. Hui Li, Dr. Kejian Yao, Dr. Christopher Hardy, Dr. Jiuyang Zhang, Dr. Perry Wilbon, Dr. Jeffery Hayat, Mitra Ganewatta, Nathan Trenor, Paras Pageni, Md Anisur Rahman, Meghan E. Lamm, Bill Floyd, Xinzhou Zhang, Tianyu Zhu and many others. It is a great pleasure to work with all of you and learn from you. Thanks for all your helps and suggestions.

Further, I want to give my sincerest gratitude to my mother, my father, my wife and other family members for their unconditional love and support. Thanks to all my friends both in USA and China for their encouragement and help.

Finally, I acknowledge all the funding supports from University of South Carolina, United Soybean Board and National Science Foundation.

ABSTRACT

ABSTRACT

In the dissertation work, new chemical intermediates, monomers and thermoplastic polymers were derived from renewable soybean oil. Elastomers were further developed using monomers and polymers from soybean oil. The properties of these polymeric materials were characterized and discussed.

In Chapter 1, the overall background and recent development polymers from renewable biomass, especially plant oils, is introduced. Major research objectives of my doctoral research were described.

The first section of the dissertation, on the preparation of renewable intermediates, novel monomers and homopolymers, is provided in Chapter 2 and Chapter 3. In Chapter 2, amidation of soybean oil with amino alcohols was developed for making hydroxyl fatty amides as novel chemical intermediates. Monomers with various polymerization groups (methacrylate, norbornene, cyclic imino ethers) were then prepared for subsequent polymerization. Chapter 3 describes a methodological study over the amidation of soybean oil with amino alcohols for sixteen (meth)acrylate monomers. Understanding on the structure-property relationship for the obtained homopolymers was provided.

The second section of the dissertation, on the preparation of elastomeric materials from soybean oil derived monomers and homopolymers. For the work in Chapter 4, an acrylate monomer (SBA) and a norbornene monomer (SBN) from soybean oil were utilized to make the elastic components of thermoplastic elastomers (TPEs). A-B-A triblock copolymer and multi-graft copolymer TPEs were prepared and compared. Chapter 5

describes how cross-linked elastomers were prepared from Diels-Alder cross-linking of furan-modified soybean oil polymers with a di-functional maleimide cross-linker. The mechanical properties of the elastomers were dependent on the polymer backbone of the precursors and the cross-linking density. The thermally reprocessed materials exhibited similar elastomer property. Chapter 6 describes the preparation of thermoset elastomers using crosslinking between azide functionalized soybean oil polymers and alkyne modified lignin through thermally promoted azide-alkyne cyclization. A model study was carried out to prove the reactivity between azide from polymers and alkyne from lignin.

Finally, a summary is given in Chapter 7. In addition, suggestions about future research directions on the preparation of polymer products from renewable plant oils are provided.

TABLE OF CONTENTS

LIST OF TABLES

LIST OF FIGURES

LIST OF ABBREVIATIONS

AIBN ....Azobisisobutyronitrile

ATRP .... Atom Transfer Radical Polymerization

DMF .... *N,N*-Dimethylformamide

DSC ....Differential Scanning Calorimetry

FTIR .... Fourier Transform Infrared Spectrometry

GPC .... Gel Permeation Chromatography

Me$_6$Tren .... Tris(2-(dimethylamino)ethyl)amine

PDI ....Polydispersity Index

PLA ....Polylactide acid

PMDETA .... *N,N,N',N'',N''*-Pentamethyldiethylenetriamine

RAFT .... Reversible Addition-Fragmentation Chain-Transfer

ROMP ....Ring-Opening Metathesis Polymerization

ROP .... Ring-Opening Polymerization

TGA .... Thermogravimetric Analysis

THF .... Tetrahydrofuran

TPE ....Thermoplastic Elastomers

CHAPTER 1

GENERAL INTRODUCTION

1.1 Polymers from renewable biomass

Polymeric materials have versatile applications in almost every single aspect of our daily lives. Most of them are made from non-renewable petroleum resources. Around 4% of the world oil production is used for plastic materials, with another 4% consumed as the energy to make them. The problem for the current polymer industry lies not only in its dependence on fossil fuels, but also in its detrimental effects to the environment as most petroleum-based polymeric materials would take hundreds of years to degrade. Sustainable polymeric materials from renewable biomass resources have been receiving a great deal of interest in the face of the depleting petroleum resources and the deteriorating environmental conditions.[1-2]

Renewable biomass resources, mainly agricultural and forestry products, can be divided into two major classes: natural polymers and natural molecular biomass.[3] Natural polymers are cheap and abundant resources such as lignin, starch, hemicellulose and cellulose. Cellulose is a polymer of D-glucose in length of 3-5 μm, comprised of about 7,000 to 12,000 glucose unites.[4] Hydrogen bonding interactions among adjacent cellulose molecules lead to the formation of bundles called elementary fibrils with about 70% crystallinity. Cellulose is the main structural polysaccharide of plant cells and makes up about 45% by weight of wood. Lignin, polyphenolic macromolecules uniquely from vascular plants, has amorphous and cross-linked structures with molecular weight ranging from thousands to hundreds of thousands daltons.[5] They are made from three cinnamyl alcohols (p-coumaryl alcohol, conifer alcohol, sinapyl alcohol) and comprise 20% to 30% of most wood. Natural molecular biomass is the second class of renewable biomass resources and can be used directly or molecularly engineered into building blocks for

2

making polymeric materials. Referring to the composition of hydrogen, carbon and oxygen, they can be classified into the following four categories: (1) oxygen-rich molecular biomass when C/O ratio is less than 5.0 such as lactic acid, itaconic acid and furans; (2) hydrocarbon-rich molecular biomass with C/O ratio larger than 5.0 such as plant oils, fatty acids and rosin acids; (3) hydrocarbon molecular biomass such as isoprene, butylene and ethylene; (4) non-hydrocarbon biomass such as carbon dioxide and carbon monoxide.[3]

Natural polymers have been used for bio-plastics and composite materials by direct blending or moderate chemical treatment.[6] Their recent applications in bio-conversions and chemical transformations help to produce renewable chemicals for biofuels and polymer preparation.[7] Lactic acid and 1,3-propanediol have been prepared from the fermentation processes of carbohydrates and used for producing biodegradable polyesters. Lignin has been broken down to phenol-rich oily products for making phenolic resins.[8] Compared to the complex natural polymers, natural molecular biomass can be facilely used as monomers or monomer precursors for polymer preparation benefiting from their well-defined chemical structures. A fast expanding area is the preparation of polymers with controlled architectures and superior properties using natural molecular biomass such as plant oils, rosin acids, furans and terpenes.[9-12]

1.2 Renewable plant oils for polymer materials

Plant oils are available world-wide at relatively low prices. Their main constituents are triglycerides, the product from the esterification of glycerol with three fatty acid molecules.[13] Figure 1.1 gives a schematic representation of a triglyceride molecule together with common saturated and unsaturated fatty acids from plant oils. Each type of plant oil has its characteristic content of fatty acids. For the industrially important plant oils such as

3

sunflower oil, palm kernel oil, soybean oil, rapeseed oil and linseed oils, the triglycerides are the esters of saturated fatty acids and unsaturated fatty acids containing double bonds, no functional group (hydroxyl, epoxy) is present. The hydroxyl group functionalized ricinoleic acid is a major component (90%) of castor oil.[14] The epoxy group containing vernolic acid is mainly from vernonia oil, which is extracted from the seeds of vernonia galamensis and has 73%-80% of vernolic acid.[15] Owning to their unique chemical structures, castor oil and vernonia oil have found great use in bioplastics, paintings, lubricants, cosmetics and etc. For example, over 3,000 products have been derived from castor oil and the production of Nylon-11 requires more than 50,000 tons of castor oil as the main raw material annually. However, these functional plant oils contribute less than 1% of the global production and have much higher market prices.

Plant oils without such functional groups show advantages in their availability and lower prices. Oleochemicals (fatty acids, fatty alcohols, fatty acid methyl ethers, *etc*.) from plant oils through chemical conversions such as hydrolysis, hydrogenation and transesterification, have been proved a great success to reduce our dependence on petroleum chemicals.[16-18] Their products include soaps, detergents, lubricants, solvents, and biodiesel. About 30% of fatty acids market and 55% of fatty alcohol markets are for the industry of soaps and detergents. Biodiesel from methyl esters of fatty acids represents the fastest growing segment of oleochemical production.

4
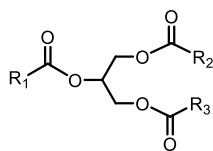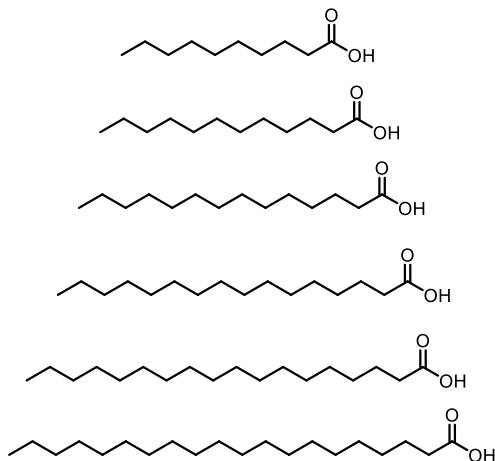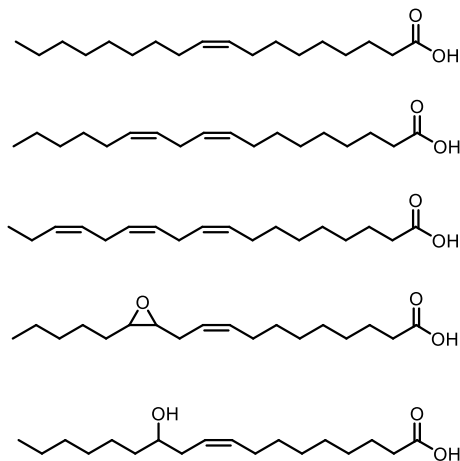
Figure 1.1 Structure of a triglyceride and common fatty acids from plant oils.

Polymer products from the industrially important plant oils have received great attention in order to release the polymer industry from its dependence on fossil fuels. Using fatty acids and fatty alcohols from plant oils as the intermediates, (meth)acrylic monomers and norbornene monomers have been prepared for subsequent polymerizations.[19-21] Plant oils have also been directed polymerized through the unsaturated double bonds via cationic polymerization with other comonomers.[22] To increase the reactivity of plant oils in polymerizations, chemical modifications have been selectively targeted on the double bonds without touching the ester groups. As shown in Figure 1.2, a variety of functional groups have been introduced to triglycerides through the double bond such as hydroxyl groups, epoxy group, azide group, alkyne group, acrylate group, etc.[23-26] These multi-functional plant oil derivatives have found applications in making thermosetting materials as epoxy resins, polyurethanes, alkyd resins. A new trend has emerged by converting plant

www.manaraa.com

oils into mono-functional monomers via modification to the ester groups. As shown in Figure 1.2, oxazoline, vinyl ether and acrylamide monomers have been reported from soybean oil.[27-29] They can be polymerized easily to get processable polymer products. It needs to be mentioned that the double bonds in the plant oils are maintained in the monomers and polymer products. This new trend provides access to plant oil based thermoplastic materials while keeping the original fatty acids compositions. However, most monomers are prepared and polymerized under harsh conditions, making it difficult for scaled production. The polymer properties need to be tailored through further engineering to meet the requirements of specific applications.[30-31]
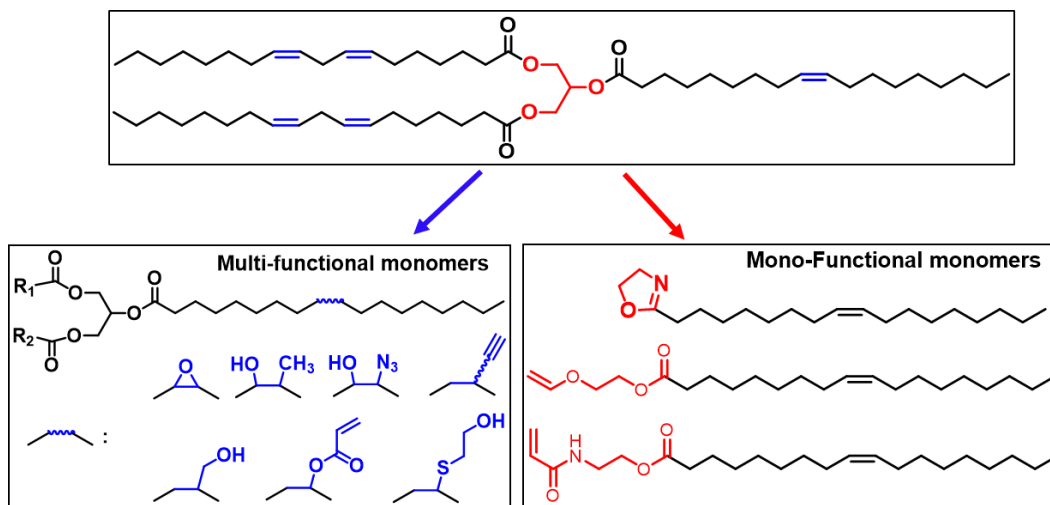
Figure 1.2 Chemical modifications of plant oil triglycerides for multi-functional monomers and mono-functional monomers toward polymer preparation.

1.3 Elastomers

Elastomers are important industry products for many applications such as tires and shoe soles, with a projected revenue of $56 billion in 2020. Elastomer materials can be classified into two categories depending on the cross-link: thermoset elastomers and thermoplastic elastomers.[32-33] Tires from the sulfur vulcanization of unsaturated rubbers are typical examples of thermoset elastomers, which have permanent chemical cross-links

6

and will not melt when heated.[34] In comparison, thermoplastic elastomers (TPE) are malleable copolymers of plastic and rubber components, which form an islands-sea structure comprising a continuous phase of the rubber component and separated phase of the plastic component due to their incompatibility.[33] The rubber phase is thus physically cross-linked by the plastic phase. Commercial TPEs include styrene block copolymers, thermoplastic copolyesters, thermoplastic polyamides and thermoplastic polyurethanes.

The global market of elastomers has been dominated by petroleum based synthetic polymers, such as styrene butadiene rubber, polybutadiene rubber and acrylonitrile butadiene rubber. Efforts are made to develop elastomer products from renewable biomass and to reduce our dependence on fossil fuels. These efforts follow a general rule: convert biomass into building blocks for making low glass transition temperature polymers and achieve property improvement through further macromolecular engineering.[35-36] Block copolymer thermoplastic elastomers have been reported using biomass based polymers as the elastic components. For example, poly(menthide) with T_g=-22 ^{o}C and poly(δ-decalactone) with T_g=-51 ^{o}C have been used as the soft component for constructing ABA triblock copolymer TPEs.[36-37] Thermoset elastomers have been reported via the cross-linking of moldable low T_g polymers from epoxidized soybean oil.[38] Exploration for new biobased elastomer building blocks and novel macromolecular engineering strategies will continuously improve the impact of biobased elastomers.

1.4 Polymerization techniques and modification chemistries

Ring-opening metathesis polymerization (ROMP). Polymers can be obtained from ROMP of cyclic olefins.[39-40] The polymerization will take place in the presence of catalysts and monomers with the driving force from releasing the ring strain energy. ROMP

7

follows a chain-growth mechanism as illustrated in Figure 1.3. The catalysts used in ROMP includes a variety of metal alkylidenes and the most well-known catalysts are ruthenium based Grubbs' catalysts, which are highly efficient. Three different generations of Grubbs' catalysts are given in Figure 1.3. The catalysts show good functional group tolerance. Polymers with various functionalities can be prepared from substituted cyclic olefins. Due to the high catalytic efficiency, cyclic olefins with bulky or polymer chain substitutions can also be polymerized to full conversion with good control in molecular weight.[41-42] Through subsequent monomer additions, polymers with block structures can be prepared.[43] Copolymerization of mixed monomers can also be carried out. ROMP provides a powerful method for synthesizing macromolecular materials with controlled functionalities and architectures.
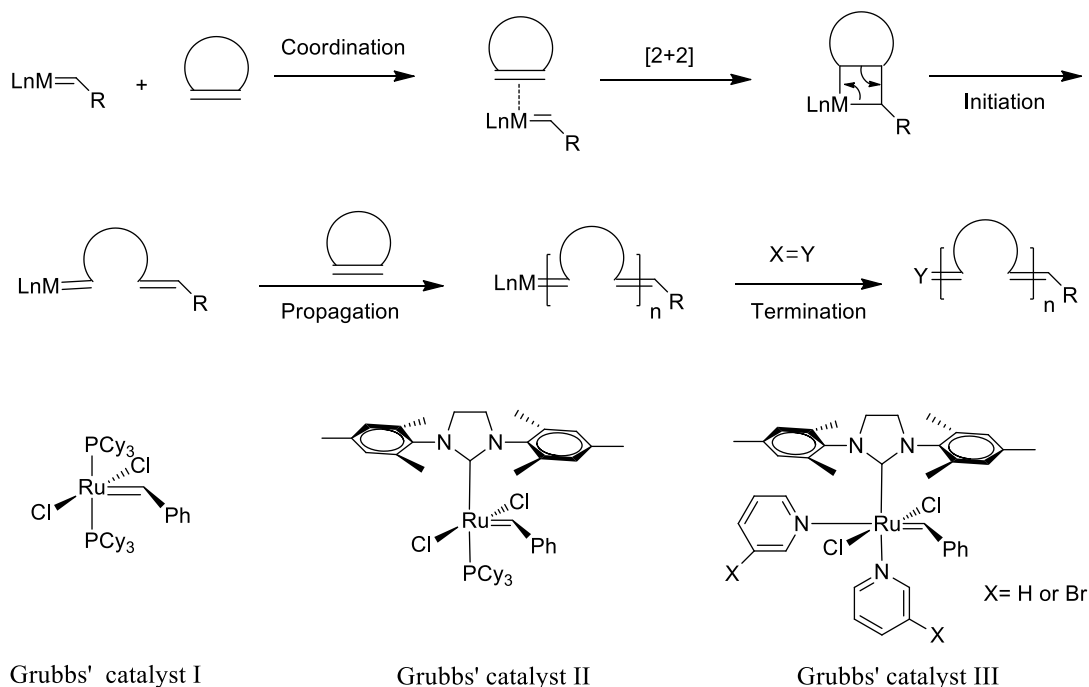
Figure 1.3 Schematic illustration of ROMP mechanism and Grubbs catalyst structures.

Atom transfer radical polymerization (ATRP). As one of the most effective and widely used methods for controlled radical polymerization, ATRP has revolutionized the

www.manaraa.com

field of polymers.[44] Figure 1.4 presents a general mechanism for ATRP. The equilibrium between propagating radicals and dormant species (initiating alkyl halides and macromolecular species PnX) is achieved through the activating effect of the transition metal complexes Mt^m/L and the deactivating effect of high oxidation state metal complexes $X-Mt^{m+1}/L$. Many redox-active transition metal complexes (Cu, Ru, Fe, Mo, Os, etc.) have been studied and Cu^I/L has been the most often used. The initiating alkyl halides can be a small organic compound or be anchored on interested substrates (particles, polymer chain end or pendent groups, one dimensional surfaces, etc.), and as a result polymers chains can be prepared as free chains or grafted from the substrates.[45-46] The halide group will be maintained at the polymer chain ends and can be used for chain extension to other monomers via ATRP. ATRP shows almost no limitation for the solvents and functional monomers since the solubility and activity of the metal/ligand complex can be tuned easily. Polymers with controlled chain topology, compositions and diverse functionalities have been synthesized using ATRP.

$$P_n\text{-}X \quad + \quad M_t{}^m/L \quad \underset{K_{deact}}{\overset{K_{act}}{\rightleftharpoons}} \quad P_n{}^\bullet \quad + \quad X\text{-}M_t{}^{m+1}/L$$

$$\left(K_p\right) \quad \overset{K_t}{\searrow} \quad P_n\text{-}P_n$$
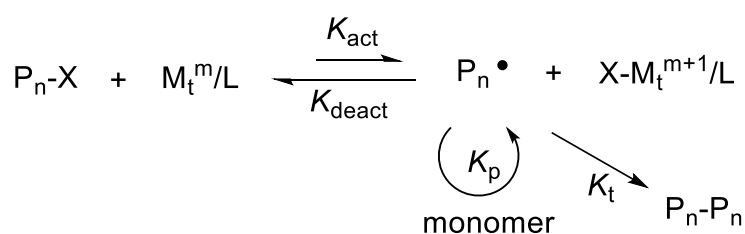
monomer

Figure 1.4 Schematic illustration of ATRP mechanism.

Ring-opening polymerization (ROP). Cyclic monomers with heteroatoms in the ring such as lactones, lactides, carbonates, lactams, ethylene oxide, N-carboxyanhydride, oxazolines and siloxanes, have been polymerized through chain-growth ROP by different mechanisms to afford linear polymers.[47] Organometallic compounds are usually added as a catalyst or initiator for the polymerization. Most ROP can be divided into cationic ROP

and anionic ROP depending on the reactive center during the polymerization. Biodegradable polymers (PLA, PCL, PLGA, etc.) by ROP of cyclic lactones and lactides are particularly attractive for their environmental friendliness and biomedical-related applications.[48] The most widely used catalyst for their industrial preparation is undoubtedly tin(II) bis(2-ethylhexanoate). Various aluminum alkoxides and zinc salts have also been explored for making biodegradable polyesters. Recently, metal-free ROP have been developed using organic catalysts such as N-heterocyclic carbenes, 4-dimethylaminopyridine and organic super bases. Figure 1.5 shows a typical polymerization of lactide to prepare polylactide (PLA), and several catalysts that have been proved effective for the polymerization.
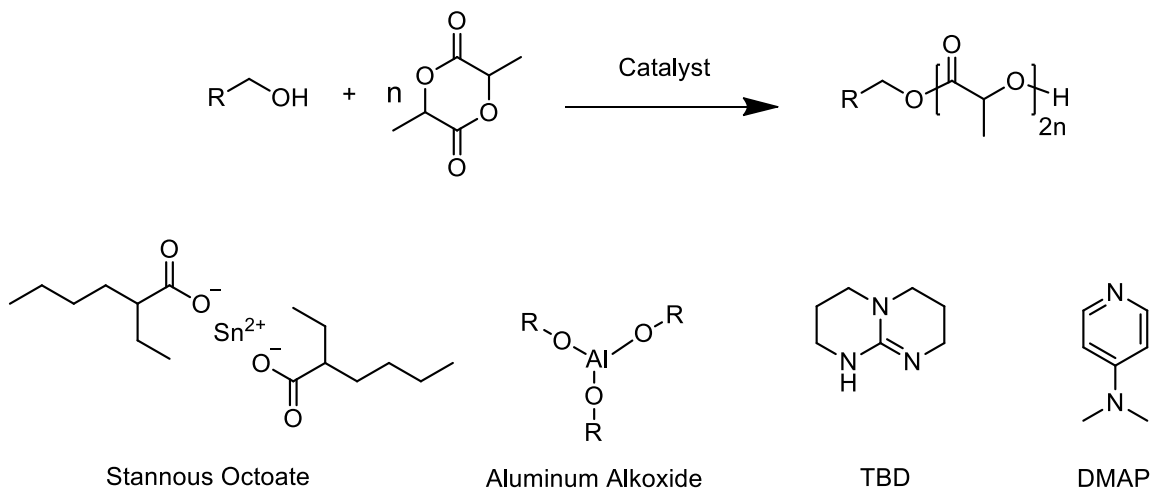
Figure 1.5 Ring-opening polymerization of lactide with the chemical structures of several catalysts.

Thermally promoted azide-alkyne cycloaddition. The formation of 1,2,3-triazoles from the copper-catalyzed azide-alkyne cycloaddition (CuAAC) have been mostly known as a standard "Click Chemistry", as introduced by K.B. Sharpless in 2011 to describe reactions with high yields and only byproducts that can be removed easily.[49]

CuAAC gives 1,4-disubstituted regioisomers specifically. The reaction can be carried out at ambient temperature in a wide scope of reaction medium. Cyclooctynes have been developed for a strain-promoted azide-alkyne cycloaddition in the absence of metal catalyst and have found extensive biological applications.[50] However, the difficulty in the preparation and functionalization of cyclooctynes makes it challenging for large-scale production. Traditionally, the azide-alkyne cycloaddition is promoted by thermal treatment at elevated temperature, known as a classic Huisgen 1,3-Dipolar Cycloaddition. A mixture of 1,4- and 1,5- disubstituted regioisomers is obtained from the reaction as shown in Figure 1.6. As alkyne and azide groups can be easily incorporated into different objects, reviving of the thermally promoted azide-alkyne cycloaddition in materials preparation has been observed.[51]

A. Thermally promoted azide-alkyne cyclization
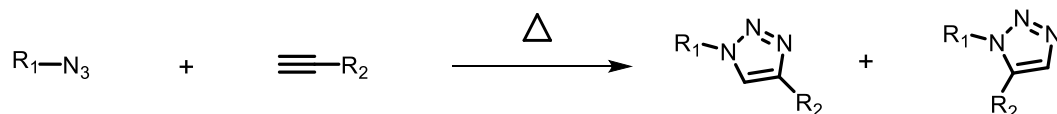
B. Diels-Alder reaction between furan and maleimide
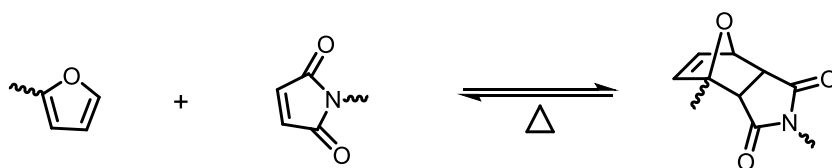
Figure 1.6 Schematic illustration of (A) thermally promoted azide-alkyne cyclization and (B) Diels-Alder reaction between furan and maleimide.

Diels-Alder reaction. The Diels-Alder (DA) reaction between furan and maleimide is thermally reversible via the retro-Diels-Alder (rDA) reaction (Figure 1.6).[52] Covalent bond linkage can be formed from DA reaction and stable at room temperature. Disconnection happens through rDA reaction at an elevated temperature. The process is

fully reversible and useful for making self-healing materials and thermally mendable polymers. Functional furan derivatives with hydroxyl group, carboxyl acid group, thiol group, aldehyde, vinyl, methacrylate, acrylate groups can be easily obtained. Polymers with furan moieties can be obtained through the polymerization of furan based monomers and post polymerization modifications. Multi-functional maleimide compounds are always used as the cross-linker for a cross-linking process. The cross-linked networks can be remolded under elevated temperatures due to the rDA reaction.[53]

1.5 Research objectives

The major objective of my dissertation work was to develop mono-functional monomers and thermoplastic polymers from renewable soybean oil. Hydroxyl fatty amides from the amidation reactions of high oleic soybean oil (HOSO) with three different amino alcohols (ethanolamine, propanolamine, N-methyl ethanolamine) were firstly prepared and converted to monomers with different polymerizable functionalities (methacrylate, norbornene, oxazoline). Polymers from free radical polymerization of methacrylate monomers and ROMP of norbornene monomers were characterized for property comparison. A subsequent methodological study was carried out to examine the amidation behaviors of 19 different amino alcohols with HOSO. Their hydroxyl fatty amides were converted to meth(acrylate) monomers and polymerized by free radical polymerization for understanding structural-property relationship.

Applications for constructing elastomers were further developed using these soybean oil based monomers and thermoplastic polymers. A-B-A triblock copolymer thermoplastic elastomers were prepared by ATRP with polystyrene as the outside block and a soybean oil based polymer as the middle block. The influence of polystyrene content

12

on the mechanical properties was examined. A multi-graft type thermoplastic elastomer was also prepared using a soybean oil based norbornene monomer and a norbornene capped polylactide by ROMP. The properties for these polymers were compared by tensile testing. Thermally remendable elastomers with high resilience were also developed through the DA cross-linking of a furan modified soybean oil derived polymers by bis-maleimide cross-linker. Control over the properties can be achieved through the choice of polymer precursors and the cross-linker ratios. Finally, composites materials with elastomer properties were prepared from an azide incorporated soybean oil based polymer and alkyne functionalized lignin through thermally promoted azide-alkyne cyclization. A model study was also carried out to demonstrate the reactivity between the involved components.

1.6 References

(1) Gandini, A. *Macromolecules* **2008,** *41*, 9491-9504.

(2) Wilbon, P. A.; Chu, F.; Tang, C. *Macromolecular rapid communications* **2013,** *34*, 8-37.

(3) Yao, K.; Tang, C. *Macromolecules* **2013,** *46*, 1689-1712.

(4) Thakur, V. K.; Thakur, M. K. *Carbohydrate polymers* **2014,** *109*, 102-117.

(5) Thakur, V. K.; Thakur, M. K.; Raghavan, P.; Kessler, M. R. *ACS Sustainable Chemistry & Engineering* **2014,** *2*, 1072-1092.

(6) Huber, T.; Müssig, J.; Curnow, O.; Pang, S.; Bickerton, S.; Staiger, M. P. *Journal of Materials Science* **2012,** *47*, 1171-1186.

(7) Kumar, R.; Singh, S.; Singh, O. V. *Journal of industrial microbiology & biotechnology* **2008,** *35*, 377-391.

(8) Effendi, A.; Gerhauser, H.; Bridgwater, A. V. *Renewable and Sustainable Energy Reviews* **2008,** *12*, 2092-2116.

(9) Meier, M. A.; Metzger, J. O.; Schubert, U. S. *Chemical Society Reviews* **2007,** *36*, 1788-1802.

(10) Gandini, A.; Coelho, D.; Gomes, M.; Reis, B.; Silvestre, A. *Journal of Materials Chemistry* **2009,** *19*, 8656-8664.

13

(11) Wilbon, P. A.; Zheng, Y.; Yao, K.; Tang, C. *Macromolecules* **2010,** *43*, 8747-8754.

(12) Firdaus, M.; Montero de Espinosa, L.; Meier, M. A. *Macromolecules* **2011,** *44*, 7253-7262.

(13) de Espinosa, L. M.; Meier, M. A. *European Polymer Journal* **2011,** *47*, 837-852.

(14) Ogunniyi, D. *Bioresource technology* **2006,** *97*, 1086-1091.

(15) Samuelsson, J.; Sundell, P.-E.; Johansson, M. *Progress in organic coatings* **2004,** *50*, 193-198.

(16) Kim, H.-J.; Kang, B.-S.; Kim, M.-J.; Park, Y. M.; Kim, D.-K.; Lee, J.-S.; Lee, K.-Y. *Catalysis Today* **2004,** *93–95*, 315-320.

(17) Satyarthi, J. K.; Srinivas, D.; Ratnasamy, P. *Applied Catalysis A: General* **2011,** *391*, 427-435.

(18) Zhao, M.-L.; Tang, L.; Zhu, X.-M.; Hu, J.-N.; Li, H.-Y.; Luo, L.-P.; Lei, L.; Deng, Z.-Y. *Journal of Agricultural and Food Chemistry* **2013,** *61*, 1189-1195.

(19) Qin, S.; Saget, J.; Pyun, J.; Jia, S.; Kowalewski, T.; Matyjaszewski, K. *Macromolecules* **2003,** *36*, 8969-8977.

(20) Maiti, B.; Kumar, S.; De, P. *RSC Advances* **2014,** *4*, 56415-56423.

(21) Mutlu, H.; Meier, M. A. *Journal of Polymer Science Part A: Polymer Chemistry* **2010,** *48*, 5899-5906.

(22) Lu, Y.; Larock, R. C. *ChemSusChem* **2009,** *2*, 136-147.

(23) Pelletier, H.; Belgacem, N.; Gandini, A. *Journal of applied polymer science* **2006,** *99*, 3218-3221.

(24) Hong, J.; Luo, Q.; Wan, X.; Petrović, Z. S.; Shah, B. K. *Biomacromolecules* **2011,** *13*, 261-266.

(25) Stemmelen, M.; Pessel, F.; Lapinte, V.; Caillol, S.; Habas, J. P.; Robin, J. J. *Journal of Polymer Science Part A: Polymer Chemistry* **2011,** *49*, 2434-2444.

(26) Desroches, M.; Caillol, S.; Lapinte, V.; Auvergne, R.; Boutevin, B. *Macromolecules* **2011,** *44*, 2489-2500.

(27) Hoogenboom, R.; Schubert, U. S. *Green Chemistry* **2006,** *8*, 895-899.

(28) Chernykh, A.; Alam, S.; Jayasooriya, A.; Bahr, J.; Chisholm, B. J. *Green Chemistry* **2013,** *15*, 1834-1838.

14

(29) Tarnavchyk, I.; Popadyuk, A.; Popadyuk, N.; Voronov, A. *ACS Sustainable Chemistry & Engineering* **2015,** *3*, 1618-1622.

(30) Alam, S.; Kalita, H.; Jayasooriya, A.; Samanta, S.; Bahr, J.; Chernykh, A.; Weisz, M.; Chisholm, B. J. *European Journal of Lipid Science and Technology* **2014,** *116*, 2-15.

(31) Huang, H.; Hoogenboom, R.; Leenen, M. A.; Guillet, P.; Jonas, A. M.; Schubert, U. S.; Gohy, J.-F. *Journal of the American Chemical Society* **2006,** *128*, 3784-3788.

(32) Song, J. S.; Huang, B. C.; Yu, D. S. *Journal of applied polymer science* **2001,** *82*, 81-89.

(33) Chen, Y.; Kushner, A. M.; Williams, G. A.; Guan, Z. *Nature chemistry* **2012,** *4*, 467-472.

(34) Milani, G.; Milani, F. *Journal of Applied Polymer Science* **2011,** *119*, 419-437.

(35) Liu, Y.; Yao, K.; Chen, X.; Wang, J.; Wang, Z.; Ploehn, H. J.; Wang, C.; Chu, F.; Tang, C. *Polymer Chemistry* **2014,** *5*, 3170-3181.

(36) Wanamaker, C. L.; O'Leary, L. E.; Lynd, N. A.; Hillmyer, M. A.; Tolman, W. B. *Biomacromolecules* **2007,** *8*, 3634-3640.

(37) Tang, D.; Macosko, C. W.; Hillmyer, M. A. *Polymer Chemistry* **2014,** *5*, 3231-3237.

(38) Wang, Z.; Zhang, X.; Wang, R.; Kang, H.; Qiao, B.; Ma, J.; Zhang, L.; Wang, H. *Macromolecules* **2012,** *45*, 9010-9019.

(39) Bielawski, C. W.; Grubbs, R. H. *Angewandte Chemie International Edition* **2000,** *39*, 2903-2906.

(40) Bielawski, C. W.; Grubbs, R. H. *Progress in Polymer Science* **2007,** *32*, 1-29.

(41) Akhani, R. K.; Clark, R. W.; Yuan, L.; Wang, L.; Tang, C.; Wiskur, S. L. *ChemCatChem* **2015,** *7*, 1527-1530.

(42) Yao, K.; Chen, Y.; Zhang, J.; Bunyard, C.; Tang, C. *Macromolecular rapid communications* **2013,** *34*, 645-651.

(43) Ganewatta, M. S.; Ding, W.; Rahman, M. A.; Yuan, L.; Wang, Z.; Hamidi, N.; Robertson, M. L.; Tang, C. *Macromolecules* **2016**.

(44) Matyjaszewski, K. *Macromolecules* **2012,** *45*, 4015-4039.

(45) Liu, J.; Lian, X.; Zhao, F.; Zhao, H. *Journal of Polymer Science Part A: Polymer Chemistry* **2013,** *51*, 3567-3571.

(46) Wright, R. A.; Wang, K.; Qu, J.; Zhao, B. *Angewandte Chemie International Edition* **2016**.

15

(47) Odian, G. *Principles of Polymerization, Fourth Edition* **2004**, 544-618.

(48) Stridsberg, K. M.; Ryner, M.; Albertsson, A.-C., Controlled ring-opening polymerization: polymers with designed macromolecular architecture. In Degradable aliphatic polyesters, Springer: **2002**; pp 41-65.

(49) Kolb, H. C.; Finn, M.; Sharpless, K. B. *Angewandte Chemie International Edition* **2001,** *40*, 2004-2021.

(50) Jewett, J. C.; Bertozzi, C. R. *Chemical Society Reviews* **2010,** *39*, 1272-1279.

(51) Han, Y.; Yuan, L.; Li, G.; Huang, L.; Qin, T.; Chu, F.; Tang, C. *Polymer* **2016,** *83*, 92-100.

(52) Froidevaux, V.; Borne, M.; Laborbe, E.; Auvergne, R.; Gandini, A.; Boutevin, B. *RSC Advances* **2015,** *5*, 37742-37754.

(53) Fan, M.; Liu, J.; Li, X.; Zhang, J.; Cheng, J. *Industrial & Engineering Chemistry Research* **2014,** *53*, 16156-16163.

CHAPTER 2

ROBUST TRANSFORMATION OF PLANT OILS INTO FATTY DERIVATIVES FOR

SUSTAINABLE MONOMERS AND POLYMERS[1]

17

2.1 Abstract

Sustainable fuels, chemicals and materials from renewable resources have recently gained tremendous momentum in a global scale, although there are numerous non-trivial hurdles for making them more competitive with petroleum counterparts. We demonstrate a robust strategy for the transformation of plant oils into polymerizable monomers and thermoplastic polymer materials. Specifically, triglycerides were converted into *N*-hydroxyalkyl fatty amides with the aid of amino alcohols via a mild base-catalyzed amidation process with nearly quantitative yields without the use of column chromatography. These fatty amides were further converted into a variety of methacrylate monomers, norbornene monomers and cyclic imino ether monomers. Representative polymers from selected monomers have exhibited drastic different physical properties from subtle structural variations, highlighting the potential of this particular amidation reaction in the field of biomass transformation.

2.2 Introduction

With the depletion of fossil oil reserves, the utilization of plant-based materials is becoming increasingly important for sustainable development.[1-17] As feedstock for the chemical industry, plant oils stand out as one of the most important renewable resources among rich raw materials and have been widely used for the preparation of surfactants, intermediates, paints and resins, polymers, and for the production of biofuels.[5, 18-25] Thus, efficient and economical transformation of their major components, triglycerides, into simple fatty derivatives is highly sought for further preparation of sustainable monomers, polymers and materials. Functional groups in triglycerides offer versatile organic reactions for derivatization, such as hydrolysis,[26] transesterification[27] and amidation[28] for ester

18

groups, hydrogenation,[29] oxidation,[30-31] polymerization,[32-33] epoxidation,[34] addition,[9, 35-36] and metathesis[37] for double bonds. Among these reactions, the most successful reaction in commercialization of triglycerides is their transesterification into fatty esters, mostly in the presence of methanol.[38] Polymeric materials based on these derivatives are mostly thermoset systems, like alkyd resins, epoxy resins and polyurethane resins, resulting from their inherent multi-functional properties. Linearly structured polymers from plant oils are rarely reported, which might be explained from the difficulty in the obtaining and polymerization of oil based mono-functional monomers. A soybean oil based 2-oxazoline monomer has been prepared and polymerized via micro-wave promoted cationic ring-opening polymerization.[39] Recently, a soy-derived vinyl ether monomer was prepared through the transesterification reaction with 2-(vinyloxy)-ethanol and polymerized by cationic polymerization to afford linear polymers with a glass transition temperature of -90 °C.[40] Such monomers are desirable as they can transport the fatty acid chains from triglycerides into thermoplastic polymer products with high atom efficiency.

In synthetic organic chemistry, amidation of un-activated esters with amino alcohols assisted by a catalyst (e.g. lipases,[41-42] inorganic base,[43] organic base[44-45]) has been widely explored to form *N*-hydroxyalkyl amides, partially because of the importance of amide group in many areas, like drug development,[46] polymers,[47-48] and asymmetric catalysis.[49] It is generally believed that the reaction between esters and amino alcohols follows consecutive transesterification and rearrangement via O-N intramolecular acyl migration to form amides.[50-52] The choice of an appropriate base is critical for obtaining high yield for this reaction. Both inorganic and organic bases were used to promote the catalytic amidation with over 80% yields. Naturally derived surfactants and lubrication

19

additives have been prepared through the amidation of triglycerides with amino alcohols using both homogeneous and solid base catalysts. [53-54]

Inspired by the above-mentioned pioneer works, herein we report efficient chemistry strategies for the preparation of oil based mono-functional monomers and thermoplastic polymers using derivatives from the base-catalyzed amidation of plant oils. Specifically, various amino alcohols were utilized in converting triglycerides into *N*-hydroxyalkyl fatty amides with the aid of sodium methoxide to provide precursors for further derivatization (Scheme 2.1). The amidation process was achieved with nearly quantitative yields in the absence of column chromatography, thus much appealing for sustainability. *N*-hydroxyalkyl fatty amides were further converted into non-cyclic methacrylate monomers, norbornene monomers and cyclic imino ether monomers (oxazoline and oxazine). Selected monomers were polymerized to validate the feasibility toward versatile polymers. The subtle structural variation in *N*-hydroxyalkyl amides led to polymers with drastically different properties, highlighting the opportunities for the amidation process in the preparation of bio-renewable polymers from plant oils.

Scheme 2.1 Derivatization of triglycerides into *N*-hydroxyalkyl fatty amides and corresponding monomers. The fatty structure was represented by oleic group only for the simplification purpose.
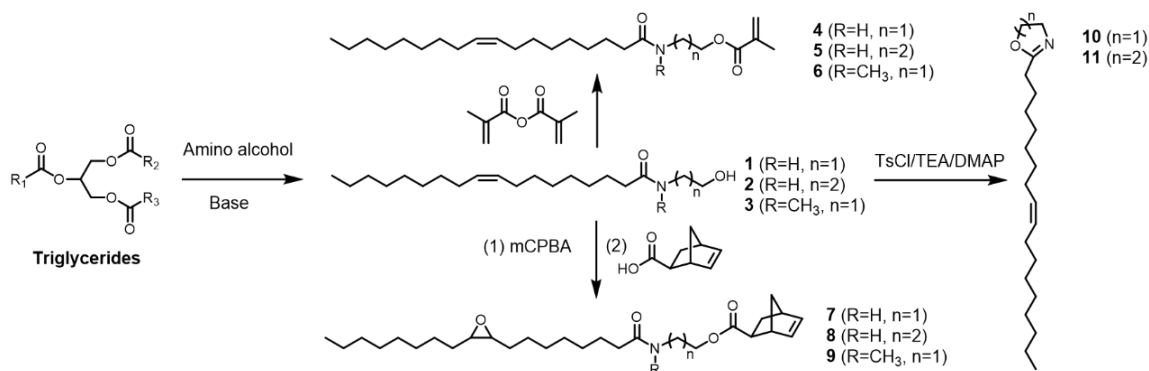
2.3 Experimental section

Materials

Plenish high oleic soybean oil (HOSO) was provided by Dupont. Ethanolamine (99%, Aldrich), 3-amino-1-propanol (99%, Aldrich), N-methyl ethanolamine (98%, Aldrich), methacrylic anhydride (94%, Aldrich), trimethylacetic anhydride (99%, Aldrich), exo-5-norbornenecarboxylic acid (97%, Aldrich), 4-Dimethylaminopyridine (DMAP, 99%, Aldrich), Grubbs Catalyst (2nd Generation, Aldrich), sodium methoxide (5.4 M solution in methanol, 30 wt.%, Acros Organics), triethylamine (TEA, 99%, Alfa Aesar), p-toluenesulfonyl chloride (TsCl, 98%, Alfa Aesar), 3-Chloroperbenzoic acid (mCPBA, 70-75%, Alfa Aesar), 5-Norbornene-2-methylamine (mixture of isomers, 98%, TCI) were used as received. Grubbs Catalyst (3rd generation) was prepared according to a previous report.[55] Azobisisobutyronitrile (AIBN, 98%, Aldrich) was recrystallized from methanol. All other reagents were from commercial resources and used as received unless otherwise mentioned.

Characterizations

^{1}H NMR and ^{13}C NMR spectra were recorded on a Varian Mercury 300 spectrometer with tetramethylsilane (TMS) as an internal reference. Molecular weights and distribution of polymers were determined using a gel permeation chromatography (GPC) equipped with a 2414 RI detector, a 1525 Binary Pump and three Styragel columns. The columns consisted of HR 1, HR 3 and HR 5E in the effective molecular weight ranges of 100-5k, 500-30k, and 2k-4M respectively. THF was used as eluent at 35 ^{o}C with a flow rate of 1.0 mL/min. The system was calibrated with polystyrene standards obtained from Polymer Laboratories. GPC samples were prepared by dissolving the sample in THF with

21

a concentration of 3.0 mg/mL and passing through microfilters with average pore size of 0.2 μm. Fourier transform infrared spectrometry (FTIR) spectra were taken on a PerkinElmer spectrum 100 FTIR spectrometer. The glass transition temperature (T_g) of polymers was tested through differential scanning calorimetry (DSC) conducted on a DSC 2000 instrument (TA instruments). Samples were firstly heated from -70 °C to 200 °C at a rate of 10 °C /min. After cooling down to -70 °C at the same rate, the data were collected from the second heating scan. 10 mg of each sample was used for DSC test with nitrogen gas at a flow rate of 50 mL/min. Thermogravimetric analysis (TGA) was conducted on a Q5000 TGA system (TA instruments), ramping from 25 °C to 600 °C with a rate of 10 °C /min. Each test cost around 10 mg of the sample. Tensile stress-strain testing was carried out with an Instron 5543A testing instrument. The films were prepared by casting a DCM solution of the polymer in a PTFE mold. After the evaporation of solvent, the film was put under vacuum for 4 hours at room temperature and 4 hours at 60 °C. Dog-bone shaped specimens were cut from the film with a length of 20 mm and width of 5.0 mm before tested at room temperature with the crosshead speed of 20 mm/min.

Synthesis of N-hydroxyalkyl Fatty Amides (1-3).

High oleic soybean oil (HOSO, 100 g, around 0.344 mol ester group) was charged into a 500 ml round bottom flask and purged with nitrogen in an 100 °C oil bath for 1 hour before cooling down to 60 °C. For the preparation of compound **1**, ethanol amine (27 g, 0.443 mol) was added to the cooled HOSO. Then, sodium methoxide dissolved in methanol (1.5 mL, 0.008 mol) was added to the mixture. The solution was kept stirring at 60 °C until the complete conversion of the ester bond as confirmed by FTIR. Normally, it took around 4 hours to obtain complete conversion for all the amidation process. The crude product was

22

poured into dichloromethane and washed twice with brine before being dried over anhydrous magnesium sulfate. After filtration and removing the solvent under reduced pressure, the product was obtained in yield between 85%-96%. Compound **2** and **3** were prepared in the same method using amino propanol and N-methyl ethanolamine as the amidation agent.

Synthesis of methacrylate monomers (4-6)

Compound **3** (102 g, 0.300 mol), methacrylic anhydride (49 g, 0.300 mol) and DMAP (0.366g, 0.003 mol) were charged together into a 500 mL round bottom flask and put into an oil bath set at 60 $^{\circ}$C. After stirring overnight, 10 ml of deionized water was added into the reactor and stirred for one hour. The solution was then poured into DCM, washed with brine for twice and dried with anhydrous magnesium sulfate. After filtration and evaporation of DCM, compound **6** was obtained in a state of liquid at room temperature. Compound **4** and **5** were prepared in the same method.

Epoxidation of N-hydroxyalkyl Fatty Amides

Compound **1** (10.2 g, 30 mmol) was dissolved together with mCPBA (9.0 g, 36 mmol) in 100 ml DCM and put into an ice-water bath. Na_2CO_3 (4.5g, 42 mmol) was added into the solution. The solution was kept in ice-water bath for 30 mins and stirred at room temperature for 3 hours. The product was subsequently washed with $Na_2S_2O_3$, $NaHCO_3$, NaCl before dried over anhydrous $MgSO_4$. The dried solution was filtered through a short column with basic Al_2O_3. With the evaporation of DCM, the epoxidized product was obtained. The epoxidized compound **1** and **2** were solid, while epoxidized compound **3** is a liquid.

23

Synthesis of norbornene functionalized monomers (7-9)

Epoxidized compound **1** (1.0 g, 2.91 mmol), pivalic anhydride (0.6 g, 3.2 mmol, exo-5-norbornenecarboxylic acid (0.441 g, 3.2 mmol) and DMAP (3.7 mg, 0.03 mmol) were dissolved in 3 mL THF and stirred in an oil bath of $60\,^{\circ}$C. After stirring for 20 hours, 1.0 ml water was added into the solution and stirred for 1 more hour. DCM was added to dissolve the product and washed with $NaHCO_3$ and NaCl aqueous solution. The product **7** was obtained after drying the organic phase and evaporation the solvent. Monomers **8** and **9** were prepared with the same method.

Synthesis of cyclic imino ethers (10-11)

Compound **1** (3.25g, 10 mmol), DMAP (0.122g, 1mmol) and TEA (3.3 ml, 22 mmol) were dissolved within 40 mL DCM in a 100 mL round bottom flask. The solution was put into an ice-water bath and stirred for 30 mins before TsCl (1.91g, 10 mmol) dissolved in DCM was added. The reaction was stirred at room temperature for 20 hours and the solution was washed subsequently by aqueous solution of NH_4Cl (twice), $NaHCO_3$ and water. The organic phase was dried by anhydrous $MgSO_4$ and flushed through silicone gel to get a liquid product **10**. Compound **11** was prepared similarly from compound **2**.

Synthesis of polymer P1 and P2 by free radical polymerization

Monomer **4** (5.0 g, 12.7 mmol) and AIBN (0.02 g, 0.12 mmol) were dissolved in 10 ml toluene. The solution was purged with nitrogen for 15 mins and put into a preheated oil bath set at 70 $^{\circ}$C. After 6 hours, the solution was directly poured slowly into methanol at room temperature under stirring. The polymer at the bottom was washed twice with methanol and dried under vacuum at 60 $^{\circ}$C to get **P1**. Polymer **P2** was prepared when monomer **5** was used.

Synthesis of polymer P3 by free radical polymerization

Monomer **6** (5.0 g, 12.7 mmol) and AIBN (0.02 g, 0.12 mmol) were dissolved in 5 ml toluene. The solution was purged with nitrogen for 15 mins and put into a preheated oil bath set at 80 ^{o}C. After polymerization for 20 hours, the solution was directly poured into methanol at room temperature under stirring. The polymer at the bottom was washed twice with methanol and dried under vacuum at 60 ^{o}C.

Synthesis of polymers P4-P6 by ROMP

Norbornene type monomer **7** (300 mg, 0.645 mmol) was dissolved in 5.0 mL DCM and nitrogen was purged through the solution for 10 mins. Grubbs 3rd catalyst (2.5 mg, 0.0034 mmol) dissolved in 1.0 ml was purged with nitrogen and transferred into the monomer solution to start the polymerization. To the reacting solution, several drops of ethyl vinyl ether were added to stop the polymerization after 20 mins and stirred for another 10 mins when full conversion of the monomer was confirmed by ^{1}H NMR. Methanol was added into the concentrated solution to precipitate the polymer out followed by washing with methanol for twice. The polymers were dried under vacuum overnight to get **P4**. **P5** and **P6** were prepared from monomer **8** and **9**.

2.4 Results and Discussion

From triglycerides to fatty amide derivatives
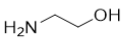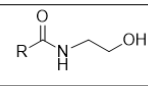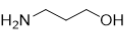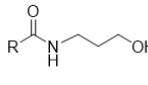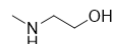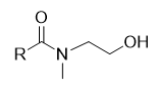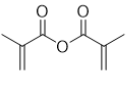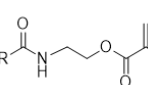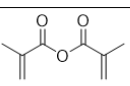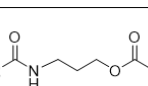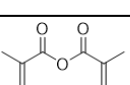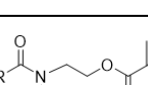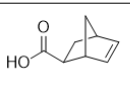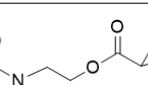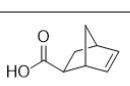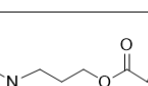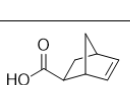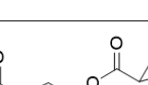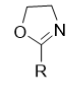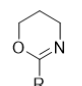
Plenish high oleic soybean oil (HOSO), which contains an average of three double bonds per triglyceride, was used as the representative plant oil in this study. Amidation of un-activated esters into *N*-hydroxyalkyl amides is typically carried out via a base-catalyzed reaction, which involves transesterification and subsequent rearrangement via O-N intramolecular acyl migration. A variety of bases have been explored, including inorganic

25

hydroxides and organic bases such as *N*-heterocyclic carbenes.[43, 45] Sodium methoxide was chosen as the base in consideration of a homogeneous reaction media and facile purification process.

In a typical procedure, an amino alcohol was mixed with HOSO, followed by the addition of sodium methoxide to promote the amidation process (Scheme 2.1). *N*-hydroxyalkyl fatty amides were obtained by washing the reaction mixture with brine water to remove the catalysts and glycerol, a side product from amidation. Using different amino alcohols, three fatty derivatives, labeled as **1**, **2** and **3**, were prepared with yields nearly 100% (Table 2.1). A typical structure of *N*-hydroxyalkyl fatty amide based on the oleic group was shown in Scheme 2.1, as 75% of the fatty acid chains in HOSO were composed of oleic acid. The fatty amide structures were confirmed by ^{1}H NMR, as presented in Figure 2.1A. The spectra show the complete disappearance of protons at 5.2 ppm (-CH-) and 4.1-4.3 ppm (-CH$_2$-), associated with the glycerol core of HOSO. New peaks appeared at 3.4 ppm (-N-CH$_2$-) and 3.7 ppm (-O-CH$_2$-) in compound **1**, 3.4 ppm and 3.6 ppm in compound **2**, and 3.5 ppm and 3.8 ppm in compound **3**, corresponding to methylene protons in the *N*-hydroxyalkyl groups. Peaks for the proton on nitrogen (-NH-) were found at 5.8 ppm in **1** and 5.9 ppm in **2**. A peak for the methyl group on nitrogen (-N-CH$_3$-) was shown at 3.0 ppm in **3**. These hydroxyl fatty amides and HOSO were also characterized by ^{13}C NMR to confirm the transformation (Figure 2.1B). As shown in many reports, a proposed mechanism of the above transformation is probably involved with cascade transesterification and O-N acyl migration (Figure 2.1C). Transesterification of esters with alcohol under basic conditions is very common. The acyl migration subsequently led to

26

more stable amides via a possible cyclic intermediate, which could be confirmed with the formation of cyclic imino ether, as described in a later section of this chapter.

Table 2.1 Amidation of HOSO with amino alcohols and further preparation of fatty monomers.

Entry	Reactant 1	Reactant 2	Product	Solvent	Yield
1	HOSO	H₂N⌒OH	**1,**	None	95%
2	HOSO	H₂N⌒⌒OH	**2,**	None	95%
3	HOSO	(CH₃)N⌒OH	**3,**	None	97%
4	**1**	methacrylic anhydride	**4,**	None	96%
5	**2**	methacrylic anhydride	**5,**	None	96%
6	**3**	methacrylic anhydride	**6,**	None	98%
7	Epoxidized **1**	norbornene carboxylic acid	**7,**	THF	96%
8	Epoxidized **2**	norbornene carboxylic acid	**8,**	THF	96%
9	Epoxidized **3**	norbornene carboxylic acid	**9,**	THF	98%
10	**1**	TsCl	**10,**	DCM	97%
11	**2**	TsCl	**11,**	DCM	97%

These fatty derivatives have quite different physical appearances. Both compounds **1** and **2** are secondary amides and are solid at room temperature, while tertiary amide

compound **3** is a liquid (Figure 2.1D). The difference in their physical states is certainly

due to the difference in their molecular structures. The presence of N-H group in **1** and **2**

promotes the formation of H-bonds.
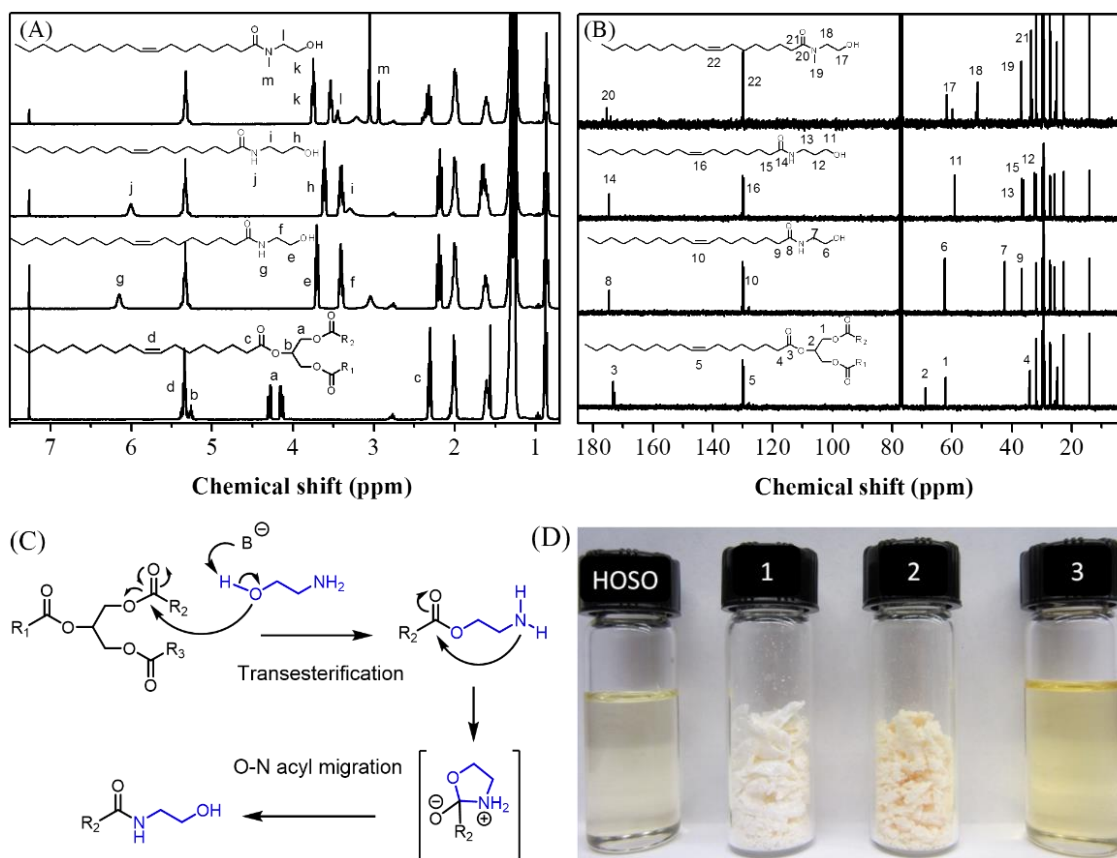
Figure 2.1 (A) ^{1}H NMR spectra and (B) ^{13}C NMR of HOSO and *N*-hydroxyalkyl fatty amides; (C) Proposed mechanism for the amidation of triglycerides with amino alcohols, ethanol amine used as an example; (D) photos of HOSO and the obtained hydroxyl fatty amides.

From *N*-hydroxyalkyl fatty amides to fatty monomers

We attempted to convert these *N*-hydroxyalkyl fatty amides into a variety of non-

cyclic and cyclic monomers using facile reactions (Scheme 2.1). We first prepared

methacrylate monomers.[56] Initially methacryloyl chloride was used for direct halide

displacement to form esters. However, it was found later that such-prepared monomers

often led to the formation of cross-linked polymers. One possible reason was associated

with the formation of dimethacrylate between methacryloyl chloride. Thus column chromatography must be needed to make highly pure monomers. We then employed a much more efficient transesterification reaction with the aid of methacrylic anhydride and catalytic DMAP. The reaction was very smooth and went to nearly 100% conversion with a ratio of 1:1 between *N*-hydroxyalkyl fatty amides and methacrylic anhydride without the use of any organic solvent.

Figure 2.2A shows ^{1}H NMR spectra of methacrylate monomers **4, 5,** and **6**. The methylene group ($-O-CH_2-$) at around 3.5 ppm shifted to 4.2 ppm after the formation of the ester group. New peaks at 6.1 ppm ($-CH_2=C-$), 5.6 ppm ($-CH_2=C-$) and 2.0 ppm ($=C-CH_3$) corresponded to vinyl and methyl protons next to the ester group. The successful synthesis of monomers **4-6** were also confirmed by ^{13}C NMR (Figure 2.2B). This process was superior to other methacrylation methods, as it only required aqueous solution wash for the purification of monomers.

We also prepared norbornene monomers from these *N*-hydroxyalkyl fatty amides for ring-opening metathesis polymerization (ROMP) to make poly(norbornene)s. In order to eliminate the influence of double bonds from the fatty chains that could interfere in ring-opening metathesis polymerization, epoxidation of **1**, **2,** and **3** was done with the aid of mCPBA to transform the double bonds into oxirane rings. Hydrogen peroxide could also be used to perform epoxidation in a more environment-benign process.[57-58] Esterification between epoxidized *N*-hydroxyalkyl fatty amides with exo-5-norbornenecarboxylic acid resulted in norbornene monomers containing oxirane groups, labeled as **7, 8,** and **9**. The coupling reaction, catalyzed by DMAP with the assistance of trimethyl acetic anhydride that would form mixed anhydride with exo-5-norbornenecarboxylic acid,[56] was more

29

efficient than an EDC/DMAP-assisted reaction. Almost 100% conversion was obtained after 12 hours at 60 °C, when the acid and anhydride were both used in 1.1 equivalent to the hydroxyl group. As shown in Figure 2.2C, the peak of the methylene protons (-O-CH$_2$-) shifted completely to 4.1-4.3 ppm with the formation of ester bonds. Also, new peaks from the carbonyl group and double bond were observed in ^{13}C NMR spectra of norbornene monomers (Figure 2.2D).
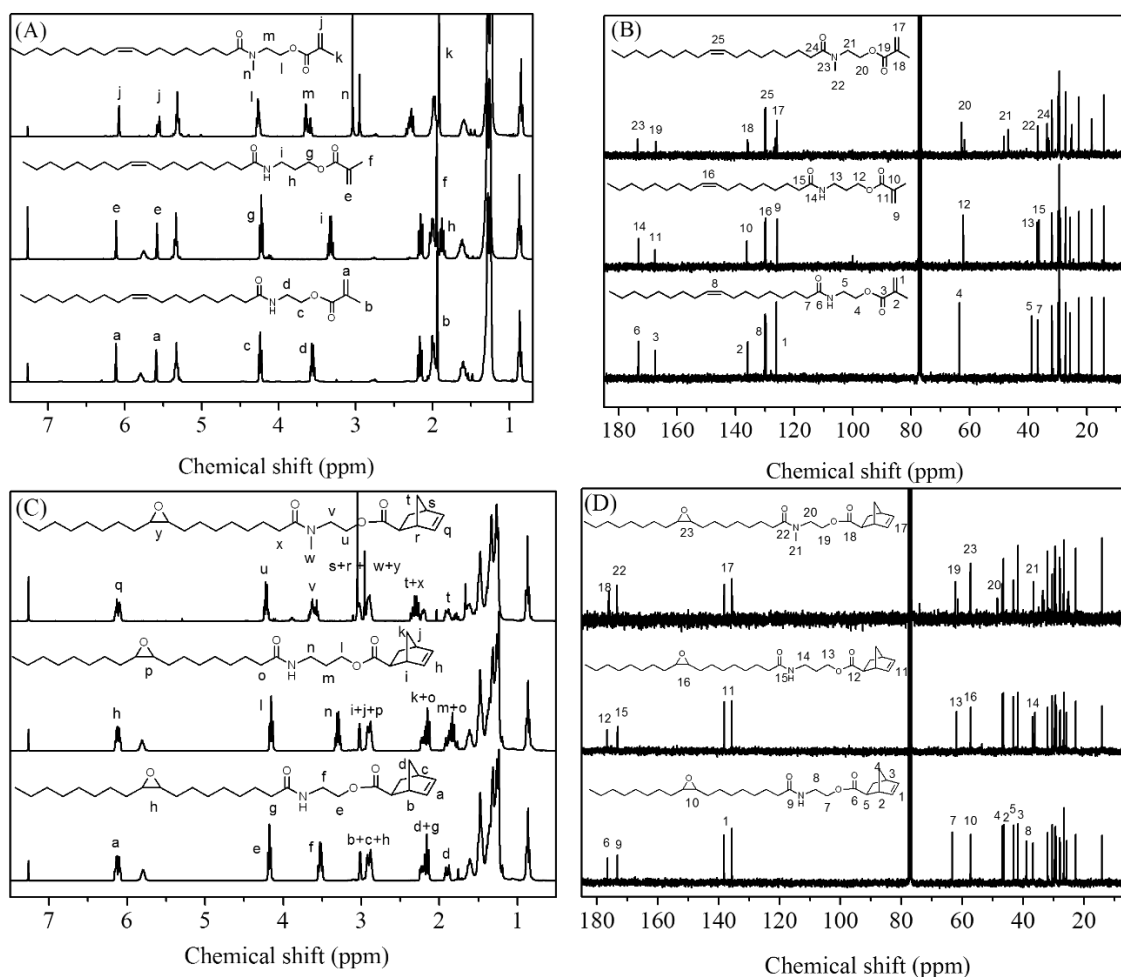
Figure 2.2 (A) ^{1}H NMR and (B) ^{13}C NMR spectra of methacrylate monomers; (C) ^{1}H NMR and (D) ^{13}C NMR spectra of norbornene monomers.

Next, we explored the possibility to prepare cyclic monomers from *N*-hydroxyalkyl fatty amides. Cyclic imino ethers of five or six-membered systems are reactive monomers

for making poly(*N*-acylalkylenimine),[59-61] which has numerous applications such as thermo-responsive hydrogels and polymer surfactants.[62-63] Such cyclic monomers are generally prepared through a condensation process between alkyl acids or nitriles with amino alcohols, which involves a catalytic high temperature system.[64] Specifically, cyclic imino ethers derived from fatty acids need high vacuum distillation for purification. One example of plant oil-derived cyclic imino ethers was a soybean oil based 2-oxazoline monomer[39], which was prepared under a harsh condition with the use of a titanium catalyst under 200 °C. We carried out a direct dehydration of *N*-hydroxyalkyl fatty amides **1** and **2** to make cyclic imino ethers **10** and **11** in a milder condition (Scheme 2.1). The dehydration was assisted with *p*-toluenesulfonyl chloride, triethylamine and DMAP in a solution of DCM at room temperature.[49] Complete conversion was observed within 12 h. Both ^{1}H NMR (Figure 2.3A) and ^{13}C NMR (Figure 2.3B) confirmed the structures of **10** and **11**. The peak from the N-H proton at around 6.2 ppm disappeared with the formation of the cyclic structure. The reaction followed a possible mechanism of in-situ tosylation and subsequent base-catalyzed cyclization (Figure 2.3C). The current process provides a facile and milder strategy to obtain vegetable oil based cyclic imino ethers.

Representative Polymers from Fatty Monomers

To validate the impact of versatile *N*-hydroxyalkyl fatty amides on the properties of soy oil-derived polymers, we first selected methacrylate monomers for free radical polymerization (Scheme 2.2). As shown in Table 2.2, all methacrylate monomers were polymerized to achieve conversions >90%. The N-H containing monomers **4** and **5** were found to be polymerized much faster than **6**. Over 90% conversion was obtained at 70 °C after 6 hours for **4** and **5**, while it took 20 hours for **6** to reach similar conversion at 80 °C.

31
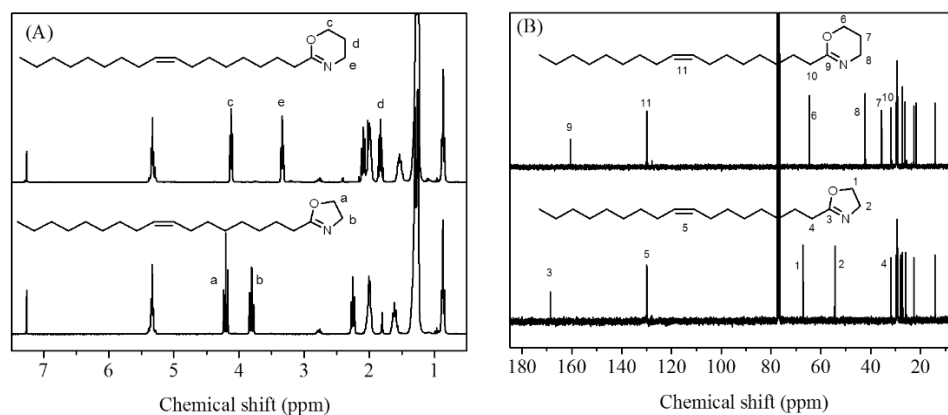
Figure 2.3 (A) ¹H NMR and ¹³C NMR spectra of cyclic imino ethers derived from *N*-hydroxyalkyl fatty amides; (C) proposed mechanism for making cyclic imino ethers.

Scheme 2.2 (A) Free radical polymerization of methacrylate fatty monomers and (B) ROMP of norbornene monomers.
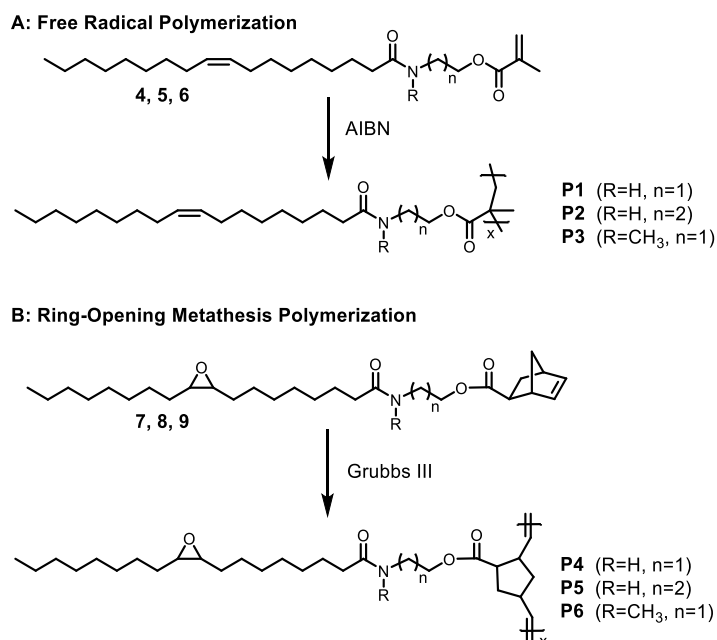
These polymers are very soluble in many organic solvents (e.g. DCM, THF, toluene), without noticeable formation of any crosslinked materials. The polymer properties are summarized in Table 2.2. ^{1}H NMR spectra of polymers **P1-P3** were shown in Figure 2.4A. The double bond in the fatty side chain was found to be stable during the polymerization process as the internal double bonds were not very active in radical polymerization, leaving it possible for further modifications.

The influence of the monomer structure on the polymer properties was firstly observed from the physical appearance of polymers **P1**, **P2**, and **P3**. Both **P1** and **P2** can form free-standing films like thermoplastics, while **P3** is very tacky and could not form free films. DSC curves showed that the glass transition temperatures (T_g) are 45 ^{o}C and 30 ^{o}C, respectively for **P1** and **P2** (Figure 2.4B), while **P3** displayed a lower T_g around -6 ^{o}C.

Table 2.2 Properties of polymers **P1-P6** prepared by free radical polymerization of methacrylate monomers (**4-6**) and ROMP of norbornene monomers (**7-9**).

Polymer	Monomer	Đ	M_n (g/mol)	T_g (^{o}C)
P1	**4**	1.5	15, 300	45.5
P2	**5**	2.2	49,100	30.0
P3	**6**	1.8	63,000	-6.2
P4	**7**	1.2	22.300	-27.0
P5	**8**	1.1	22.900	-30.7
P6	**9**	1.2	89.100	-32.7
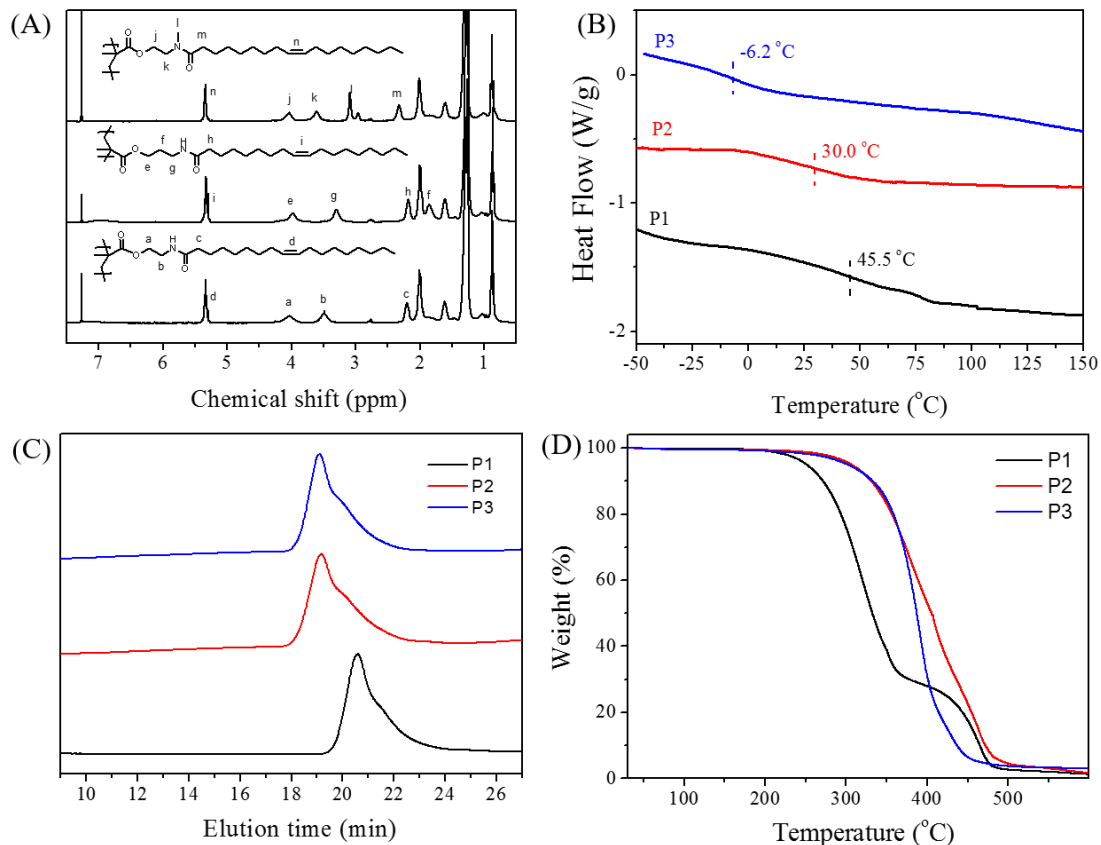
Figure 2.4 (A) ^{1}H NMR spectra, (B) DSC curves, (C) GPC curves and TGA characterization of polymers **P1-P3** prepared by free radical polymerization.

Compared with **P3**, the higher T_g of **P1** and **P2** could be explained by the presence of hydrogen bonding from the secondary amide group. As shown in Figure 2.2 and Figure 2.4A, the signal for the amide proton underwent a low-field shift from a narrow peak at 5.8 ppm to a broadened peak around 7.0 ppm after the polymerization, indicating the formation of hydrogen bonding between pendant amide groups.[65] GPC characterization for these polymers (Figure 2.4C) give characteristic distribution of polymers from free radical polymerization (Table 2.2). Thermogravimetric analysis (TGA) indicated that polymer **P1** shows two degradation stages. According to the derivative TGA curves of **P1**-**P3**, the two maximum degradation temperature of **P1** was calculated to be 320.7 °C and 465.2 °C, while **P2** and **P3** presented better thermal stability with maximum degradation temperatures of

34

378.2 ºC, 412.5 ºC, 465.2 ºC, and 388.5 ºC, 432.2 ºC respectively (Figure 2.4D). These results demonstrated that methacrylate polymers **P1-P3** have high thermal stability.

Due to the intermolecular hydrogen bonding and thus high T_g, **P1** and **P2** may exhibit mechanical properties like thermoplastics. Moreover, as the facile preparation, we carried out the synthesis of polymer **P2** at a one pound scale. Figure 2.5A presents a picture of ~ one pound **P2** in a two litter beaker with a free-standing film of **P2**. Dog-bone specimens were cut from the film for tensile testing (Figure 2.5B). A photo of **P3** was also given in Figure 2.5C, and the polymer was too soft to form a film. A typical nominal stress-nominal strain curve of **P2** obtained at room temperature was shown in Figure 2.5D. The elongation at break was found to be 140% with stress at break about 2.0 MPa. The drastic difference between **P2** and **P3** probably results from the chemical structure of the side chains as illustrated in Figure 2.5E. Polymer chains of **P2** can form strong interaction with each other through hydrogen bonding with N-H bond on the secondary amide group as the donor and carbonyl oxygen as the acceptor, while no such significant interaction presents between polymer chains of **P3**, which has tertiary amide group.

Ring-opening metathesis polymerization (ROMP) of norbornene monomers **7, 8,** and **9** were then carried out in the presence of Grubbs III catalyst.[66] The properties of norbornene polymers **P4-P6** were summarized in Table 2.2. The polymerization went to nearly complete conversion in less than 20 minutes. Newly formed double bond in the polymer backbone at 5.1-5.5 ppm were observed in the polymers (Figure 2.6A). Peaks associated with the pendant chains were retained after the polymerization, which indicated no cross-linking occurred in the absence of double bond in the side chain.

35
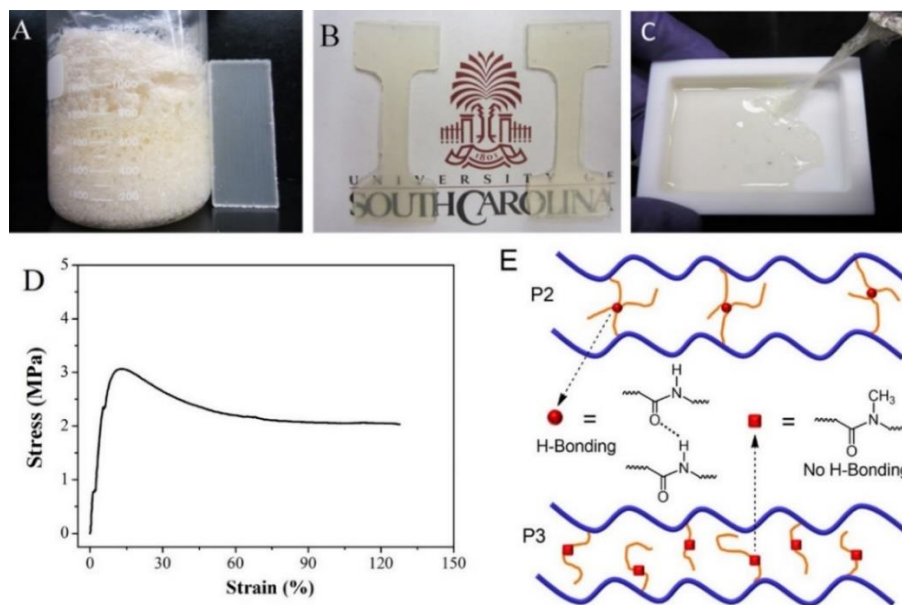
Figure 2.5 (A) One pound polymer **P2** with a solvent-cast film; (B) specimens for tensile-stress test; (C) **P3** in a mold, (D) stress-strain curve of **P2**; (E) illustration of H-bonding in **P2**, in comparison with **P3**.
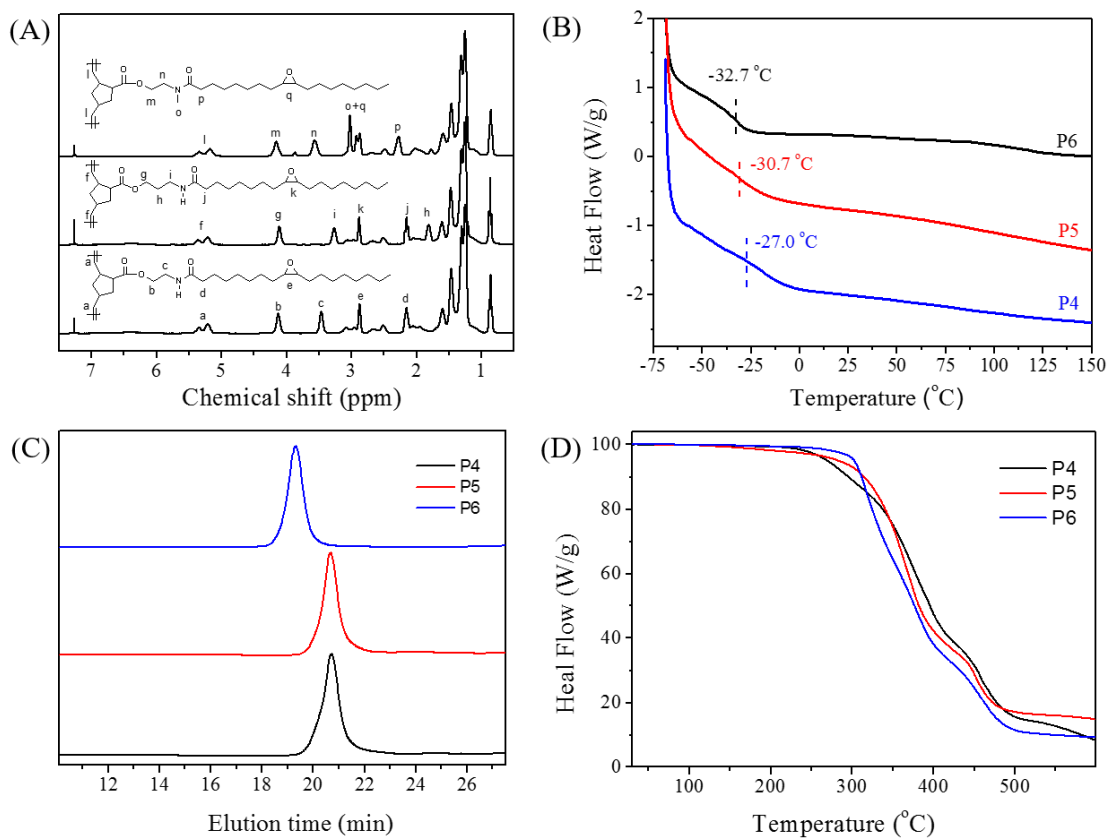
Figure 2.6 (A) ^{1}H NMR spectra, (B) DSC curves, (C) GPC curves and (D) TGA characterization of polymers **P4-P6** prepared by ROMP.

The T_g of **P4-P6** was determined from DSC characterization, as shown in Figure 2.6B. The T_g of all polymers prepared by ROMP was around -30 ºC. The presence of secondary amide groups in the side chains of **P4** and **P5** did not lead to appreciable difference from polymer **P6** with tertiary amide group. It suggested that hydrogen bonds from the pendant amide groups in **P4** and **P5** could be weaker than those in polymers **P1** and **P2**. Additional evidence can be found by comparing ^{1}H NMR spectra of these polymers (Figure 2.4 and Figure 2.6A), the chemical shifts of amide proton in **P4** and **P5** were less than those in **P1** and **P2** after the polymerization. The T_g of **P4**-**P6** are comparable with that of poly(norbornene)s from saturated C_{18} fatty ester of norbornene methanol (T_g = -32 ºC and T_m = 5.9 ºC).[67] However, no melting point was observed for **P4**-**P6**, possibly due to the presence of oxirane ring within the side chain and the varied side chain length from soybean oil. The polymers from ROMP show narrow molecular distribution than those from free radical polymerization (Figure 2.6C and Table 2.2). **P4-P6** showed good thermal stability with similar two stage degradation behaviors to **P1-P3** (Figure 2.6D).

2.5 Conclusions

In conclusion, highly efficient amidation reactions between plant oils with varied amino alcohols were utilized for the preparation of fatty amide derivatives, which were used as a powerful chemical platform for further derivatization into a variety of monomers and thermoplastic polymers. The plant oil derived intermediates and monomers were obtained with nearly quantitative yields without the utilization of laborious column separation. Specifically, cyclic imino ethers were prepared for the first time in a milder condition compared with traditional condensation method. Selected monomers were further polymerized to yield polymers that exhibit appreciable structure-dependent

properties. The strategy developed might pave the path for the facile preparation of renewable monomers and thermoplastic polymers with targeted properties from plant oils.

2.6 References

(1) Balandrin, M. F.; Klocke, J. A.; Wurtele, E. S.; Bollinger, W. H. *Science* **1985,** *228*, 1154-1160.

(2) Gandini, A. *Macromolecules* **2008,** *41*, 9491-9504.

(3) Williams, C. K.; Hillmyer, M. A. *Polymer reviews* **2008,** *48*, 1-10.

(4) Wilbon, P. A.; Chu, F.; Tang, C. *Macromolecular rapid communications* **2013,** *34*, 8-37.

(5) Meier, M. A.; Metzger, J. O.; Schubert, U. S. *Chemical Society Reviews* **2007,** *36*, 1788-1802.

(6) Coates, G. W.; Hillmyer, M. A. *Macromolecules* **2009,** *42*, 7987-7989.

(7) Xiong, M.; Schneiderman, D. K.; Bates, F. S.; Hillmyer, M. A.; Zhang, K. *Proceedings of the National Academy of Sciences* **2014**, 201404596.

(8) Yao, K.; Tang, C. *Macromolecules* **2013,** *46*, 1689-1712.

(9) Billiet, S.; De Bruycker, K.; Driessen, F.; Goossens, H.; Van Speybroeck, V.; Winne, J. M.; Du Prez, F. E. *Nature chemistry* **2014,** *6*, 815-821.

(10) Mathers, R. T. *Journal of Polymer Science Part A: Polymer Chemistry* **2012,** *50*, 1-15.

(11) Mecking, S. *Angewandte Chemie International Edition* **2004,** *43*, 1078-1085.

(12) Miller, S. A. *ACS Macro Letters* **2013,** *2*, 550-554.

(13) Ragauskas, A. J.; Beckham, G. T.; Biddy, M. J.; Chandra, R.; Chen, F.; Davis, M. F.; Davison, B. H.; Dixon, R. A.; Gilna, P.; Keller, M.; Langan, P.; Naskar, A. K.; Saddler, J. N.; Tschaplinski, T. J.; Tuskan, G. A.; Wyman, C. E. *Science* **2014,** *344*, 709-719.

(14) Dodds, D. R.; Gross, R. A. *Science* **2007,** *318*, 1250-1251.

(15) Sun, L.; Pitto-Barry, A.; Kirby, N.; Schiller, T. L.; Sanchez, A. M.; Dyson, M. A.; Sloan, J.; Wilson, N. R.; O'Reilly, R. K.; Dove, A. P. *Nat Commun* **2014,** *5*.

(16) Chung, Y.-L.; Olsson, J. V.; Li, R. J.; Frank, C. W.; Waymouth, R. M.; Billington, S. L.; Sattely, E. S. *ACS Sustainable Chemistry & Engineering* **2013,** *1*, 1231-1238.

(17) Kamber, N. E.; Jeong, W.; Waymouth, R. M.; Pratt, R. C.; Lohmeijer, B. G. G.; Hedrick, J. L. *Chem. Rev.* **2007,** *107*, 5813-5840.

(18) Montero de Espinosa, L.; Meier, M. A. *European Polymer Journal* **2011,** *47*, 837-852.

(19) Biermann, U.; Bornscheuer, U.; Meier, M. A. R.; Metzger, J. O.; Schäfer, H. J. *Angewandte Chemie International Edition* **2011,** *50*, 3854-3871.

(20) Alam, S.; Kalita, H.; Kudina, O.; Popadyuk, A.; Chisholm, B. J.; Voronov, A. *ACS Sustainable Chemistry & Engineering* **2012,** *1*, 19-22.

(21) Russo, D.; Dassisti, M.; Lawlor, V.; Olabi, A. *Renewable and Sustainable Energy Reviews* **2012,** *16*, 4056-4070.

(22) Xia, Y.; Larock, R. C. *Green Chemistry* **2010,** *12*, 1893-1909.

(23) Lligadas, G.; Ronda, J. C.; Galià, M.; Cádiz, V. *Biomacromolecules* **2010,** *11*, 2825-2835.

(24) Hong, J.; Luo, Q.; Wan, X.; Petrović, Z. S.; Shah, B. K. *Biomacromolecules* **2011,** *13*, 261-266.

(25) Bähr, M.; Mülhaupt, R. *Green Chemistry* **2012,** *14*, 483-489.

(26) Satyarthi, J.; Srinivas, D.; Ratnasamy, P. *Applied Catalysis A: General* **2011,** *391*, 427-435.

(27) Kim, H.-J.; Kang, B.-S.; Kim, M.-J.; Park, Y. M.; Kim, D.-K.; Lee, J.-S.; Lee, K.-Y. *Catalysis today* **2004,** *93*, 315-320.

(28) Delatte, D.; Kaya, E.; Kolibal, L. G.; Mendon, S. K.; Rawlins, J. W.; Thames, S. F. *Journal of Applied Polymer Science* **2014,** *131*.

(29) Zhao, M.-L.; Tang, L.; Zhu, X.-M.; Hu, J.-N.; Li, H.-Y.; Luo, L.-P.; Lei, L.; Deng, Z.-Y. *Journal of agricultural and food chemistry* **2013,** *61*, 1189-1195.

(30) Petrović, Z. S.; Milić, J.; Xu, Y.; Cvetković, I. *Macromolecules* **2010,** *43*, 4120-4125.

(31) Louis, K.; Vivier, L.; Clacens, J.-M.; Brandhorst, M.; Dubois, J.-L.; Vigier, K. D. O.; Pouilloux, Y. *Green Chemistry* **2014,** *16*, 96-101.

(32) Andjelkovic, D. D.; Valverde, M.; Henna, P.; Li, F.; Larock, R. C. *Polymer* **2005,** *46*, 9674-9685.

(33) Li, F.; Larock, R. C. *Journal of Applied Polymer Science* **2000,** *78*, 1044-1056.

(34) Tehfe, M.-A.; Lalevée, J.; Gigmes, D.; Fouassier, J. P. *Macromolecules* **2010,** *43*, 1364-1370.

(35) Petrović, Z. S.; Guo, A.; Javni, I.; Cvetković, I.; Hong, D. P. *Polymer International* **2008,** *57*, 275-281.

(36) Desroches, M.; Caillol, S.; Lapinte, V.; Auvergne, R.; Boutevin, B. *Macromolecules* **2011,** *44*, 2489-2500.

(37) Chikkali, S.; Mecking, S. *Angewandte Chemie International Edition* **2012,** *51*, 5802-5808.

(38) Borges, M. E.; Díaz, L. *Renewable and Sustainable Energy Reviews* **2012,** *16*, 2839-2849.

(39) Huang, H.; Hoogenboom, R.; Leenen, M. A.; Guillet, P.; Jonas, A. M.; Schubert, U. S.; Gohy, J.-F. *Journal of the American Chemical Society* **2006,** *128*, 3784-3788.

(40) Chernykh, A.; Alam, S.; Jayasooriya, A.; Bahr, J.; Chisholm, B. J. *Green Chemistry* **2013,** *15*, 1834-1838.

(41) Adamczyk, M.; Gebler, J. C.; Grote, J. *Bioorganic & Medicinal Chemistry Letters* **1997,** *7*, 1027-1030.

(42) Whitten, K. M.; Makriyannis, A.; Vadivel, S. K. *Tetrahedron Letters* **2012,** *53*, 5753-5755.

(43) Caldwell, N.; Jamieson, C.; Simpson, I.; Watson, A. J. *ACS Sustainable Chemistry & Engineering* **2013,** *1*, 1339-1344.

(44) Caldwell, N.; Jamieson, C.; Simpson, I.; Tuttle, T. *Organic letters* **2013,** *15*, 2506-2509.

(45) Movassaghi, M.; Schmidt, M. A. *Organic letters* **2005,** *7*, 2453-2456.

(46) Noble, M. E.; Endicott, J. A.; Johnson, L. N. *Science* **2004,** *303*, 1800-1805.

(47) Yang, J.; Zhang, M.; Chen, H.; Chang, Y.; Chen, Z.; Zheng, J. *Biomacromolecules* **2014,** *15*, 2982-2991.

(48) Chen, Y.; Guan, Z. *Chemical Communications* **2014,** *50*, 10868-10870.

(49) Evans, D. A.; Seidel, D.; Rueping, M.; Lam, H. W.; Shaw, J. T.; Downey, C. W. *Journal of the American Chemical Society* **2003,** *125*, 12692-12693.

(50) Skwarczynski, M.; Sohma, Y.; Kimura, M.; Hayashi, Y.; Kimura, T.; Kiso, Y. *Bioorganic & medicinal chemistry letters* **2003,** *13*, 4441-4444.

(51) Skwarczynski, M.; Sohma, Y.; Noguchi, M.; Kimura, M.; Hayashi, Y.; Hamada, Y.; Kimura, T.; Kiso, Y. *Journal of medicinal chemistry* **2005,** *48*, 2655-2666.

(52) Sohma, Y.; Sasaki, M.; Hayashi, Y.; Kimura, T.; Kiso, Y. *Chem. Commun.* **2004**, 124-125.

(53) Boshui, C.; Nan, Z.; Jiang, W.; Jiu, W.; Jianhua, F.; Kai, L. *Green Chemistry* **2013,** *15*, 738-743.

(54) Zhang, J.; Cai, D.; Wang, S.; Tang, Y.; Zhang, Z.; Liu, Y.; Gao, X. *The Canadian Journal of Chemical Engineering* **2014,** *92*, 871-875.

(55) Sanford, M. S.; Love, J. A.; Grubbs, R. H. *Organometallics* **2001,** *20*, 5314-5318.

(56) Sakakura, A.; Kawajiri, K.; Ohkubo, T.; Kosugi, Y.; Ishihara, K. *Journal of the American Chemical Society* **2007,** *129*, 14775-14779.

(57) Mungroo, R.; Pradhan, N. C.; Goud, V. V.; Dalai, A. K. *Journal of the American Oil Chemists' Society* **2008,** *85*, 887-896.

(58) Dinda, S.; Patwardhan, A. V.; Goud, V. V.; Pradhan, N. C. *Bioresource technology* **2008,** *99*, 3737-3744.

(59) Gress, A.; Völkel, A.; Schlaad, H. *Macromolecules* **2007,** *40*, 7928-7933.

(60) Hoogenboom, R. *Angewandte Chemie International Edition* **2009,** *48*, 7978-7994.

(61) Kempe, K.; Hoogenboom, R.; Jaeger, M.; Schubert, U. S. *Macromolecules* **2011,** *44*, 6424-6432.

(62) Farrugia, B. L.; Kempe, K.; Schubert, U. S.; Hoogenboom, R.; Dargaville, T. R. *Biomacromolecules* **2013,** *14*, 2724-2732.

(63) Kobayashi, S.; Igarashi, T.; Moriuchi, Y.; Saegusa, T. *Macromolecules* **1986,** *19*, 535-541.

(64) Hoogenboom, R. *European Journal of Lipid Science and Technology* **2011,** *113*, 59-71.

(65) Gellman, S. H.; Dado, G. P.; Liang, G. B.; Adams, B. R. *Journal of the American Chemical Society* **1991,** *113*, 1164-1173.

(66) Bielawski, C. W.; Grubbs, R. H. *Angewandte Chemie* **2000,** *112*, 3025-3028.

(67) Mutlu, H.; Meier, M. A. *Journal of Polymer Science Part A: Polymer Chemistry* **2010,** *48*, 5899-5906.

CHAPTER 3

METHODOLOGICAL AMIDATION OF TRIGLYCERIDES BY AMINO ALCOHOLS

AND THEIR IMPACT ON PLANT OIL-DERIVED POLYMER[2]

3.1 Abstract

Amidation of plant oils with amino alcohols was methodologically examined. Twenty one amino alcohols, varied in alcohol substitutions, linkers and amino substitutions, were respectively reacted with high oleic soybean oil. The structure factors in amino alcohols dictated their reactivity in amidation. While most of them resulted in quantitative conversion of triglycerides, steric hindrance on secondary amines resulted in much lower yields. Subsequent synthesis and radical polymerization of (meth)acrylates led to polymers with a distinct dependence essentially originating from the amino alcohols. Depending on the backbone and amide structures in the side chain, these polymers exhibited wide glass transition temperatures with difference more than 100 $^{\circ}$C, ranging from tacky materials to thermoplastics. A proof-of-concept hydrogenation of unsaturated double bonds was carried out, providing an approach to precisely controlling thermal and mechanical properties of plant oil-derived polymers.

3.2 Introduction

Presently, plastic production consumes about 7% of fossil fuels, which will be depleted in the future. To reduce the dependence on these finite resources, biomass feedstocks have been explored for the production of sustainable plastics and elastomers.[1-16] Plant oils are among the most important renewable raw materials for the chemical industry. Composed of triglycerides, plant oils can be converted into useful industrial commodities without extensive downstream processing, such as biodiesels, fatty alcohols, fatty acids, surfactants, etc.[17-19] Plant oils have been extensively utilized to make thermoset materials for coating and resin applications.[20-30] On the other hand, recent attempts have been targeted toward thermoplastic polymers from triglycerides.[31-40]

Conversion of triglycerides into mono-functional monomers presents one of the major challenges. Hoogenboom et al. prepared a soy-based oxazoline monomer (SoyOx), which was polymerized by microwave-assisted cationic ring-opening polymerization.[33] Chisholm et al. prepared a vinyl ether monomer (2-VOES) by transesterification of plant oils with ethylene glycol vinyl ether and further carried out living carbocationic polymerization.[36] High vacuum monomer distillation and relatively strict polymerization conditions were required for both procedures. As an improvement in monomer preparation and polymerization, a vinyl monomer was recently prepared by transesterification with *N*-hydroxyethyl acrylamide and polymerized by free radical polymerization.[37] The above three different polymers were reported to be tacky with glass transition temperature (T_g) lower than 0 ^{o}C. There is a lack of an approach to prepare polymers with a wider scope of physical properties that could offer benefits for further applications.

Recently, we reported the preparation of methacrylate monomers via a facile amidation process using soybean oil with amino alcohols. A few polymers with T_gs above and below room temperature were obtained.[38] An acrylate monomer was also obtained to make low T_g polymers, which were used for preparing triblock copolymer thermoplastic elastomers.[41] The physical properties of polymers was greatly dependent on the chemical structure of monomers, which was further dictated by the amino alcohols used in the amidation step. For example, a polymer with $T_g \approx 46\,^o$C is brittle, while a polymer with $T_g \approx -6\,^o$C is tacky. The only difference originates from the amino alcohols (ethanolamine vs. *N*-methyl ethanolamine) used in the amidation reaction.

Given the abundance of amino alcohols with various structures, it is strongly needed to examine the role of amino alcohols in a systematic approach. Herein we report

44

a methodological investigation of twenty one commercial mono-hydroxyl amino alcohols in the amidation reaction with soybean oil (Scheme 3.1). Except four amino alcohols, all others led to quantitative conversion of HOSO into mono-hydroxyl fatty amides. After esterification reactions, thirteen methacrylate monomers and three acrylate monomers were prepared and polymerized by free radical polymerization. The T_gs of ten polymers are in the range of 20 °C to 61 °C, exhibiting plastic behaviors, while six other polymers are tacky with T_gs in the range of -6 °C to -51 °C. A proof-of-concept hydrogenation of polymers was carried out to allow the tuning of mechanical properties.

Scheme 3.1 (A) Synthesis and free radical polymerization of soybean oil-derived (meth)acrylate monomers; (B) proposed mechanism of amidation between amino alcohol and triglyceride; (C) mono-hydroxyl amino alcohols examined for the amidation process.

(A) Converting soybean oil into (meth)acrylate monomers for radical polymerization
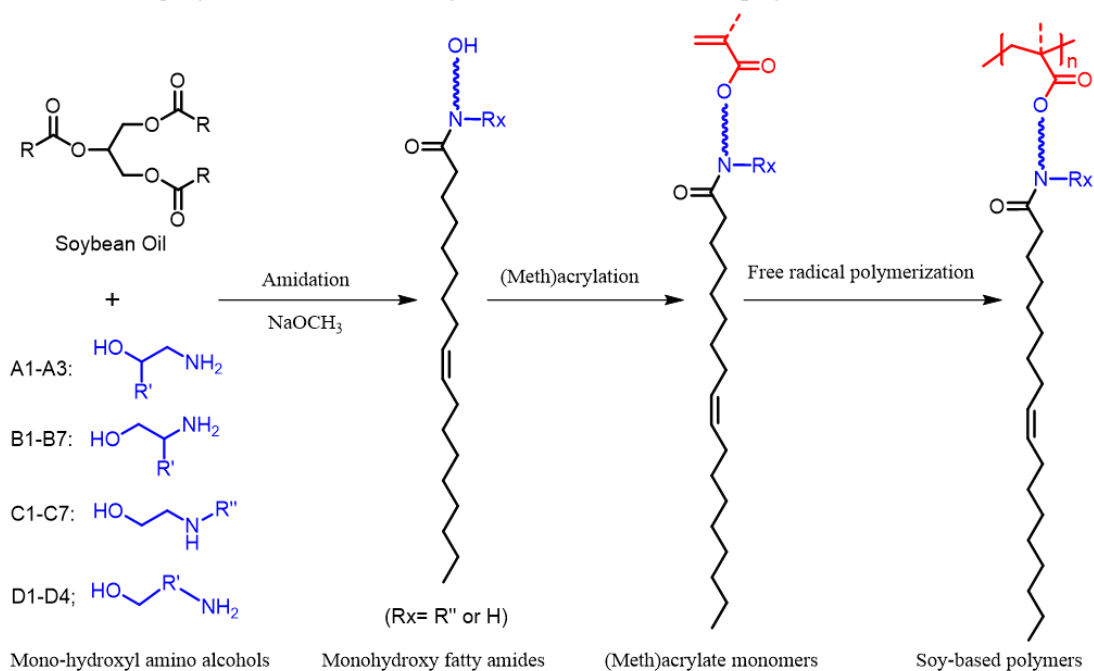
(B) Mechanism of amidation between amino alcohol and triglyceride
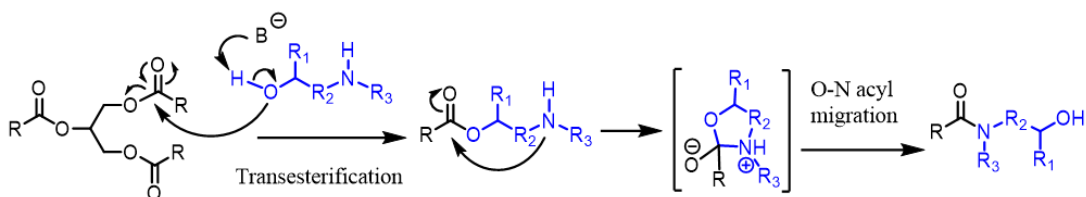
(C) Mono-hydroxyl amino alcohols for amidation
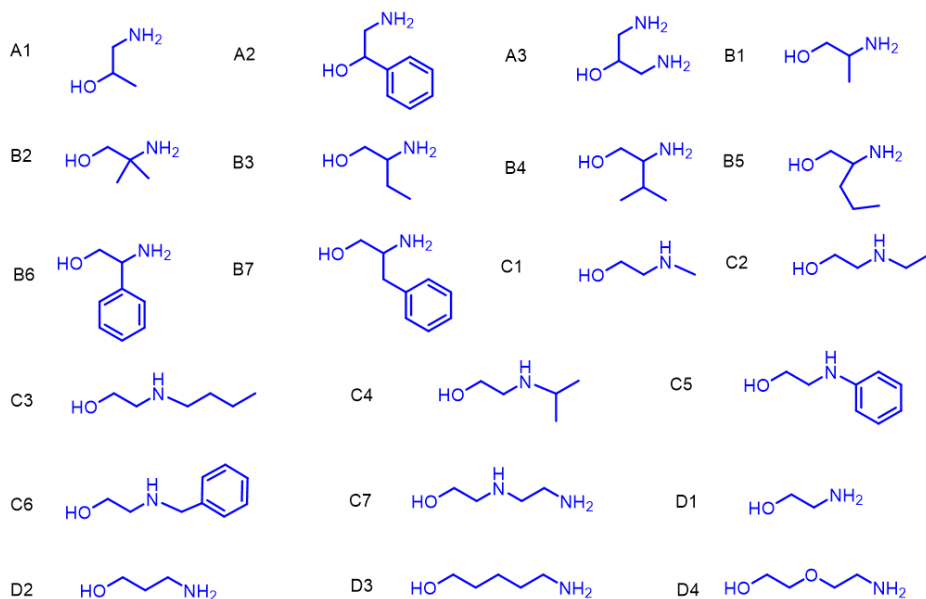
3.3 Experimental section

Materials

Plenish high oleic soybean oil (HOSO) was provided by DuPont. DL-1-amino-2-propanol (A1, 98%, TCI AMERICA), 2-amino-1-phenylethanol (A2, 97%, TCI AMERICA), 1,3-diamino-2-propanol (A3, 97%, Alfa Aesar), DL-2-amino-1-propanol (B1, 98%, TCI AMERICA), 2-amino-2-methyl-1-propanol (B2, 99%, Sigma-Aldrich), DL-2-amino-1-butanol (B3, 97%, Acros Organics), 2-amino-3-methyl-1-butanol (B4, 97%, Sigma-Aldrich), DL-2-amino-1-pentanol (B5, 97%, Sigma-Aldrich), (R)-(-)-2-Phenylglycinol (B6, 98%, Alfa Aesar), L-phenylalaninol (B7, 98%, Alfa Aesar), N-methyl ethanoamine (C1, 98%, Sigma-Aldrich), 2-(ethylamino)ethanol (C2, 98%, Sigma-Aldrich), 2-(butylamino)ethanol (C3, 98%, TCI AMERICA), 2-(isopropylamino)ethanol (C4, 99%, TCI AMERICA), 2-anilinoethano (C5, 98%, TCI AMERICA), N-benzylethanolamine (C6, 99%, TCI AMERICA), 2-(2-aminoethylamino)ethanol (C7, 99%, TCI AMERICA), ethanolamine (D1, 99%, Sigma-Aldrich), 3-amino-1-propanol

(D2, 99%, Sigma-Aldrich), 5-amino-1-pentanol (D3, 95%, TCI AMERICA), 2-(2-aminoethox)ethanol (D4, 98%, Sigma-Aldrich), sodium methoxide (5.4 M solution in methanol, 30 wt%, Acros Organics), methacrylic anhydride (94%, Sigma-Aldrich), acryloyl chloride (97%, Sigma-Aldrich), triethylamine (TEA, 99%, Alfa Aesar), 4-dimethylaminopyridine (DMAP, 99%, Sigma-Aldrich), p-toluenesulfonyl hydrazide (TSH, 97%, Sigma-Aldrich) and benzoyl peroxide (BPO, Fisher Science Education) were used as received. Azobis(isobutyronitrile) (AIBN, 98%, Sigma-Aldrich) was recrystallized from methanol. All other reagents and solvents were obtained from commercial resources and used as received. Methacrylate monomers (M1-M13) were prepared from thirteen selected hydroxyl fatty amides (SBOH-1 - SBOH-6 & SBOH-11 – SBOH-17), which can be obtained easily in 5 g scale, and polymer (P1-P13) were prepared following similar procedures reported in our previous work.[38] Since secondary amides are reactive with acryloyl chloride, only three acrylate monomers (M13-M16) were obtained by acrylation of hydroxyl fatty tertiary amides (SBOH-11 - SBOH-13) with acryloyl chloride.[41]

Characterizations

300 MHz ^{1}H NMR and 75 MHz ^{13}C NMR measurements were taken on a Varian Mercury 300 spectrometer with tetramethylsilane (TMS) as an internal reference. A gel permeation chromatography (GPC) system composed of a 2414 RI detector, a 1525 Binary Pump and three Styragel columns was used to determine molecular weight and molecular weight distribution of polymers. The columns consist of HR 1, HR 3 and HR 5E with molecular weight in the range of 1×10^5 - 5×10^3 g/mol, 5×10^5 - 3×10^4 g/mol and 2×10^3 - 4×10^6 g/mol respectively. The eluent was tetrahydrofuran (THF) at 35 °C with a flow rate of 1.0 mL/min. Polystyrene standards from Polymer laboratories were used for calibration.

47

GPC samples were prepared by filtering a 3.0 mg/mL solution in THF through microfilters with an average pore size of 200 nm. Differential scanning calorimetry (DSC) analysis of polymer samples (around 10 mg) was conducted on a DSC 2000 instrument (TA Instruments). Using a rate of 10 ^{o}C/min, a sample was heated from -70 ^{o}C to 200 ^{o}C, cooled down to -70 ^{o}C, then re-heated to 200 ^{o}C and cooled down to -70 ^{o}C. Nitrogen gas was used at a flow rate of 50 ml/min. The data was collected from the 2nd heating scan. Tensile stress-strain testing was conducted on an Instron 5543A testing instrument. Polymer films were prepared by casting 10 ml THF solution of polymer (1.25 g) in a PTFE mold (inner size 2.0 inch $\times$ 2.75 inch). After evaporation of the solvent, the films were dried under vacuum for 12 hours at room temperature before the temperature was increased to 60 ^{o}C for further drying. Dog-bone shaped specimens with cross-section length of 20 mm and width of 5.0 mm were cut from the polymer films. The thickness of films were between 0.29-0.31 mm. A photo picture of the PTFE mold and the dog-bone samples from polymer P4 was given in Fig. S10. For polymer P4, P8, P10, 3 samples were tested. For the more brittle hydrogenated polymers P8-12 and P8-40, two samples were tested. All the tests were done at room temperature with a crosshead speed of 10 mm/min.

Synthesis of N-hydroxyalkyl fatty amides (SBOH-1 to SBOH-17)

The preparation of SBOH-11, SBOH-14 and SBOH-15 was reported in our previous report.[38] Other SBOHs (except SBOH-3) were prepared following the same feeding ratios of amino alcohols and HOSO (Table 3.1). For the preparation of SBOH-3, amino alcohol A3 was used as the limiting agent, and the procedure is given as follows: HOSO (36.9 g, 0.126 mol ester) was heated at 100 ^{o}C and purged N$_2$ for 30 mins. After cooling to 60 ^{o}C, 1,3-diamino-2-propanol (5.56 g, 0.06 mol), 30 wt% NaOCH$_3$/CH$_3$OH

(0.5 mL) and 10 mL THF were added to HOSO. After 10 hours, the hot solution was poured into methanol, and product SBOH-3 crystallized out. After filtration, the product was recrystallized twice from methanol after dissolving at 70 °C to obtain a white solid product.

Synthesis of acrylate polymers (P14-P16)

Polymers (P14-P16) were prepared by free radical polymerization of corresponding monomers (M14-M16) using BPO as the initiator. The preparation of P16 is given as an example. Monomer M16 (2.2 g, 5.1 mmol) and BPO (10 mg, 0.041 mmol) were dissolved together in 2.2 mL dry toluene in a 10.0 mL Schlenk flask and purged N_2 for 20 mins. The flask was stirred in an oil bath preheated at 100 °C for 7 hours. Then the solution was precipitated from cold methanol and further dried under vacuum overnight.

Hydrogenation of polymer P8

Hydrogenation of P8 was realized using *p*-toluenesulfonyl hydrazide, and the degree of hydrogenation can be tuned by simply changing the feed ratio of TSH and P8 as well as the reaction time. The procedure for P8-H100 (100% hydrogenation) is given as follows. Polymer P8 (1.00 g, 2.45 mmol), TSH (0.91 g, 4.9 mmol) and TEA (0.8 mL, 5.9 mmol) were dissolved together in 7.0 mL dry toluene in a 25 mL round bottle flask connected with a condenser. After purging N_2 for 20 mins, the flask was placed in an oil bath preheated at 115 °C and stirred for 2 hours. Release of bubbles was observed during the reaction as nitrogen gas was formed after the decomposition of TSH. The solution was cooled down to room temperature when no more bubbles were generated, and precipitated from cold methanol to yield the hydrogenated polymer product P8-H100.

49

3.4 Results and discussion

Amidation between amino alcohols with triglycerides

Fatty acid ethanolamides are important oleochemicals from plant and animal oils for a broad spectrum of applications, such as sulfosuccinate surfactants, lubricants and cosmetics.[19] With the presence of a mono-hydroxyl functional group, a methacrylate monomer was prepared from high oleic soybean oil (HOSO) derived fatty ethanolamides, and further polymerized by free radical polymerization. The polymer turned out to be brittle with T_g = 46 °C. By replacing ethanolamine (D1, Scheme 3.1) with propanol amine (D2, Scheme 3.1), a polymer with T_g = 30 °C was prepared to obtain a flexible polymer. In contrast, when *N*-methyl ethanolamine (C1, Scheme 3.1) was used, a rubbery polymer with T_g = -6 °C was obtained.[38] These initial study proved that HOSO based polymers could be easily prepared via hydroxyl fatty amides, and their property can be controlled by selecting amino alcohols. Polymers covering a wider scope of properties can be obtained by simply varying the structure of amino alcohols.

Methodologically twenty one mono-hydroxyl amino alcohols (Scheme 3.1C) were selected to examine their amidation reactivity with high oleic soybean oil (HOSO). Using ethanolamine (D1) as a basic structure, amino alcohols were grouped into four categories: (A) substitution on the methylene next to alcohol (A1-A3: secondary alcohols); (B) substitution on the methylene next to amine (B1-B7); (C) direct substitution on the amino group (C1-C7: secondary amines); (D) change of linkages between hydroxyl (–OH) and amino (–NH$_2$) groups (D1-D4). The guiding principle is to cover all possibilities to insert structural variability of amino alcohols. The amidation reaction was carried out by mixing an amino alcohol, HOSO and catalysts (CH$_3$ONa/CH$_3$OH). In most reactions, the amino

alcohols were used in excess to the ester group in HOSO (4:3). For A3 and C7, which contain two amino groups, the amino alcohols were used as the limiting reactant (it will be completely consumed during a reaction), as compared to the ester group. No solvent was utilized, except A3, B6 and B7, where a small amount of THF was added to increase their miscibility with HOSO.

As summarized in Table 3.1, seventeen mono-hydroxyl fatty amides (SBOH-1 to SBOH-17) were obtained in nearly quantitative yields after conversion of HOSO. For amino alcohols in group A, full conversions of HOSO were achieved using 2° alcohols A1 and A2 with methyl and phenyl substitutions, irrespective of steric effects. When A3 was used, both primary amines were converted to secondary amide groups in the presence of excess HOSO. Two fatty chains were incorporated into one molecule of A3 to yield SBOH-3, which was recrystallized from methanol with a yield of 53%.

For amino alcohols in the second group (B1-B7), all amidation reactions also ended with a quantitative conversion of HOSO. However, higher temperatures (70-90 ^{o}C) and a longer reaction time were necessary for those with larger substitutions (di-methyl, isopropyl, propyl, phenyl, benzyl for B3-B7), indicating there is a steric effect. Products from B1-B6 (SBOH-4 to SBOH-9) were purified by washing with brine solution, while SBOH-10 from B7 was purified by washing with dilute HCl solution, as the excess B7 was relatively more hydrophobic and could not be removed by simple aqueous washing.

The amino alcohols with 2° amines (C1-C7) exhibited distinctly different efficiency in the amidation reaction with HOSO. With linear alkyl substituents (methyl, ethyl, butyl in C1-C3), quantitative conversion of HOSO was achieved at 60 ^{o}C within hours. The amidation of C1 was finished in less than 1 hour, while it took about 4 hours for C2 and

C3. When larger substitutions (isopropyl, benzyl, phenyl in C4-C6) were present, a high

conversion could not be reached even after the temperature was increased to 115 ºC, with

a longer reaction time and excess amino alcohols. As proposed in Scheme 3.1B, the

Table 3.1 Results of amidation reactions between amino alcohols and HOSO.

Product	Structure	Amino alcohol	Temp.	Time	Yield	Appearance
SBOH-1		A1	65 ºC	6 h	95%	Liquid
SBOH-2		A2	80 ºC	3 h	98%	Solid
SBOH-3		A3	60 ºC	10 h	53%	Solid
SBOH-4		B1	60 ºC	2 h	96%	Waxy
SBOH-5		B2	60 ºC	2 h	96%	Liquid
SBOH-6		B3	70 ºC	6 h	96%	Waxy
SBOH-7		B4	80 ºC	9 h	96%	Liquid
SBOH-8		B5	90 ºC	12 h	95%	Waxy
SBOH-9		B6	80 ºC	4 h	97%	Solid
SBOH-10		B7	80 ºC	4 h	96%	Liquid
SBOH-11		C1	60 ºC	1 h	97%	Liquid
SBOH-12		C2	60 ºC	4 h	97%	Liquid
SBOH-13		C3	60 ºC	4 h	97%	Liquid
SBOH-14		D1	60 ºC	3 h	95%	Solid
SBOH-15		D2	60 ºC	3 h	95%	Solid
SBOH-16		D3	115 ºC	72 h	97%	Solid
SBOH-17		D4	80 ºC	24 h	94%	Solid

الم ـنارة للاستشارات

www.manaraa.com

amidation process follows consecutive transesterification and O-N intramolecular acyl migration.[42-43] It involves a cyclic intermediate by nucleophilic addition of amino group on the carbonyl group. The formation of such intermediate would be influenced by both the electronic effect and steric effect. *N*-methyl ethanolamine gave the fastest conversion of HOSO in less than 1 hour at 60 °C, probably due to the stabilization of the methyl group on the quaternary ammonium. Ethyl and butyl groups on N (C2 & C3) increased the steric hindrance and slowed down the intermediate formation (Table 3.1). Larger groups (in C4-C6) made it even more difficult. For C7, the primary amine would be more nucleophilic to participate the formation of cyclic intermediate. However, thermodynamically, it is less favorable to form an eight-member ring. Thus the steric effect on amino alcohols with 2° amines plays a more important role in the amidation process.

The influence of linkage between –OH and –NH$_2$ was evaluated with D1-D4. For –CH$_2$CH$_2$– and –CH$_2$CH$_2$CH$_2$– as linkers (in D1 & D2), quantitative conversion of HOSO was achieved at 60 °C in three hours. When 5-amino-1-pentanol (D3) was used, a high conversion was reached only after 72 hours at a much higher temperature (115 °C). As described above, the formation of an intermediate with either five or six member ring (via D1 and D2) was preferred. An eight-member ring intermediate via D3 would be less energetically favored. However, when the carbon in the middle of the five carbon linkage was replaced by oxygen (D4), nearly quantitative conversion was achieved after 24 hours at 80 °C. ^{1}H NMR spectra of representative products from each amino alcohol groups (A-D) with clear assignments are given in Figure 3.1.
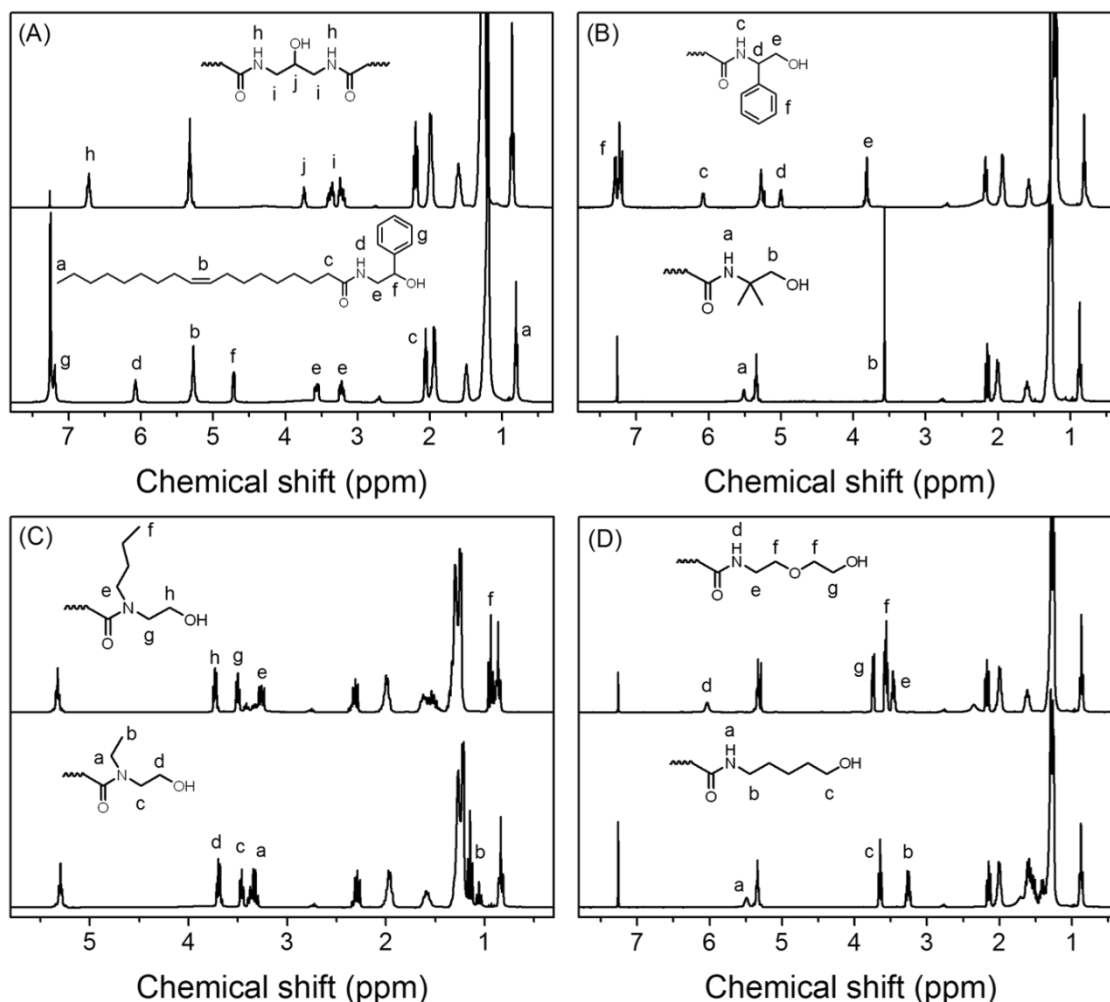
Figure 3.1 ^{1}H NMR spectra of representative products after amidation between amino alcohol and HOSO: (A) SBOH-2 & SBOH-3, (B) SBOH-5 & SBOH-9, (C) SBOH-12 & SBOH-13, and (D) SBOH-16 & SBOH-17.

Synthesis and free radical polymerization of monomers

After elucidating the amidation behavior of amino alcohols with HOSO, (meth)acrylation of mono-hydroxyl fatty amides (SBOHs) was carried out. Methacrylation of thirteen selected SBOHs was carried out by reacting them with methacrylic anhydride catalyzed via DMAP.[44] Methacrylate monomers (M1-M13) were obtained by washing with aqueous solution of NaHCO$_3$. Three acrylate monomers (M14-M16) were prepared by reacting mono-hydroxyl fatty tertiary amides (SBOH-11, SBOH-12, SBOH-13) with

54

acryloyl chloride. Table 3.2 presents the monomer structures with reference to their SBOH precursors. For methacrylate monomers (M1-M13), ^{1}H NMR spectra indicated the complete disappearance of the –CH_2OH protons, with new peaks appearing at 5.5 ppm and 6.1 ppm from the CH_2=CCH_3– group together with the methyl protons (CH$_2$=CCH_3–) at 1.9 ppm. Three peaks at 5.7 ppm, 6.0 ppm, 6.4 ppm were found for the acrylate monomers (M14-M16). All the monomers presents these characteristic peaks and two representatives were given in Figure 3.2. It is worthy to mention that monomer M4, prepared from the fatty amides containing two fatty chains (SBOH-3), was a waxy product, while all other monomers were liquid at room temperature.

Free radical polymerization was carried out for all monomers (M1-M16). Methacrylate monomers were initiated by AIBN at 70 ^{o}C - 80 ^{o}C, while acrylate monomers were initiated by BPO at 100 ^{o}C. The use of different initiators was only due to the difference in reactivity of methacrylates and acrylates. Polymerization conditions are given in Table 3.3, detailing the amount of monomer, initiator, solvent and polymerization time. Representative ^{1}H NMR spectra of polymers are given and paired with each precursor monomer (Figure 3.2). In addition, Table 3.2 presents molecular weight information from GPC and glass transition temperatures (T_gs) from DSC. Polymers (P1-P10) prepared from monomers containing secondary amide exhibited T_gs in the range of 20 ^{o}C - 61 ^{o}C. Among them, polymer P3 shows the highest T_g due to the phenyl substitution (-CHPhOOC-). The bulky phenyl group is close to the backbone and could greatly reduce the mobility of polymer chain. With other substitutions, T_gs of polymers fell in the range of 45 ^{o}C - 55 ^{o}C (Figure 3.2C). After increasing the linkage to five methylene carbons, the polymer (P9) showed T_g of 55 ^{o}C, while with an O atom in the middle of the five carbon linkage it

reduced T_g to 20 °C (P10). It is believed that hydrogen bonding between secondary amides in the side chains played a crucial role in determining higher T_gs.[45-47]

In contrast to polymers with secondary amide groups (P1-P10), polymers with tertiary amides (P11-P16) showed T_gs below 0 °C. When the substitutions on the N atom increased from methyl to ethyl to butyl in methacrylate polymers P11-P13, the reduction of T_gs from -6 °C to -29 °C was observed (Figure 3.2D). Even lower T_gs were observed for acrylate polymers (P14-P16). The lowest T_g (-51 °C) was found with P16, which has an acrylate backbone and a butyl substitution on the N atom.
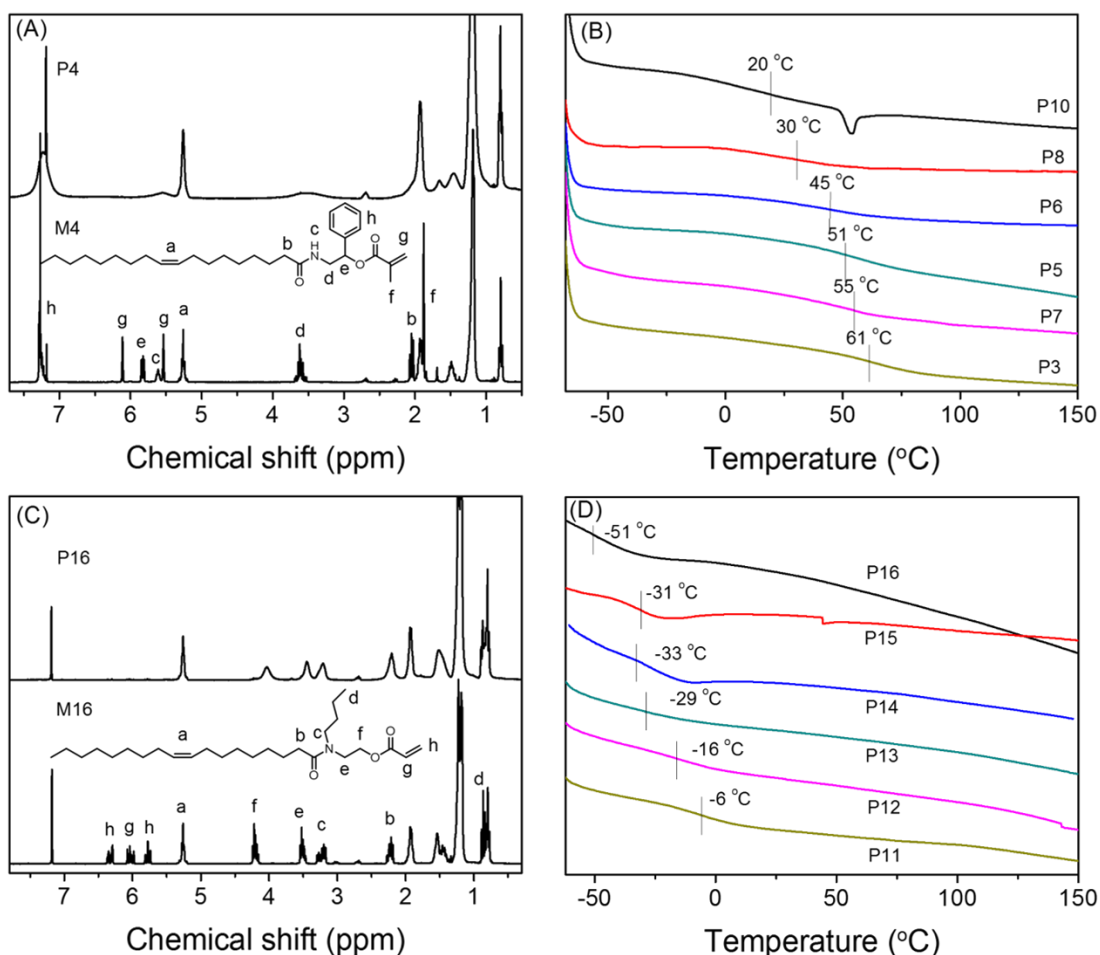
Figure 3.2 Representative ^{1}H NMR spectra of (A) P3 vs. M3 and (C) P16 vs. M16; representative DSC curves of polymers: (B) T_g above 0 °C and (D) T_g below 0 °C.

56

Overall, these polymers have T_gs in the range of ~ -50 °C and ~ 60 °C (Figure 3.3), a substantial difference over 100 °C depending on the backbone, substitution and hydrogen bonding. The wide range of T_gs could allow these polymers to be used for various applications.
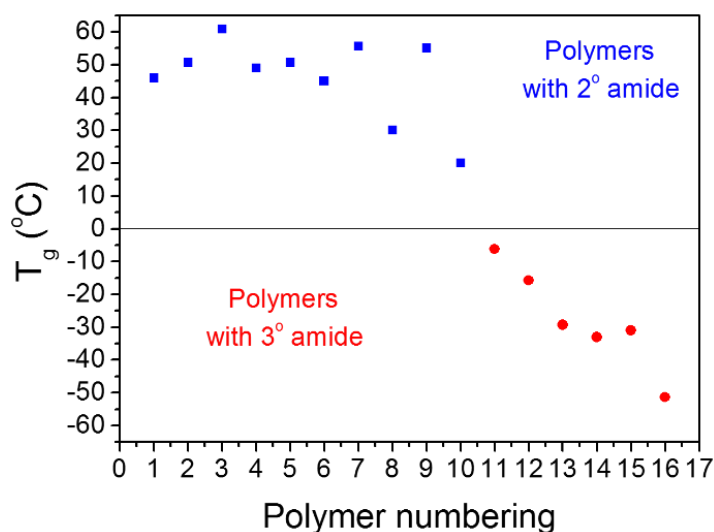
Figure 3.3 Glass transition temperature distribution of polymers from soybean oil.

Mechanical properties of higher T_g polymers.

While most side-chain fatty-containing polymers reported in literature have very low T_gs, many of our polymers with secondary amide groups have T_gs above 20 °C, which could allow them to be used as thermoplastic materials. Thus their mechanical properties were evaluated. P1-P10 were respectively dissolved in THF, and then polymer films were prepared by casting the solutions in Teflon molds after complete removal of solvent. As summarized in Table 3.2, it is easy to get free standing flexible films from P4, P8 and P10, while other polymers are brittle (cannot be removed from the mold without breaking).Tensile tests were carried out with dog-bone shaped specimens. Stress-strain curves of representative polymer samples P4, P8 and P10 are presented in Figure 3.4. These films exhibited plastic properties with characteristic yield points at 0.9±0.1 MPa for P10,

57

2.1±0.1 MPa for P4, and 3.1±0.1 MPa for P8. P8 exhibited the highest yield strength, probably due to the stronger hydrogen bonding between polymers chains. Strain-at-break was found to be 400±20 % for P10, 110±10 % for P4, and 140±20 % for P8. P10 showed the highest extensibility due to the flexible linkage between the ester and amide groups.

Table 3.2 Monomer structures and polymer properties after free radical polymerization.

Polymer	Monomer structure	Precursor	M_n (g/mol)[a]	Đ[a]	T_g (°C)[b]	Film
P1	M1	SBOH-14	15,300	1.5	46.0	Brittle
P2	M2	SBOH-1	49,800	2.4	50.7	Brittle
P3	M3	SBOH-2	32,700	1.7	60.8	Brittle
P4	M4	SBOH-3	203,000	2.2	49.0	Flexible
P5	M5	SBOH-4	55,000	2.2	50.7	Brittle
P6	M6	SBOH-5	45,700	2.0	45.0	Brittle
P7	M7	SBOH-6	56,000	2.2	55.6	Brittle
P8	M8	SBOH-15	60,600	2.2	30.0	Flexible
P9	M9	SBOH-16	32,300	1.7	55.0	Brittle
P10	M10	SBOH-17	33,000	1.9	20.0	Flexible
P11	M11	SBOH-11	63,000	1.8	-6.2	Sticky
P12	M12	SBOH-12	31,600	1.7	-15.7	Sticky
P13	M13	SBOH-13	25,200	1.7	-29.3	Sticky
P14	M14	SBOH-11	19,300	2.0	-33.0	Sticky
P15	M15	SBOH-12	19,900	1.9	-31.0	Sticky
P16	M16	SBOH-13	14,000	1.7	-51.3	Sticky

a. The molecular weight (M_n) and molecular weight distribution (Đ) were determined via GPC.
b. The glass transition temperatures of polymers were determined by DSC.

58

Table 3.3 Polymerization parameters of M1-M16.

Monomer	Monomer amount	Toluene (mL)	Initiator Amount [a]	Temperature (^{o}C)	Time (h)
M1	3.14 g (8.0 mmol)	3.6	13.2 mg (0.08 mmol)	80	12
M2	3.0 g (7.4 mmol)	6.0	12.0 mg (0.074 mmol)	75	4.5
M3	2.0 g (4.3 mmol)	4.0	10.0 mg (0.061 mmol)	75	6
M4	4.0 g (5.8 mmol)	12.0	13.0 mg (0.079 mmol)	70	2
M5	2.0 g (4.9 mmol)	5.0	10.0 mg (0.061 mmol)	75	5.5
M6	2.3 g (5.4 mmol)	5.0	10.0 mg (0.061 mmol)	75	5.5
M7	2.0 g (4.8 mmol)	4.0	8.0 mg (0.052 mmol)	80	5.5
M8	3.26 (8 mmol)	3.6	13.2 mg (0.08 mmol)	80	12
M9	2.4 g (5.5 mmol)	6.0	7.4 mg (0.048 mmol)	80	2.5
M10	4.4 g (10 mmol)	6.0	16.4 mg (0.1 mmol)	80	3.5
M11	5.0 g (12 mmol)	9.0	20 mg (0.12 mmol)	80	20.0
M12	2.0 g (4.7 mmol)	4.0	10 mg (0.061 mmol)	75	6
M13	2.0 g (4.4 mmol)	4.0	10 mg (0.061 mmol)	75	6
M14	2.0 g (5.1 mmol)	2.0	10 mg (0.041 mmol)	100	7
M15	2.0 g (4.9 mmol)	2.0	10 mg (0.041 mmol)	100	7
M16	2.2 g (5.1 mmol)	2.2	10 mg (0.041 mmol)	100	7

[a] For entries 1-13, the initiator is azobisisobutyronitrile (AIBN). For entries 14-16, the initiator is benzoyl peroxide (BPO).
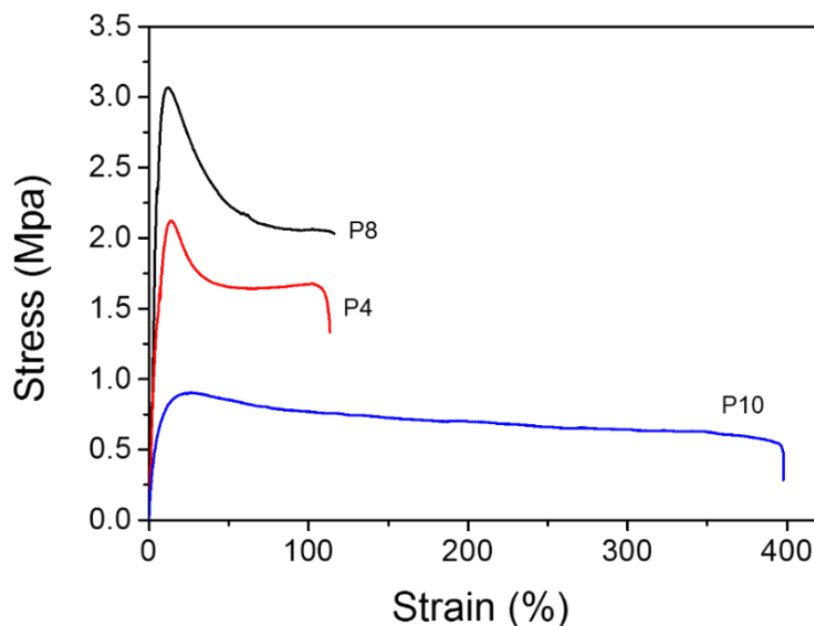
Figure 3.4 Tensile stress-strain curves of P4, P8, and P10.

Proof-of-concept hydrogenation of polymers

The presence of unsaturated double bonds on the fatty side chains of polymers provides opportunities for post-polymerization modification. A handful of chemical strategies are available for modifying the double bonds, such as epoxidation,[48-49] hydroformylation,[50] acrylation and hydrogenation.[51-53] We attempted to hydrogenate these double bonds and evaluated change of mechanical behaviors. Polymer P8 was chosen for a proof-of-concept study. Hydrogenation was carried out by *p*-toluenesulfonyl hydrazide (TSH, Scheme 3.2) in the presence of triethylamine. The reaction was refluxed in toluene at 115 °C.[53] By adjusting the reaction time and the feed ratio of TSH and double bond, the level of hydrogenation could be controlled. The degree of hydrogenation was calculated by ^{1}H NMR, using the methylene protons (–CH_2OOC–) next to the ester group as a reference (Figure 3.5A). The ester groups and amide groups remained stable during the hydrogenation process. Six samples with precisely controlled hydrogenation (12%, 30%, 40%, 56%, 83%, 100%) were prepared. The hydrogenated samples were labeled as P8-

60

HX, in which H indicates hydrogenation, and X represents the percentage of hydrogenation. The overall decrease of molecular weight with hydrogenation indicated the nature of polymer chain flexibility. The more hydrogenated, the more coiled the chain. Thus highly hydrogenated polymers (e.g. P8-H83 and P8-H100) should exhibit a lower hydrodynamic volume in THF, as confirmed from GPC characterization (Figure 3.5B).

DSC curve of fully hydrogenated polymer P8-H100 shows two melting points at 51 ^oC and 134 ^oC. The melting peak at 51 ^oC (T_m1) was much stronger than the one at 134 ^oC (T_m2) (Figure 3.5C). In a control study, fully hydrogenated polymer P11, which does not contain hydrogen bonding, gave only one melting point at 25 ^oC. This control study indicated that the melting point in the low temperature region (51 ^oC) of P8-H100 originated from the hydrogenated alkyl side chain, and the melting point at a higher temperature region (134 ^oC) might be due to the hydrogen bonding.

Scheme 3.2 Hydrogenation of polymer P8.
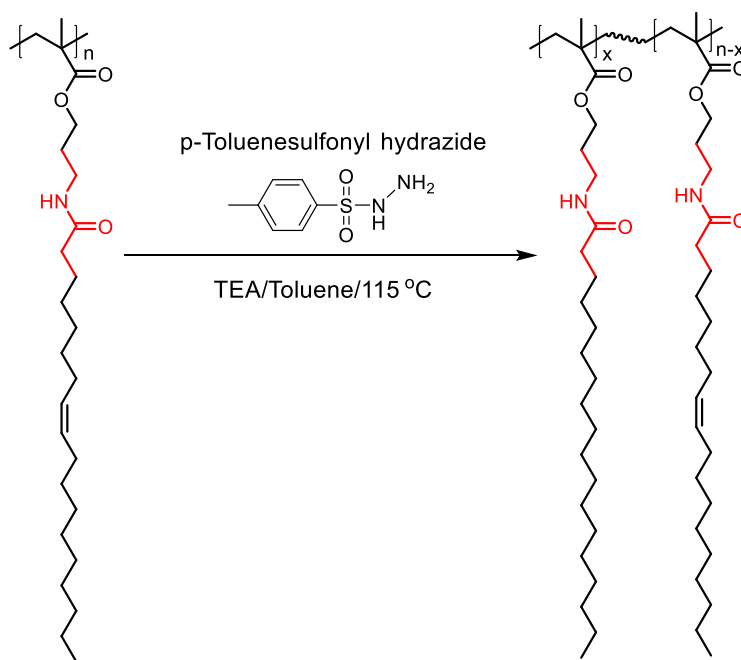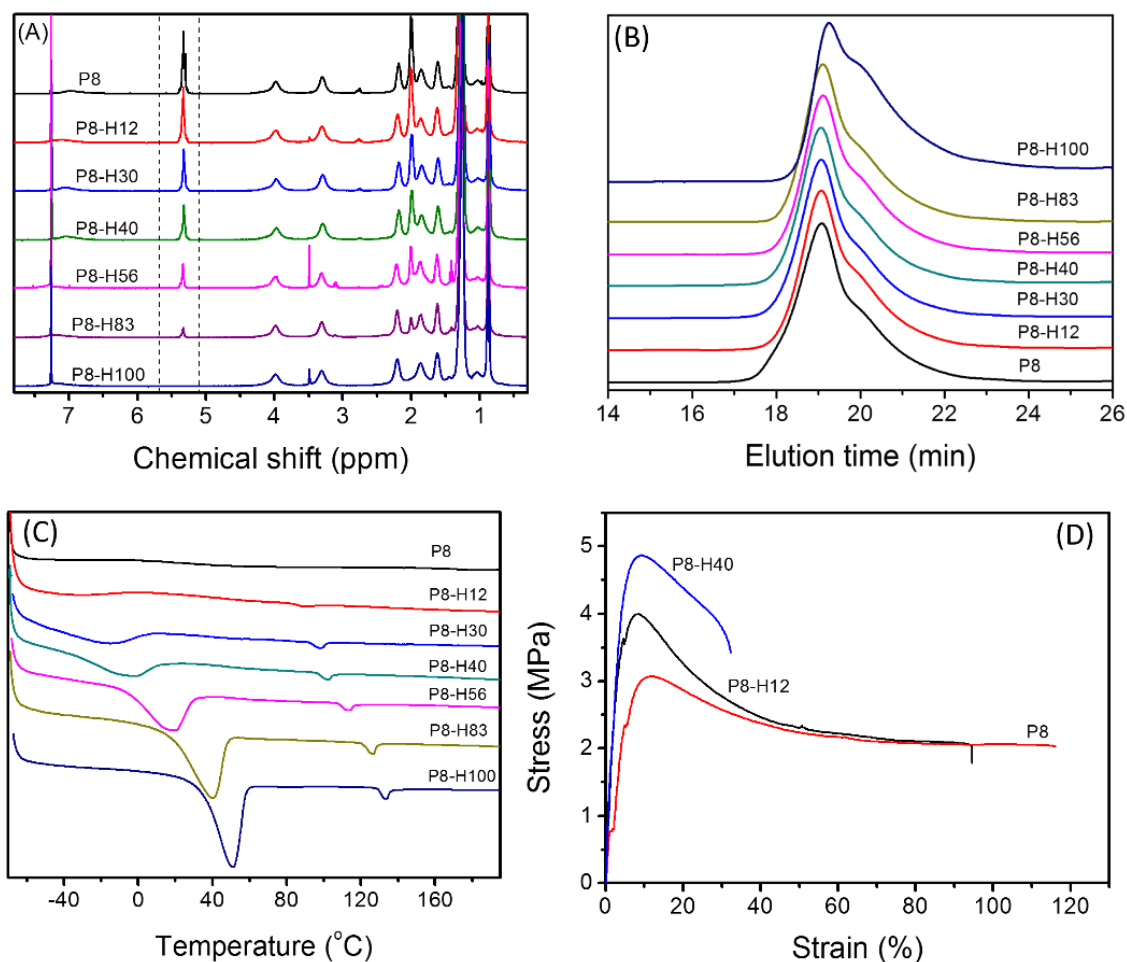
Figure 3.5 (A) ^{1}H NMR spectra and (B) DSC curves of hydrogenated P8 with various degree of hydrogenation; (C) Stress-strain curves of P8, P8-H12, and P8-H40.

Crystallization is common for polymers with repetitive saturated fatty chains.[54-55] As shown in Figure 3.5C, these melting points (T_m1 & T_m2) were present even with 12% hydrogenation and increased gradually with higher hydrogenation. At the same time, T_g of the hydrogenated polymers increased from 30 ^{o}C (P8) to 52°C (P8-H56), and could not be detected in polymers with an even higher degree of hydrogenation. These results suggested that hydrogenation in the side chain would induce the crystallization from both the side chain and the hydrogen bonding segments.

Crystallization after hydrogenation could be interpreted as increased polymer chain interactions, which might impact the mechanical properties. Unlike the tough crystalline

plastic polyethylene (PE), the polymers become increasingly more brittle with higher hydrogenation degree. No free standing films could be made with hydrogenation degree higher than 60%. Absence of chain entanglements from the comb-like polymers could be the reason for the brittleness.[41] As indicated in Figure 3.5D, the hydrogenated samples give increasing tensile strength from 3.1±0.1 MPa (P8) to 4.0±0.2 MPa (P8-H12) and 4.9±0.2 MPa (P8-H40), and a sacrifice of tensile strain was observed.

3.5 Conclusions

Amidation of soybean oils with mono-hydroxyl amino alcohols was systematically examined over the structural factors of amino alcohols, such as alcohol substitutions, linkers and amino substitutions. Those with primary amino groups could unexceptionally lead to quantitative conversion with reactivity influenced by the alcohol substitution and linkers. Small substitution on the N atom (methyl, ethyl, butyl) did not change the reactivity greatly, while larger groups (isopropyl, benzyl, phenyl, ethyl amine) inserted significant steric effect and resulted in lower conversion. (Meth)acrylate monomers were prepared from the obtained fatty amide alcohols and polymerized by free radical polymerization. Depending on the monomer structures, sixteen polymers with T_gs between -51 ^{o}C and 61 ^{o}C were obtained, showing properties from tacky to thermoplastic materials. Proof-of-concept hydrogenation of of soybean oil-derived polymers influenced the physical properties, such as glass transition temperature, crystallization and mechanical properties.

3.6 References

(1) Mecking, S. *Angewandte Chemie International Edition* **2004,** *43*, 1078-1085.

(2) Meier, M. A.; Metzger, J. O.; Schubert, U. S. *Chemical Society Reviews* **2007,** *36*, 1788-1802.

(3) Gandini, A. *Macromolecules* **2008,** *41*, 9491-9504.

(4) Coates, G. W.; Hillmyer, M. A. *Macromolecules* **2009,** *42*, 7987-7989.

(5) Biermann, U.; Bornscheuer, U.; Meier, M. A.; Metzger, J. O.; Schäfer, H. J. *Angewandte Chemie International Edition* **2011,** *50*, 3854-3871.

(6) Hillmyer, M. A.; Tolman, W. B. *Accounts of Chemical Research* **2014,** *47*, 2390-2396.

(7) Wilbon, P. A.; Chu, F.; Tang, C. *Macromolecular rapid communications* **2013,** *34*, 8-37.

(8) Thakur, V. K.; Thakur, M. K.; Raghavan, P.; Kessler, M. R. *ACS Sustainable Chemistry & Engineering* **2014,** *2*, 1072-1092.

(9) Yao, K.; Tang, C. *Macromolecules* **2013,** *46*, 1689-1712.

(10) Miller, S. A. *ACS Macro Letters* **2013,** *2*, 550-554.

(11) Xiong, M.; Schneiderman, D. K.; Bates, F. S.; Hillmyer, M. A.; Zhang, K. *Proceedings of the National Academy of Sciences* **2014,** *111*, 8357-8362.

(12) Liu, X.; Xin, W.; Zhang, J. *Green Chemistry* **2009,** *11*, 1018-1025.

(13) Chung, Y.-L.; Olsson, J. V.; Li, R. J.; Frank, C. W.; Waymouth, R. M.; Billington, S. L.; Sattely, E. S. *ACS Sustainable Chemistry & Engineering* **2013,** *1*, 1231-1238.

(14) Zheng, Y.; Yao, K.; Lee, J.; Chandler, D.; Wang, J.; Wang, C.; Chu, F.; Tang, C. *Macromolecules* **2010,** *43*, 5922-5924.

(15) Liu, Y.; Yao, K.; Chen, X.; Wang, J.; Wang, Z.; Ploehn, H. J.; Wang, C.; Chu, F.; Tang, C. *Polymer Chemistry* **2014,** *5*, 3170-3181.

(16) Yu, J.; Liu, Y.; Liu, X.; Wang, C.; Wang, J.; Chu, F.; Tang, C. *Green Chemistry* **2014,** *16*, 1854-1864.

(17) Carlsson, A. S. *Biochimie* **2009,** *91*, 665-670.

(18) Meher, L.; Sagar, D. V.; Naik, S. *Renewable and sustainable energy reviews* **2006,** *10*, 248-268.

(19) Kamalakar, K.; Satyavani, T.; Mohini, Y.; Prasad, R. N.; Karuna, M. L. *J Surfact Deterg* **2014,** *17*, 637-645.

(20) Khot, S. N.; Lascala, J. J.; Can, E.; Morye, S. S.; Williams, G. I.; Palmese, G. R.; Kusefoglu, S. H.; Wool, R. P. *Journal of Applied Polymer Science* **2001,** *82*, 703-723.

(21) Xia, Y.; Larock, R. C. *Green Chemistry* **2010,** *12*, 1893-1909.

(22) Wang, Z.; Zhang, X.; Wang, R.; Kang, H.; Qiao, B.; Ma, J.; Zhang, L.; Wang, H. *Macromolecules* **2012,** *45*, 9010-9019.

(23) Hong, J.; Luo, Q.; Wan, X.; Petrović, Z. S.; Shah, B. K. *Biomacromolecules* **2012,** *13*, 261-266.

(24) Lligadas, G.; Ronda, J. C.; Galia, M.; Cádiz, V. *Biomacromolecules* **2010,** *11*, 2825-2835.

(25) Raquez, J.-M.; Deléglise, M.; Lacrampe, M.-F.; Krawczak, P. *Progress in Polymer Science* **2010,** *35*, 487-509.

(26) Türünç, O.; Billiet, S.; De Bruycker, K.; Ouardad, S.; Winne, J.; Du Prez, F. E. *European Polymer Journal* **2015,** *65*, 286-297.

(27) Türünç, O.; Meier, M. A. *European Journal of Lipid Science and Technology* **2013,** *115*, 41-54.

(28) Pan, X.; Sengupta, P.; Webster, D. C. *Biomacromolecules* **2011,** *12*, 2416-2428.

(29) Lu, Y.; Larock, R. C. *Biomacromolecules* **2008,** *9*, 3332-3340.

(30) Eren, T.; Küsefoğlu, S. H. *Journal of applied polymer science* **2004,** *91*, 4037-4046.

(31) Alam, S.; Chisholm, B. J. *Journal of coatings technology and research* **2011,** *8*, 671-683.

(32) Maiti, B.; Kumar, S.; De, P. *RSC Advances* **2014,** *4*, 56415-56423.

(33) Hoogenboom, R.; Schubert, U. S. *Green Chemistry* **2006,** *8*, 895-899.

(34) Huang, H.; Hoogenboom, R.; Leenen, M. A.; Guillet, P.; Jonas, A. M.; Schubert, U. S.; Gohy, J.-F. *Journal of the American Chemical Society* **2006,** *128*, 3784-3788.

(35) Alam, S.; Kalita, H.; Kudina, O.; Popadyuk, A.; Chisholm, B. J.; Voronov, A. *ACS Sustainable Chemistry & Engineering* **2012,** *1*, 19-22.

(36) Chernykh, A.; Alam, S.; Jayasooriya, A.; Bahr, J.; Chisholm, B. J. *Green Chemistry* **2013,** *15*, 1834-1838.

(37) Tarnavchyk, I.; Popadyuk, A.; Popadyuk, N.; Voronov, A. *ACS Sustainable Chemistry & Engineering* **2015,** *3*, 1618-1622.

(38) Yuan, L.; Wang, Z.; Trenor, N. M.; Tang, C. *Macromolecules* **2015,** *48*, 1320-1328.

(39) Wang, S.; Vajjala Kesava, S.; Gomez, E. D.; Robertson, M. L. *Macromolecules* **2013,** *46*, 7202-7212.

(40) Wang, S.; Robertson, M. L. *ACS Applied Materials & Interfaces* **2015,** *7*, 12109-12118.

(41) Wang, Z.; Yuan, L.; Trenor, N. M.; Vlaminck, L.; Billiet, S.; Sarkar, A.; Du Prez, F. E.; Stefik, M.; Tang, C. *Green Chemistry* **2015,** *17*, 3806-3818.

(42) Sohma, Y.; Sasaki, M.; Hayashi, Y.; Kimura, T.; Kiso, Y. *Chemical communications* **2004**, 124-125.

(43) Skwarczynski, M.; Sohma, Y.; Kimura, M.; Hayashi, Y.; Kimura, T.; Kiso, Y. *Bioorganic & medicinal chemistry letters* **2003,** *13*, 4441-4444.

(44) Sakakura, A.; Kawajiri, K.; Ohkubo, T.; Kosugi, Y.; Ishihara, K. *Journal of the American Chemical Society* **2007,** *129*, 14775-14779.

(45) Chen, Y.; Kushner, A. M.; Williams, G. A.; Guan, Z. *Nature chemistry* **2012,** *4*, 467-472.

(46) Chen, Y.; Guan, Z. *Chemical Communications* **2014,** *50*, 10868-10870.

(47) Neal, J. A.; Mozhdehi, D.; Guan, Z. *Journal of the American Chemical Society* **2015,** *137*, 4846-4850.

(48) Mungroo, R.; Pradhan, N. C.; Goud, V. V.; Dalai, A. K. *Journal of the American Oil Chemists' Society* **2008,** *85*, 887-896.

(49) Tehfe, M.-A.; Lalevée, J.; Gigmes, D.; Fouassier, J. P. *Macromolecules* **2010,** *43*, 1364-1370.

(50) Frankel, E.; Pryde, E. *Journal of the American Oil Chemists' Society* **1977,** *54*, A873-A881.

(51) Zhang, P.; Xin, J.; Zhang, J. *ACS Sustainable Chemistry & Engineering* **2013,** *2*, 181-187.

(52) Zhao, M.-L.; Tang, L.; Zhu, X.-M.; Hu, J.-N.; Li, H.-Y.; Luo, L.-P.; Lei, L.; Deng, Z.-Y. *Journal of agricultural and food chemistry* **2013,** *61*, 1189-1195.

(53) Petzetakis, N.; Stone, G. M.; Balsara, N. P. *Macromolecules* **2014,** *47*, 4151-4159.

(54) Mutlu, H.; Meier, M. A. R. *Journal of Polymer Science Part A: Polymer Chemistry* **2010,** *48*, 5899-5906.

(55) Fei, P.; Cavicchi, K. A. *ACS Applied Materials & Interfaces* **2010,** *2*, 2797-2803.

CHAPTER 4

SUSTAINABLE THERMOPLASTIC ELASTOMERS FROM SOYBEAN OIL DERIVED

MONOMERS

4.1 Abstract

Soybean oil based monomers are used as building blocks for the elastic components of thermoplastic elastomers. First, triblock copolymers via atom transfer radical polymerization (ATRP) of a soybean oil derived acrylate monomer (SBA) and subsequent chain extension to styrene were prepared. The resulting PS-*b*-PSBA-*b*-PS triblock copolymers exhibited properties from thermoplastics to thermoplastic elastomers (TPE) depending on the weight percentage of PS. The double bond from PSBA was employed for selective "click coupling" with triazolinedione (TAD) chemistry to create chemical cross-links inside the elastic phase to improve the mechanical properties. Multi-graft copolymers PSBN-g-PLA were prepared from the copolymerization of a soybean oil derived norbornene monomer (SBN) and a norbornene capped polylactide (PLA) macromonomer by ring-opening metathesis polymerization (ROMP). These polymers exhibited improved elastic properties compared to those triblock copolymers from ATRP.

4.2 Introduction

Synthetic polymers from fossil fuels have found numerous applications during the past several decades. The energy shortage and environmental concerns have directed researchers' attention to naturally renewable materials.[1-4] On one hand, efforts have been made to improve the physical properties of natural polymers by chemical modification, enzymatic treatment and by blending of natural polymers with synthetic polymers.[5-7] On the other hand, small molecular biomasses (plant oils, fatty acid, lactic acid, rosin acids, furfural, etc.) have opened new routes to renewable polymers that could replace synthetic polymers manufactured from petroleum chemicals.[8-10]

Plant oils and their derivatives have been used to prepare thermoplastics, thermoset

resins, thermoset elastomers, and nanocomposites.[11-12] Soybean oil comprises about 90% of the U.S. oil seed business, which has reached 107 million tons in 2015. Soybean oil is consisted of more than 99% triglycerides, the esters of glycerol with three fatty acids such as oleic acid, linoleic acid and linolenic acid. Methods were developed to transform the unsaturation to more reactive groups for subsequent polymerization.[13-14] Larock and coworkers prepared low saturation soybean oil as well as conjugated low saturation soybean oil for copolymerization with divinylbenzene to obtain thermosets with a wide range of properties.[15-16] The product from acrylation of epoxidized soybean oil (ESO) was employed to prepare renewable thermoset materials by free radical polymerization.[17-18] Most of these research are for thermoset materials, which could not be reprocessed after use.

Thermoplastic elastomers (TPEs) combine the elasticity from elastomers and the plasticity of plastics.[19-21] TPEs have a phase separated morphology, with hard domains dispersed in a soft and elastic matrix to form a well-defined network structure. The most studied model of TPEs is linear ABA triblock copolymer, such as poly(styrene-*b*-butadiene-*b*-styrene) (SBS) or poly(styrene-*b*-isoprene-*b*-styrene) (SIS).[22-23] Another model is multi-graft copolymer, which has an elastic polymer backbone and multi-grafted pendant rigid polymers.[24-26] Generally, the rigid phase of TPEs is composed of a high glass transition temperature (T_g) polymer and the elastic phase is composed of a low T_g polymer.

Here, we prepared copolymers with A-B-A triblock and multi-graft copolymers using soybean oil based monomers for constructing the elastic component. A soybean oil based acrylate monomer (SBA) was firstly polymerized by ATRP using a di-functional initiator and chain extended to styrene to achieve poly(styrene)-*b*-poly(soybean oil

69

acrylate)-*b*-poly(styrene) (PS-*b*-PSBA-*b*-PS). A norbornene capped polylactide (PLA) was prepared by ROP of lactide using norbornene methanol as the initiator.[27] The copolymerization of a soybean oil based norbornene monomer (SBN) and the norbornene capped PLA by ROMP was applied for making multi-graft copolymers PSBN-g-PLA. These triblock and multi-graft copolymers show phase separated morphologies and act as typical TPEs. The triblock copolymers from ATRP show low stress-at-break and strain-at-break due to the absence of chain entanglements and limited elasticity from PSBA backbone. A new click chemistry was used to selectively crosslink the soft middle block PSBA. Du Prez and coworkers developed a versatile click chemistry platform based on the reactivity of 1,2,4-triazoline-3,5-dione (TAD) with double bonds and found that the same reaction occurred very efficiently with double bonds present in plant oils.[28-29] A di-functional molecule bis-TAD was used to "click-couple" the soft middle block of triblock copolymers and achieved controllable mechanical strength improvement for the triblock copolymers.[30] The multi-graft type PSBN-g-PLA exhibited higher strain-at-break than the triblock copolymers due to the increased elasticity of PSBN compared to PSBA.

4.3 Experimental section

Materials

Soybean oil based acrylate monomer (SBA) and norbornene monomer (SBN) were prepared using methods in previous chapters. 4,4′-(1,4-Phenylene)-bis(1,2,4-triazoline-3,5-dione) (bis-TAD) was prepared according to a published procedure. Dimethylformamide (DMF), methanol, styrene, 5-norbornene-2-methanol, tin(II) 2-ethylhexanoate, Hoveyda-Grubbs catalyst 2nd generation (97%), ethyl vinyl ether, ethyl bis(2-bromoisobutyrate) (EBIB), CuBr, CuCl, tris (2-(dimethylamino)ethyl) amine

(Me$_6$TREN), and 2,2'-bipyridine (bpy) were purchased from Sigma-Aldrich and used directly. Lactide is purchased from Sigma-Aldrich, recrystallized three times from toluene and dried under vacuum before use. Toluene is refluxed with sodium-benzophenone to dry and distilled before use.

Synthesis of poly(soybean oil acrylate) (PSBA) macroinitiator by ATRP

As shown in Scheme 4.1, A-B-A triblock copolymers PS-b-PSBA-b-PS were prepared by ATRP. A typical polymerization procedure for PSBA is described as follows. EBIB (144 mg, 0.4 mmol), SBA (15.6 g, 40.0 mmol), Me$_6$TREN (92 mg, 0.4 mmol), and DMF (2 mL) were introduced to a Schlenk flask equipped with a magnetic stirring bar and degassed by three freeze-pump-thaw cycles before CuBr (57.6 mg, 0.4 mmol) was added under nitrogen. The sealed flask was immersed into an oil bath set at 90 $^{\circ}$C. After 12 h, the polymerization was stopped by opening the flask and exposing the reactive mixture to air. THF was then added to dilute the solution before passing it through an aluminum oxide column. The concentrated solution was precipitated from cold methanol to recover the polymer product PSBA, which was subsequently dried at 40 $^{\circ}$C. Polymerizations of SBA with different molar ratios to the initiator EBIB were performed in a similar way.

Synthesis of poly(styrene-b-soybean oil acrylate-styrene) triblock copolymers

Styrene was passed through an aluminum oxide column to remove inhibitors. As shown in Scheme 4.1, the triblock copolymers were prepared by chain extension of PSBA with monomer styrene. A representative chain-extension polymerization is described as follows: PSBA (1.5 g, 0.05 mmol) and bpy (31.2 mg, 0.2 mmol) were dissolved together with a mixture of styrene (1.2 ml, 10 mmol) and toluene (0.9 mL) in a 10 mL Schlenk flask. The solution was degassed by three freeze-pump-thaw cycles before CuCl (10 mg, 0.1

mmol) was added under nitrogen. The sealed flask was immersed into an oil bath of 100 ℃ and polymerized for 12 h before being stopped by opening the flask and exposing the reactive mixture to air. The THF diluted solution was passed through an aluminum oxide column, concentrated under reduced pressure, and precipitated in methanol. The resulting product was collected and dried under vacuum at 40 ℃. Chain extension polymerizations of styrene with different molar ratios to PSBA macroinitiators were performed similarly.

"Click-Coupling" of PS-b-PSBA-b-PS with bis-TAD

Bis-TAD was used to couple the PSBA block of PS-b-PSBA-b-PS due to the reaction between TAD group and the double bond. The cross-linking joints can act like pseudo-chain entanglements to increase the mechanical properties of triblock copolymers. A typical procedure is described as follows: PS-PSBA-PS (2.0 g) was completely dissolved in THF (5 ml), and then bis-TAD (68.6 mg, 2.5 mmol) was added. After bis-TAD was completely dissolved, the solution was degassed and poured into a Teflon mold. The film was completely dried by leaving in the hood for 24 h and keeping under vacuum at 40 ℃ for another 12 h to obtain "click-coupled" product.

Synthesis of norbornene capped poly(lactide) (PLA) by ring-opening polymerization

A norbornene capped PLA was prepared by ROP of lactide using norbornene methanol as the initiator (Scheme 4.2). Recrystallized lactide (1.73 g, 12 mmol), norbornene methanol (25 mg, 0.2 mmol), tin(II) 2-ethylhexanoate (48 mg, 0.12 mmol) and toluene (1.8 mL) were firstly charged into a 10 mL flame-dried Schlenk flask and degassed by three freeze-pump-thaw cycles before refilled with nitrogen. The flask was put into a preheated oil-bath at 125 ℃ to start the polymerization for 2.5 h. DCM (5.0 mL) was added to dilute the cooled product before it was precipitated into methanol to recover PLA.

72

Ring-opening metathesis polymerization copolymerization of PLA and SBN

ROMP is a highly efficient polymerization strategy for norbornene functionalized bulky monomers and macromonomers.[31-32] Full conversions of monomers were always reported. Multi-graft type copolymers were prepared from a soybean oil based norbornene monomer (SBN) and the norbornene capped PLA (Scheme 4.2). The weight ratio between them can be tuned easily through their feeding ratios. For making a copolymer with 30 wt% of PLA, SBN (0.5 g, 1.0 mmol) and PLA (0.21 g, 0.03 mmol) were dissolved together in a 25 mL round-bottomed flask with DCM (12 mL) and purged with N_2 for 10 mins. In a separate flask, a stock solution of 5.8 mg H-G 2nd catalyst was dissolved in 2.2 mL nitrogen-purged DCM and protected under N_2. A portion of the stock solution (0.5 mL, 1.3 mg catalyst, 0.002 mmol) was added directly into the monomer solution under fast stirring. After 30 min, the polymerization was terminated by adding 0.2 mL of ethyl vinyl ether and stirred for another 20 min. The polymer product was precipitated from cold methanol to yield the final product.

Characterization

^{1}H NMR spectra of the synthesized polymers were recorded on a Bruker AVANCE 300 spectrometer in solutions of CDCl$_3$ with tetramethylsilane (TMS) as the internal standard. Molecular weights and molecular weight distributions of polymer products were determined on a Waters system equipped with a 515 HPLC pump, a 2410 refractive index detector, and three Styragel columns (HR1, HR3, HR5 in the effective molecular weight range of 100~5,000 g/mol, 500~30,000 g/mol, and 5,000~500,000 g/mol, respectively) with HPLC grade THF as the eluent at 30 °C and a flow rate of 1.0 mL/min. Polymer solutions (3 mg/mL) in THF were filtered through microfilters with a pore size of 0.2 μm

(Nylon, Millex-HN 13 mm Syringes Filters, Millipore, USA). The columns were calibrated against polystyrene standards. DSC measurements were conducted using a TA Q2000 DSC (TA Instruments) under nitrogen atmosphere. Approximately 10 mg of each sample were used in the measurement. First, the sample was heated from room temperature to 100 °C, held at this temperature for 5 min to remove thermal history, and then cooled to −70 °C at a rate of 10 °C/min. Then the sample was heated from −70 °C to 150 °C at a heating rate of 10 °C/min. To determine the glass transition temperatures (T_g), the DSC data were analyzed using the Universal Analysis 2000 software (TA Instruments). The data were collected from the second heating scan. Dog-bone shape specimens with width of 5 mm and length of 22 mm were cut from the hot-press or solution cast films. Tensile testing was carried out with an Instron 5500 tensile tester with a 100 N load cell at a speed of 20 mm/min at room temperature to obtain stress versus strain curves. The cyclic tensile deformation was conducted stepwise to a tensile strain of 50% for the cross-linked PS-PSBA-PS. In each step, once the sample reached the appropriate tensile strain, the crosshead direction was reversed and the sample strain was decreased at the same nominal strain rate (1 mm/min) until zero stress was achieved. Once the stress was fully released, the crosshead was immediately reversed, and the sample was then extended again at the same constant strain rate until it reached 50% strain. The cyclic deformation was repeated for 5 times. For the cyclic tensile test of PLA-g-PSBN, a maximum strain is set at 200% with a nominal strain rate of 5 mm/min.

4.4 Results and Discussion

Synthesis and characterization of poly(styrene-b-soybean oil acrylate-b-styrene)

A-B-A triblock structured thermoplastic elastomers have been widely reported using biomass derived monomers to construct the elastic component which has a low T_g.[33-35]

74

From our previous study, homopolymer PSBA from the free radical polymerization of SBA has a T_g of -33 °C, making it promising to serve as the elastic component of TPEs. As shown in Scheme 4.1, triblock copolymers were prepared by ATRP with PSBA as the middle block and polystyrene as the outside rigid blocks.[36] Ethyl bis(2-bromoisobutyrate) (EBIB) was used as a difunctional initiator for the polymerization of SBA. Me$_6$TREN/CuBr complex was used as the catalyst and DMF as solvent to achieve high conversion and good control over the molecular weight distribution of PSBA. Chain extension using PSBA as the macroinitiator to styrene was achieved using bpy/CuCl as the catalyst and toluene as solvent.

Scheme 4.1 Synthesis of PSBA and PS-PSBA-PS triblock copolymers by ATRP.
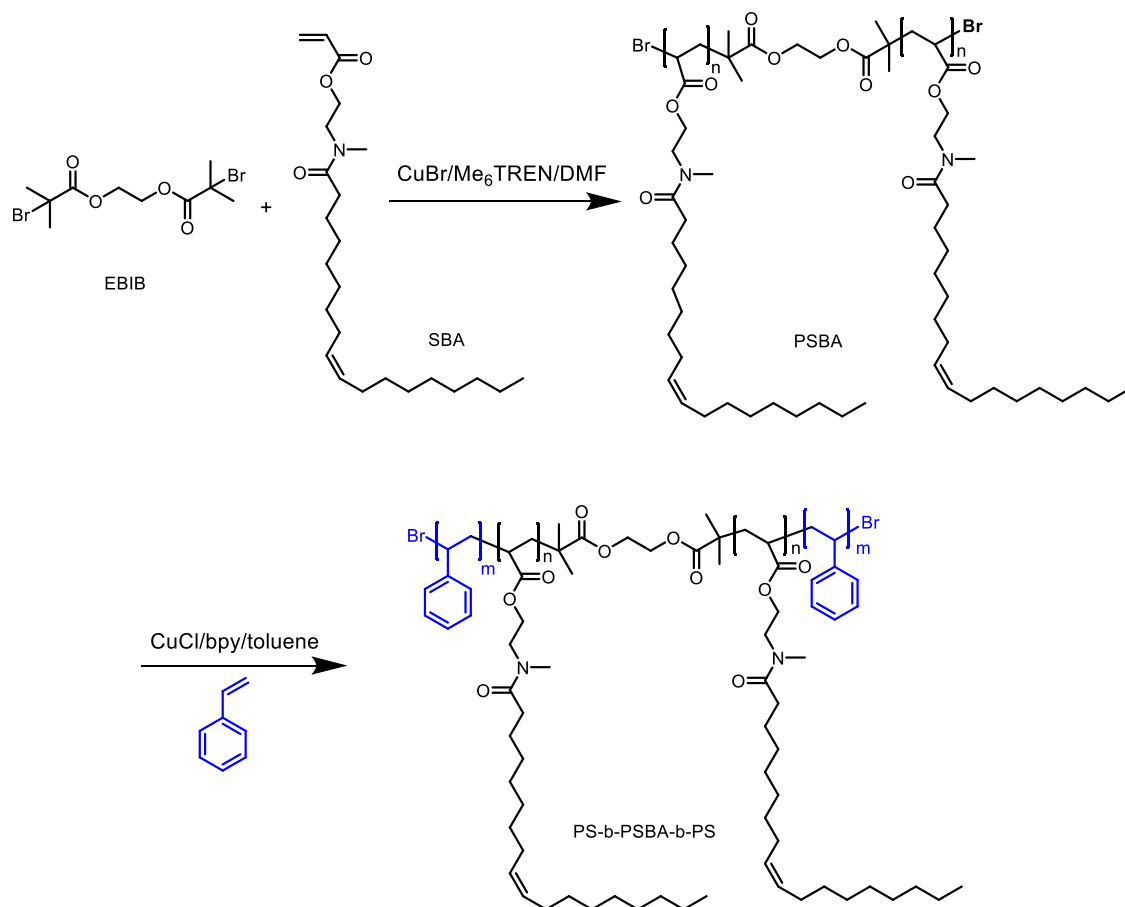
The ^{1}H NMR spectrum of PSBA is shown in Figure 4.1. The peaks at 5.33, 4.10, 3.56, 3.04, 2.26, 2.00, 1.25, and 0.84 ppm show the incorporation of SBA monomers. A small peak at 4.30 ppm indicates the presence of the functional groups of the ATRP initiator, which allows for the subsequent chain extension for obtaining triblock copolymers. New signals for the aromatic protons of polystyrene end block appeared at 6.54 and 7.06 ppm after the chain extension. The theoretical molecular weights of the synthesized polymers were calculated based on the monomer conversions and listed in Table 4.1.
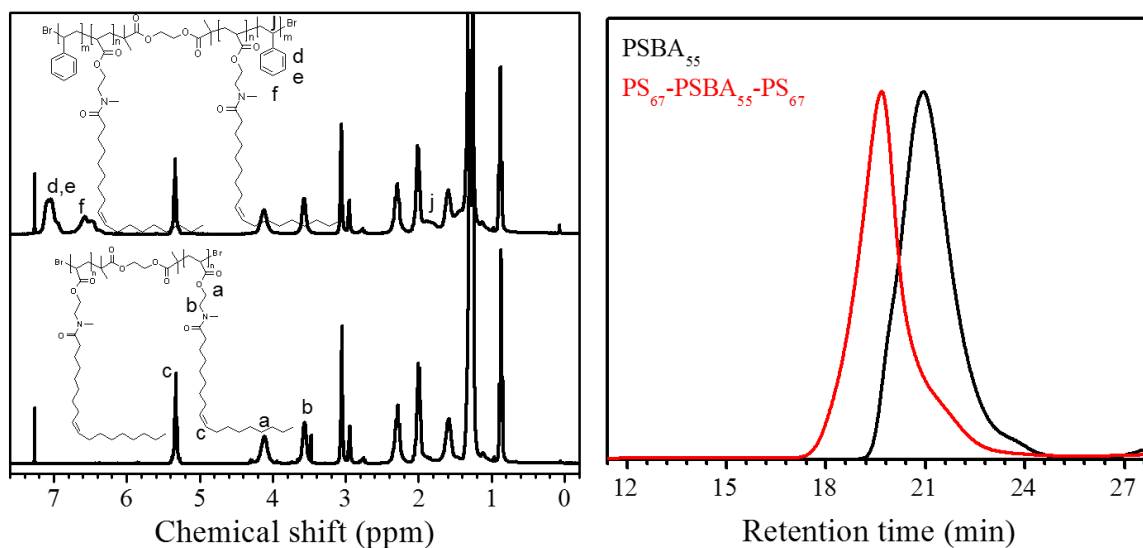
Figure 4.1 ^{1}H NMR spectra of PSBA and PS-PSBA-PS triblock copolymer (left); SEC traces for PSBA$_{55}$ and PS$_{67}$-PSBA$_{55}$-PS$_{67}$ triblock copolymers (right).

The prepared triblock copolymers were also characterized using SEC. As shown in Figure 4.1, the formation of triblock copolymers was demonstrated by a clear shift of SEC traces relative to the respective macroinitiator PSBA. The SEC trace of PS-PSBA-PS triblock copolymer was almost unimodal with a negligible shoulder on the low molecular weight side, demonstrating that the chain extension of styrene from the PSBA macroinitiator was well controlled. As listed in Table 4.1, four PS-*b*-PSBA-*b*-PS triblock

copolymers with the same PSBA middle block and different PS chain lengths were prepared by controlling the feed ratios of styrene to PSBA macroinitiator. Three PS-*b*-PSBA-*b*-PS triblock copolymers with different PSBA chain lengths and similar PS chains were also prepared by using different PSBA macroinitiators. The polymers were characterized by ^{1}H NMR, SEC, and DSC. The weight percentage of styrene (wt %), dispersity (Đ), molecular weights (M_n), and T_g of copolymers are summarized in Table 4.1.

Table 4.1 Characteristics of PS-PSBA-PS triblock copolymers.

Sample code[a]	Molar ratio[b]	Middle block		Triblock		St wt% (NMR)[d]	T_g (St, °C)[e]
		M_n[c] (g/mol)	Đ[c]	M_n[c] (g/mol)	Đ[c]		
PS$_{118}$-PSBA$_{82}$-PS$_{118}$	600:1:2:2	20,400	1.37	59,500	1.71	49.4 %	99
PS$_{102}$-PSBA$_{82}$-PS$_{102}$	400:1:2:2	20,400	1.37	46,000	1.72	40.1%	98
PS$_{70}$-PSBA$_{82}$-PS$_{70}$	300:1:2:2	20,400	1.37	41,200	1.53	32.5 %	86
PS$_{49}$-PSBA$_{82}$-PS$_{49}$	200:1:2:2	20,400	1.37	34,300	1.63	27.4 %	67
PS$_{67}$-PSBA$_{55}$-PS$_{67}$	300:1:2:2	16,500	1.32	35,200	1.78	37.3 %	-
PS$_{65}$-PSBA$_{104}$-PS$_{65}$	300:1:2:2	30,300	1.38	73,300	1.65	24.6 %	-

[a]Sample codes are defined as follows: the numbers behind "PS" and "PSBA" represent the degree of polymerization. [b]Molar ratio: St/PSBA/CuCl/bpy. [c]Measured by SEC. [d]The St weight percentage were calculated from ^{1}H NMR spectroscopy. [e]Measured by DSC.

Microphase separation and mechanical behavior

The microphase separation behavior of triblock copolymers were studied by DSC. DSC heat flow curves for PS-*b*-PSBA-*b*-PS triblock copolymers displayed two distinct T_gs, implying a two-phase morphology (Figure 4.2). The T_g values of PSBA phase varied from -26 °C to -21 °C, which were slightly higher than that of the homopolymer, presumably due to the grafting of rigid polystyrene to the chain ends. In contrast, the T_g values of the

polystyrene phase decreased from 100 °C to 67 °C with the increase of PSBA. These results

suggest partial phase mixing between PSBA and PS.
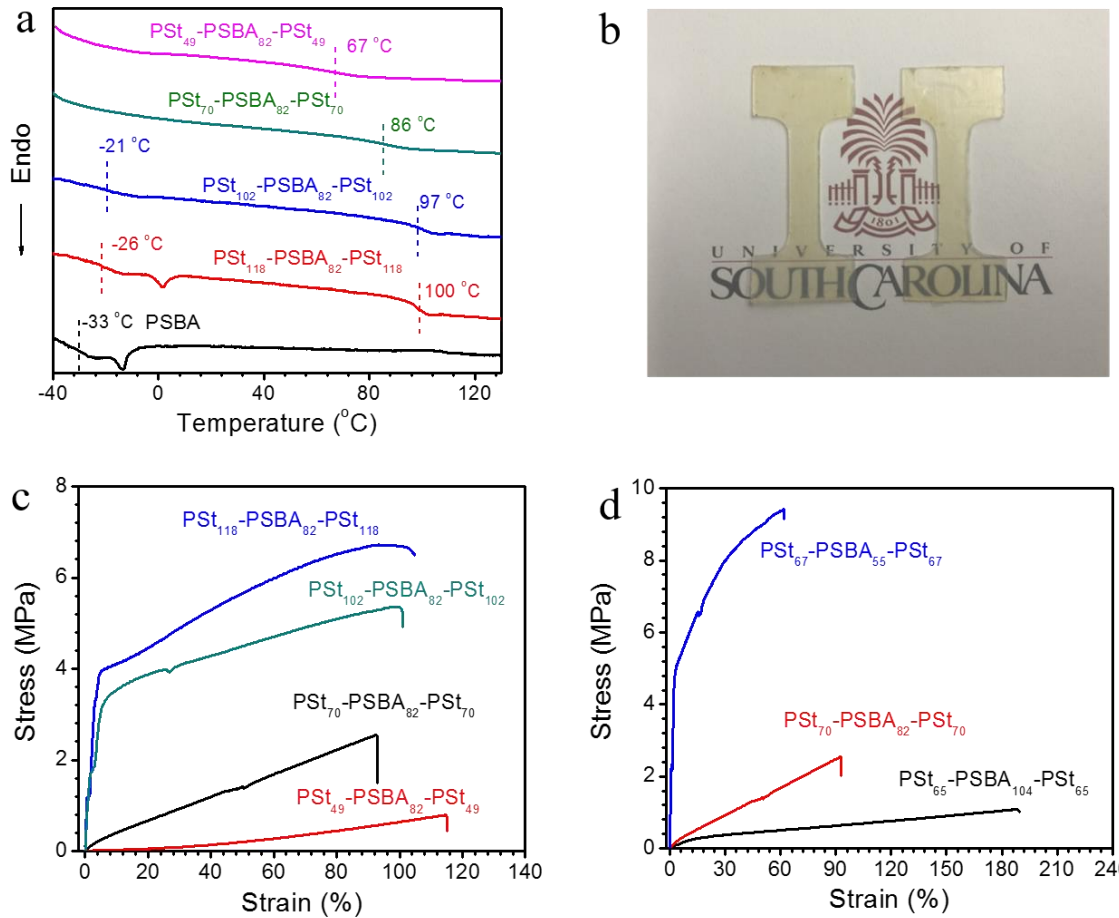
Figure 4.2 (a) DSC curves of PSBA and PS-PSBA-PS triblock copolymers, (b) picture of PS$_{118}$-PSBA$_{82}$-PS$_{118}$ dog-bone samples. Nominal stress-nominal strain curve of (c) PS-PSBA-PS triblock copolymers with the same PSBA block and different PS blocks (d) PS-PSBA-PS triblock copolymers with similar PS blocks and different PSBA blocks.

Mechanical properties of PS-*b*-PSBA-*b*-PS triblock copolymers were measured by

monotonic tensile tests (Figure 4.2). Polymer films of PS-*b*-PSBA-*b*-PS samples were

prepared by hot-press and then cut into dog-bone specimens with a length of 22 mm, a

width of 5 mm and a thickness of about 0.25 mm (Figure 4.2). Stress-strain curves of PS-

b-PSBA-*b*-PS samples with the same middle PSBA block (N=82) and different PS weight

percentage (Figure 4.2a) clearly show that all these samples maintain elongations at break

close to 100%. The PS content has an important effect on the mechanical properties of PS-*b*-PSBA-*b*-PS copolymers. With the increase of PS weight percentage (from 27.4 % to 49.4 %), their ultimate tensile strength increased from 0.9 ± 0.1 to 6.6 ± 0.4 MPa. This result is in accordance with T_g of these triblock copolymers as shown in Figure 4.2. It should be mentioned that PS-*b*-PSBA-*b*-PS triblock copolymers with a PS weight percentage lower than 32.5 % exhibited typical elastic behavior, while triblock copolymers with higher PS content displayed plastic behavior. Stress-strain curves of PS-*b*-PSBA-*b*-PS samples with similar PS block (N=65-70) and different PSBA chain lengths are shown in Figure 4.2. With the increase of molecular weight of PSBA from 16,500 to 30,300 g/mol, the failure strain increased from 60 ± 7 % to 189 ± 11 %, illustrating that the elongation at break of the triblock copolymer were largely influenced by the length of soft middle block PSBA.

"Click coupling" of the soft middle block via TAD chemistry

PS-PSBA-PS triblock copolymers with lower styrene contents show typical elastomeric behavior, and their mechanical strength is higher than that of the saturated fatty acid derived triblock copolymers reported by Robertson and coworkers.[21] However, the mechanical strength of those triblock copolymers is still lower than that of commercial SBS and SIS. As shown in Figure 4.3, chain entanglement of the soft middle block is important for the mechanical properties of SBS and SIS. Chain entanglement of the soft middle blocks plays an important role in the mechanical strength of triblock TPEs. It requires the molecular weight of the middle block 2-3 times to the entanglement molecular weight (M_e). The M_e values for the middle blocks of SBS and SIS are 1.7 and 6.1 kg/mol, respectively.[37-38] This means chain entanglements can be easily formed in SBS and SIS. However, the M_e values for polymers with long fatty acid side chains, are much higher.

79

For example, the M_e for poly(lauryl methacrylate) was reported to be 225 kg/mol and we presume the M_e for PSBA to be even higher. As shown in Figure 4.3, our triblock copolymers would not show sufficient chain entanglement, which results in inferior mechanical properties.[39] We anticipated that if covalent "click coupling" could be applied to the soft middle block, the chemical joints may act like pseudo-chain entanglements, which could enhance the mechanical properties of the triblock copolymers (Figure 4.3).
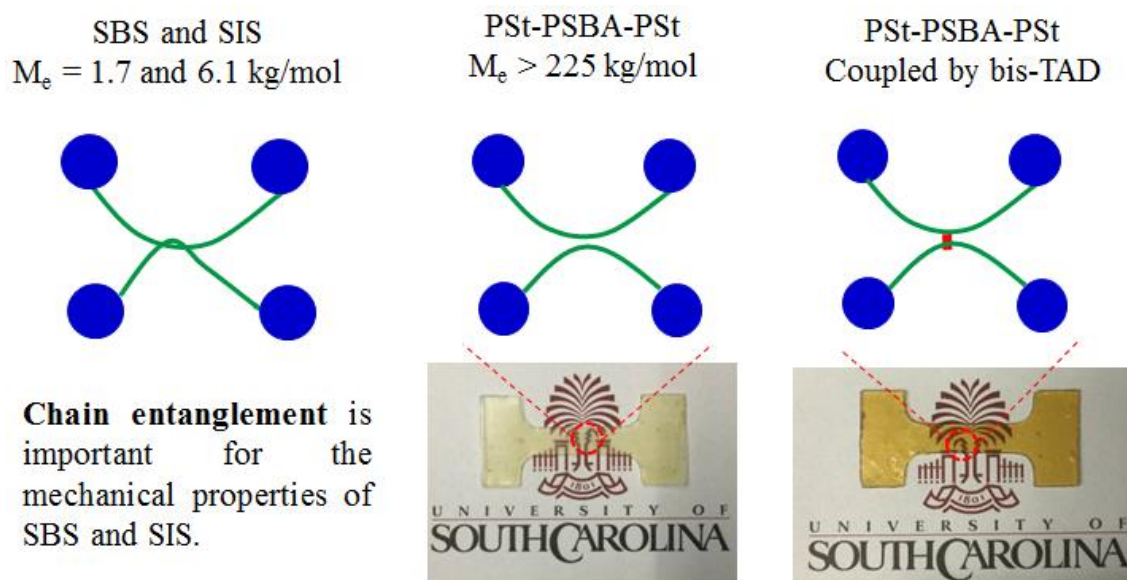
Figure 4.3 Microstructure models for commercial SBS and PS-PSBA-PS triblock copolymers before and after "click coupling".

Recently, the Du Prez group developed triazolinedione (TAD) based click chemistry, in which TAD could react with relatively inert alkenes under ambient conditions without the presence of a catalyst.[28] This click reaction of TAD was found to be efficient for double bonds in plant oils.[29] Since plant oil derived double bonds are present in the soft middle block of PS-b-PSBA-b-PS, bis-triazolinediones were introduced to "click couple" the soft middle block PSBA.

Then, bis-TAD was used to "click couple" the middle block of PS-PSBA-PS triblock copolymers. As shown in Figure 4.4, when 5 mol% of bis-TAD (relative to the

80

double bonds in PSBA) was added to a solution of PS-PSBA-PS in THF (20 wt%), a chemically crosslinked gel formed within 1 h, which was probably due to the high concentration of intermolecular chemical joints formed via "click coupling" between double bonds on PSBA block and bis-TAD. The observation indicated the efficiency of bis-TAD for "click coupling" the middle block of PS-PSBA-PS triblock copolymers. When PS-PSBA-PS triblock copolymers were "click coupled" with 1 mol% of bis-TAD, the dried film could be well dissolved in THF (Figure 4.4). This result indicated that slightly "click coupled" PS-PSBA-PS triblock copolymers did not show 3D chemical network structures and could still be processed like typical thermoplastic elastomers. To demonstrate that the click junctions can act like pseudo-chain entanglements and increase the mechanical strength, PS_{49}-$PSBA_{82}$-PS_{49} were "click coupled" with 1 mol%, 2 mol%, and 5 mol% of bis-TAD respectively. Monotonic stress-strain curves of the "click coupled" samples are shown in Figure 4.4. Doubled tensile strength of the triblock copolymers was achieved after adding 1 mol% of bis-TAD, while the elongation at break maintained. When bis-TAD was increased to 2 mol%, the tensile strength further increased, and the samples still showed typical elastic behavior. However, when 5 mol% bis-TAD was used, the mechanical strength of the "click coupled" samples increased greatly and exhibited plastic behavior. This is due to the high concentration of joints, which limits the chain extension of the PSBA block.

The elasticity of PS-PSBA-PS "click coupled" with 1 mol% bis-TAD was examined by repetitive cyclic tensile deformation to a strain of 50 % (Figure 4.4).We observed the accumulation of a small residual deformation after relaxation and a slight decline of peak stress that stabilized after several cycles of deformation. The small residual

strain was largely due to the plastic deformation of PS domains. After five loading cycles, the "click coupled" sample exhibited excellent elasticity close to 100 %.
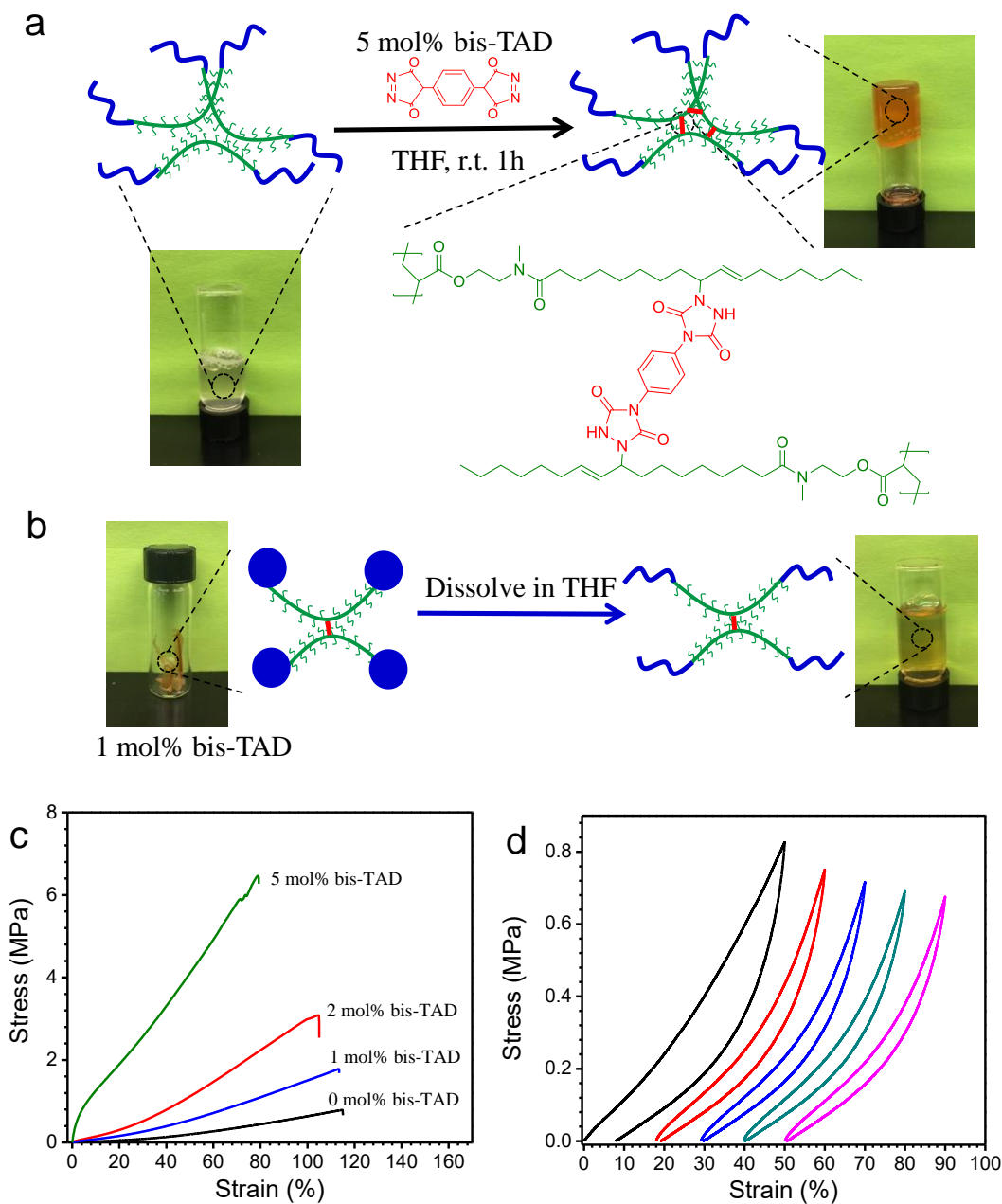

Figure 4.4 (a) "Click coupling" of PS-PSBA-PS with 5 mol% of bis-TAD leads to the formation of gel. (b) Redissolution of 1 mol% bis TAD crosslinked sample. (c) Tensile stress-stain courves of PS_{49}-$PSBA_{82}$-PS_{49} "click coupled" with 1 mol%, 2 mol%, and 5 mol% of bis-TAD. (d) Representative cyclic stress−strain curves of PS_{49}-$PSBA_{82}$-PS_{49} "click coupled" with 1 mol%.

Multi-graft type TPEs from ROMP of SBN and PLA

PS-PSBA-PS triblock copolymers show TPE properties when the content of PS is lower than 32.5 %. A close examination over the tensile properties of PS_{49}-$PSBA_{82}$-PS_{49} and PS_{70}-$PSBA_{82}$-PS_{70} revealed that stress-at-break and strain-at-break are relatively low. The low mechanical stress is explained by the absence of chain entanglements in the PSBA matrix and can be improved through TAD chemistry cross-linking. However, this cross-linking process further reduced the stain-at-break of the polymer products. The low strain-at-break for PS-PSBA-PS triblock copolymers can be attributed to the limited elasticity of PSBA polymer backbone. Linear pendant groups of 23 atoms were connected to the PSBA C-C backbone and separated from each other by a distance of only two C-C bonds. This fact makes the space around the C-C backbone highly crowded and reduced the elasticity of the C-C backbone. The elasticity of the C-C backbone can be improved by separating these long fatty chains away from each other and making the space around the backbone less crowded. As reported in Chapter 2, norbornene monomers are prepared from soybean oil and their polymers show T_g around -30 °C. The pendant long fatty chains are more separated from each other (6 atoms) and might make their polymer backbone more elastic than that of PSBA.

As a proof-of-concept study, multi-graft type copolymers PSBN-g-PLA were prepared using SBN and a norbornene functionalized PLA (Scheme 4.2). ^{1}H NMR characterization confirmed the preparation of norbornene capped PLA as a macromonomer (Figure 4.5a). After the copolymerization, ^{1}H NMR of the polymer product shows characteristic peaks from both PLA and SBN. SEC characterization for PLA and PSBN-g-PLA presents clear shift of the elution curve without any residual PLA peak, which proves

that all PLA chains were incorporated into the final graft copolymers (Figure 4.5b). DSC characterization confirmed the phase separation between PLA and PSBN as two distinct T_gs are found for PLA and PSBN (Figure 4.5c). Tensile testing results of PSBN-g-PLA with 28 wt% and 50 wt% PLA are presented in Figure 4.6. In comparison with those of PS-b-PSBA-b-PS triblock copolymers, which have a similar weight percentage of the hard phase, higher strain-at-break and stress-at-break are clearly observed. PSBN-g-PLA with 28 % of PLA was also tested by cyclic tensile test with a maximum strain of 200 % and found to exhibit over 90 % elastic recovery in the first cycle and close to 100 % elastic recovery thereafter.

Scheme 4.2 Preparation of multi-graft copolymer PSBN-g-PLA through the combination of ROP and ROMP.
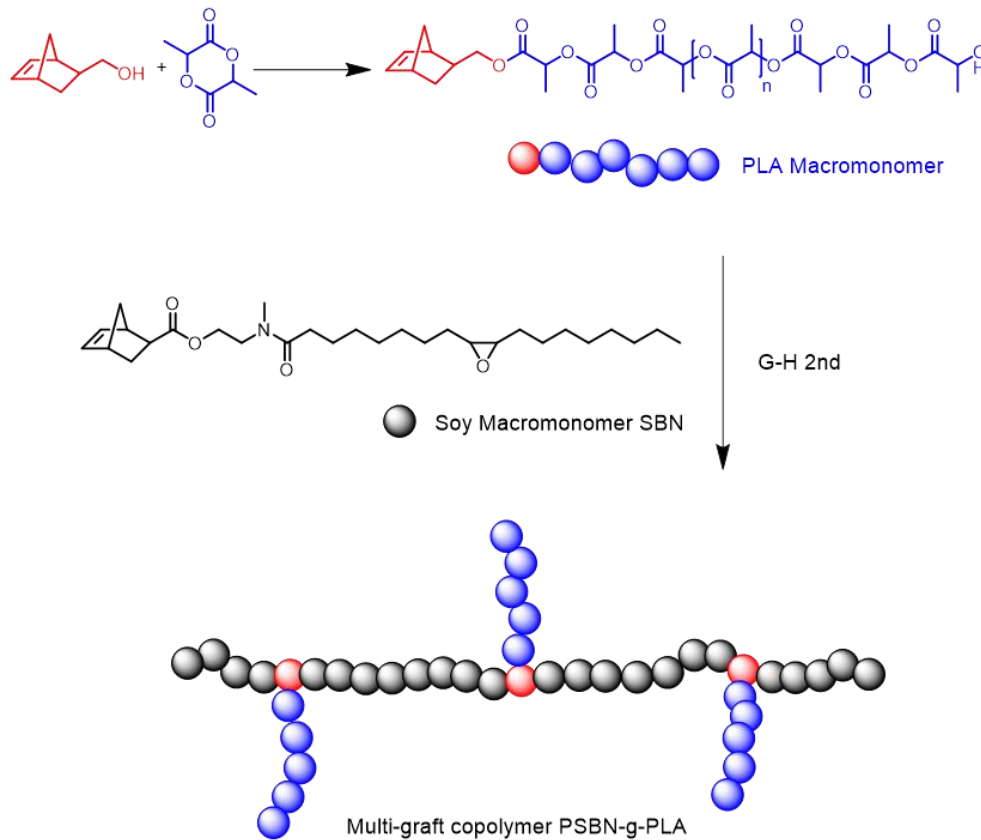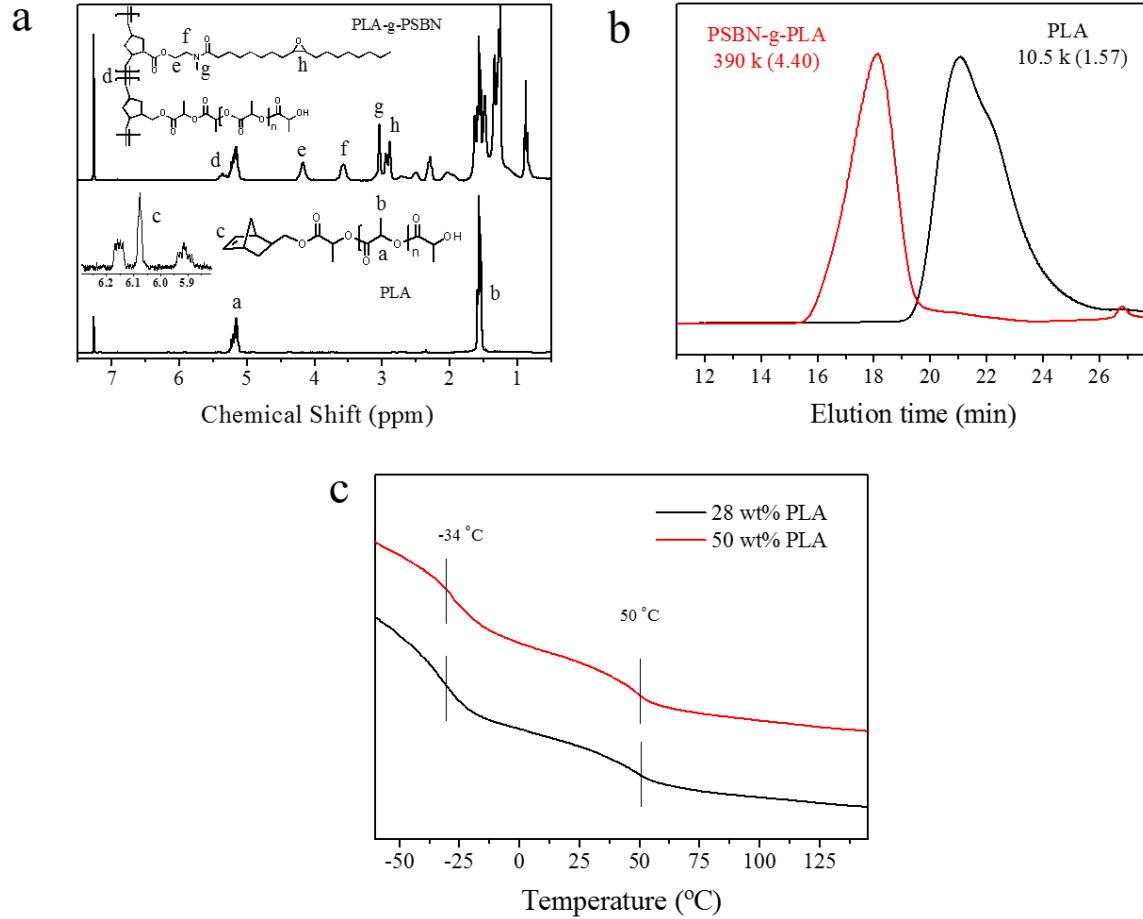
Figure 4.5 (a) ^{1}H NMR spectra of norbornene capped PLA and multi-graft copolymer PSBN-g-PLA with 28 wt% of PLA; (b) SEC curves of PLA and PSBN-g-PLA with 28 wt% of PLA; (c) DSC characterization of PSBN-g-PLA.
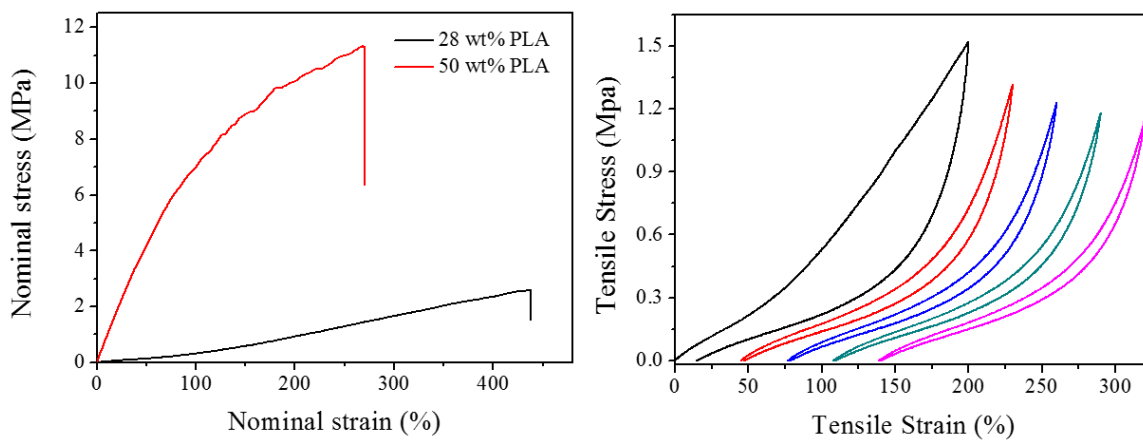

Figure 4.6 Tensile test of PSBN-g-PLA copolymers and cyclic tensile test of PSBN-g-PLA with 28 wt% PLA.

4.5 Conclusions

We demonstrated the preparation of thermoplastic elastomers using soybean oil derived monomers (SBA and SBN) as the elastic component. Triblock copolymers PS-PSBA-PS were prepared and exhibited thermoplastic elastomer properties with relatively lower stress-at-break and strain-at-break than commercial TPEs. A new "click coupling" strategy was used to overcome the lack of chain entanglement for the triblock copolymer TPEs by cross-linking with bivalent triazolindiones. Improved tensile strengths are achieved with minimum sacrifice of the tensile strain. The low strain-at-break for the triblock copolymers are attributed to the reduced polymer backbone elasticity of PSBA in a crowded environment. We did a proof-of-concept study by making multi-graft type TPE from the copolymerization of a norbornene capped PLA and SBN. PSBN has a better polymer elasticity than PSBA, and the obtained PSBN-g-PLA exhibited a 3 times higher strain-at-break than the triblock with similar weight ratio of the hard phase.

4.6 References

(1) Mecking, S. *Angewandte Chemie International Edition* **2004,** *43*, 1078-1085.

(2) Dodds, D. R.; Gross, R. A. *Science* **2007,** *318*, 1250-1251.

(3) Yao, K.; Tang, C. *Macromolecules* **2013,** *46*, 1689-1712.

(4) Thakur, V. K.; Thakur, M. K.; Raghavan, P.; Kessler, M. R. *ACS Sustainable Chemistry & Engineering* **2014,** *2*, 1072-1092.

(5) Ajjan, F.; Casado, N.; Rębiś, T.; Elfwing, A.; Solin, N.; Mecerreyes, D.; Inganäs, O. *Journal of Materials Chemistry A* **2016,** *4*, 1838-1847.

(6) Gavilà, L.; Constantí, M.; Medina, F. *Cellulose* **2015,** *22*, 3089-3098.

(7) Tang, Y.; Shen, X.; Zhang, J.; Guo, D.; Kong, F.; Zhang, N. *Carbohydrate polymers* **2015,** *125*, 360-366.

(8) Maiti, B.; Kumar, S.; De, P. *RSC Advances* **2014,** *4*, 56415-56423.

(9) Gandini, A.; Coelho, D.; Gomes, M.; Reis, B.; Silvestre, A. *Journal of Materials Chemistry* **2009,** *19*, 8656-8664.

(10) Meier, M. A.; Metzger, J. O.; Schubert, U. S. *Chemical Society Reviews* **2007,** *36*, 1788-1802.

(11) de Espinosa, L. M.; Meier, M. A. *European Polymer Journal* **2011,** *47*, 837-852.

(12) Xia, Y.; Larock, R. C. *Green Chemistry* **2010,** *12*, 1893-1909.

(13) Desroches, M.; Caillol, S.; Lapinte, V.; Auvergne, R.; Boutevin, B. *Macromolecules* **2011,** *44*, 2489-2500.

(14) Hong, J.; Luo, Q.; Wan, X.; Petrović, Z. S.; Shah, B. K. *Biomacromolecules* **2011,** *13*, 261-266.

(15) Li, F.; Larock, R. C. *Journal of Applied Polymer Science* **2001,** *80*, 658-670.

(16) Li, F.; Larock, R. C. *Journal of Polymer Science Part B: Polymer Physics* **2001,** *39*, 60-77.

(17) Lee, K.-Y.; Wong, L. L. C.; Blaker, J. J.; Hodgkinson, J. M.; Bismarck, A. *Green Chemistry* **2011,** *13*, 3117-3123.

(18) Fu, L.; Yang, L.; Dai, C.; Zhao, C.; Ma, L. *Journal of applied polymer science* **2010,** *117*, 2220-2225.

(19) Jiang, F.; Wang, Z.; Qiao, Y.; Wang, Z.; Tang, C. *Macromolecules* **2013,** *46*, 4772-4780.

(20) Dufour, B.; Tang, C.; Koynov, K.; Zhang, Y.; Pakula, T.; Matyjaszewski, K. *Macromolecules* **2008,** *41*, 2451-2458.

(21) Wang, S.; Vajjala Kesava, S.; Gomez, E. D.; Robertson, M. L. *Macromolecules* **2013,** *46*, 7202-7212.

(22) Ruzette, A.-V.; Leibler, L. *Nat Mater* **2005,** *4*, 19-31.

(23) Pedemonte, E.; Turturro, A.; Bianchi, U.; Devetta, P. *Polymer* **1973,** *14*, 145-150.

(24) Zhu, Y.; Burgaz, E.; Gido, S. P.; Staudinger, U.; Weidisch, R.; Uhrig, D.; Mays, J. W. *Macromolecules* **2006,** *39*, 4428-4436.

(25) Schlegel, R.; Duan, Y. X.; Weidisch, R.; Hölzer, S.; Schneider, K.; Stamm, M.; Uhrig, D.; Mays, J. W.; Heinrich, G.; Hadjichristidis, N. *Macromolecules* **2011,** *44*, 9374-9383.

(26) Wang, W.; Wang, W.; Li, H.; Lu, X.; Chen, J.; Kang, N.-G.; Zhang, Q.; Mays, J. *Industrial & Engineering Chemistry Research* **2015,** *54*, 1292-1300.

87

(27) Zhao, C.; Wu, D.; Huang, N.; Zhao, H. *Journal of Polymer Science Part B: Polymer Physics* **2008,** *46*, 589-598.

(28) Billiet, S.; De Bruycker, K.; Driessen, F.; Goossens, H.; Van Speybroeck, V.; Winne, J. M.; Du Prez, F. E. *Nature chemistry* **2014,** *6*, 815-821.

(29) Türünç, O.; Billiet, S.; De Bruycker, K.; Ouardad, S.; Winne, J.; Du Prez, F. E. *European Polymer Journal* **2015,** *65*, 286-297.

(30) Wang, Z.; Zhang, Y.; Yuan, L.; Hayat, J.; Trenor, N. M.; Lamm, M. E.; Vlaminck, L.; Billiet, S.; Du Prez, F. E.; Wang, Z. *ACS Macro Letters* **2016,** *5*, 602-606.

(31) Bielawski, C. W.; Grubbs, R. H. *Progress in Polymer Science* **2007,** *32*, 1-29.

(32) Bielawski, C. W.; Grubbs, R. H. *Angewandte Chemie International Edition* **2000,** *39*, 2903-2906.

(33) Tang, D.; Macosko, C. W.; Hillmyer, M. A. *Polymer Chemistry* **2014,** *5*, 3231-3237.

(34) Wanamaker, C. L.; O'Leary, L. E.; Lynd, N. A.; Hillmyer, M. A.; Tolman, W. B. *Biomacromolecules* **2007,** *8*, 3634-3640.

(35) Yu, J.; Wang, J.; Wang, C.; Liu, Y.; Xu, Y.; Tang, C.; Chu, F. *Macromolecular rapid communications* **2015,** *36*, 398-404.

(36) Matyjaszewski, K. *Macromolecules* **2012,** *45*, 4015-4039.

(37) Roovers, J.; Toporowski, P. M. *Rubber Chemistry and Technology* **1990,** *63*, 734-746.

(38) Gotro, J. T.; Graessley, W. W. *Macromolecules* **1984,** *17*, 2767-2775.

(39) Chatterjee, D. P.; Mandal, B. M. *Macromolecules* **2006,** *39*, 9192-9200.

CHAPTER 5

A New Sustainable Approach to Mendable High Resilient Elastomer

5.1 Abstract

Sustainable bioelastomers with high elastic recovery, high resilience and mendability are conceptualized with low chain-entanglement polymers that are predominantly originated from renewable biomass. Polymers with plant oil-derived fatty group at the side chain were installed with furan, which allowed Diels-Alder addition to introduce dynamic covalent crosslinking. These elastomers are mendable via retro Diels-Alder. Reprocessing of these polymers led to the formation of elastomers with preservation of excellent resilience and elastic recovery.

5.2 Introduction

High resilient materials have many important applications particularly in the context of biological purposes as bioelastomers.[1-3] Resilience is the ability of a material to recover energy during mechanical deformation. Proteins such as resilin show resilience typically over 92%, indicating the minimal energy loss during dynamic deformation recovery.[4] These natural materials exhibit unique mechanical and energy-store properties responsible for movement and in some cases for sound production of a living object.[2] It has been well demonstrated that a well-defined network and low intermolecular friction dictate high resilience of natural resilin.[5-7] Many synthetic materials have been designed to mimic these fascinating natural materials: most notably polypeptides and hydrogels.[7-9]

A common strategy on the reduction of intermolecular friction uses plasticizers.[10-12] Most of these resilin-mimicking polypeptides and hydrogels are in the hydrated state, because water serves as a plasticizer to reduce the interchain friction. Another approach is to reduce chain entanglement by stretching polymer chains through deformation-induced mechanical processing of polymeric materials.[13-17] Both strategies rely on external agents

90

or force to reduce energy loss due to friction between polymer chains. On the other hand, a well-defined network has been achieved via various means of crosslinking chemistry, which mostly leads to permanent crosslinking without recyclability.[16-18]

Scheme 5.1 A concept to achieve high resilience with the use of low chain-entanglement polymers.
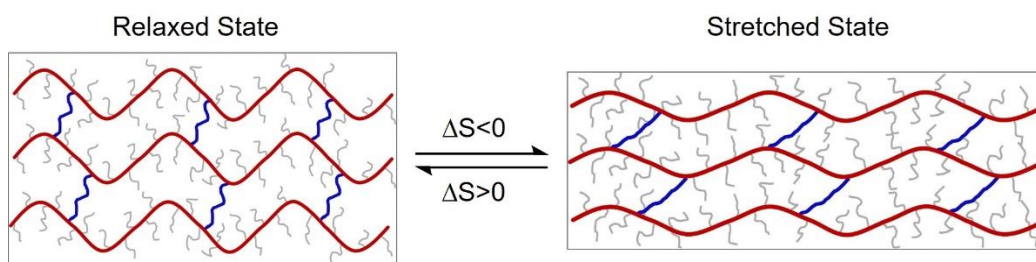
Scheme 5.2 High resilient bioelastomers by crosslinked fatty-containing polymers.
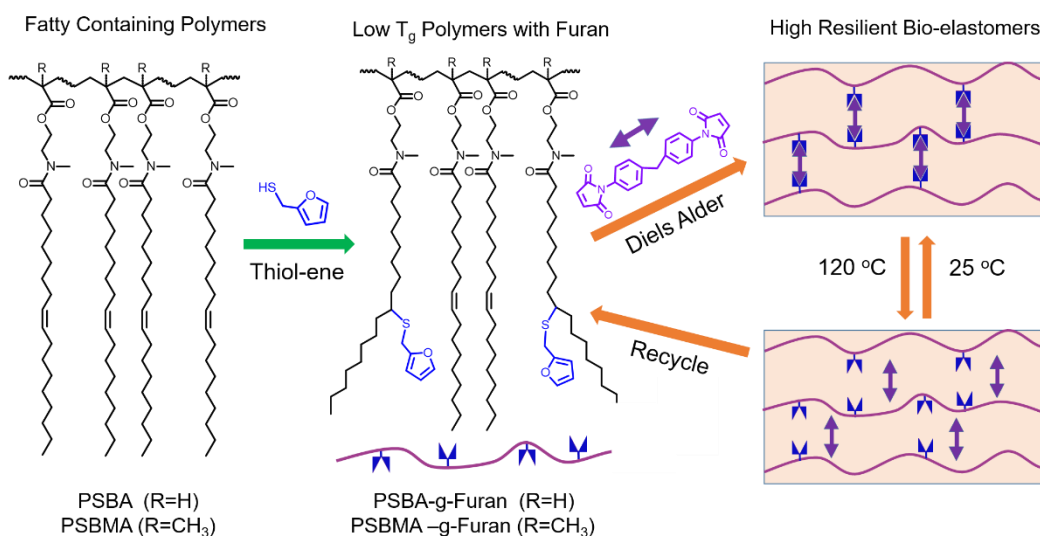
Herein we develop a novel approach to designing high resilient polymers with intrinsically low chain entanglement to reduce intermolecular friction, thus no need of additional force or agents (Scheme 5.1). On top of these polymers we further introduce dynamic covalent bonds to form reversible crosslinking structures that allow recyclability (Scheme 5.2).[19-23] On the other hand, we have recently explored sustainable chemicals, polymers and materials from biomass including plant oils.[24-28] The aforementioned

91

resilient polymers are derived from renewable biomass, thus making them sustainable materials.[29-31] Specifically we explore plant oil-derived fatty polymers, which are well known to have low chain entanglement due to the long side chain of fatty groups.[32-34] Reversible Diels-Alder reaction is introduced for crosslinking on the double bond of fatty group at the side chain. Not only are the resources rich, but also the chemistry is simple and well-demonstrated, thus making this strategy appealing for wide applications of high resilient materials.

5.3 Experimental section

Materials

Furfuryl mercaptan (98%) and 4,4'-bismaleimido-diphenylmethane (BMD, 95%) were obtained from TCI Chemicals. 1-Hydroxycyclohexyl phenyl ketone (99%) was obtained from Sigma Aldrich. PSBMA and PSBA were prepared from high oleic soybean oil according to a reported method.[24] All other solvents and chemicals were obtained from commercial providers and used as received.

Modification of PSBA and PSBMA with furfuryl mercaptan *via* thiol-ene reaction

Polymers PSBA and PSBMA were both subjected to a thiol-ene modification process. The reaction was carried out under UV-vis irradiation with 1-hydroxycyclohexyl phenyl ketone as a light sensitive radical initiator. The modification of PSBA is given as an example. PSBA (8.0 g, 0.02 mol C=C), furfuryl mercaptan (16.0 mL, 0.16 mol) and 1-hydroxycyclohexyl phenyl ketone (0.25 g, 1.2 mmol) were dissolved in 25 mL THF in a 250 mL round bottle flask. The solution was purged with N_2 for 30 min and kept under UV (254 nm, 15 Watt) irradiation for 16 hours. Methanol (200 mL) was added dropwise into the solution under stirring. The supernatant was poured out, and the precipitate was washed

twice with methanol (2×100 mL) by stirring. The polymer in the flask was dried under vacuum overnight. The product was named as PSBA-g-Furan. PSBMA-g-Furan was prepared with a similar method to the synthesis of PSBMA.

Preparation of bioelastomers from PSBA-g-Furan and PSBMA-g-Furan

BMD was used as a cross-linker for polymers PSBA-g-Furan and PSBMA-g-Furan. The Diels-Alder reaction occurred between the furan and maleimide groups. For polymer films, 1.0 gram of a polymer was used and the amount of cross-linker was varied to control the level of cross-linking. For PSBA-g-Furan, six films were prepared, with the amount of BMD respectively at 2.0 wt%, 4.0 wt%, 6.0 wt%, 8.0 wt%, 10.0 wt%, 12.0 wt% to PSBA-g-Furan. Five films with 2.0 wt%, 4.0 wt%, 6.0 wt%, 8.0 wt% and 10.0 wt% of BMD were prepared for PSBMA-g-Furan. The cured film was named as PSBA-X or PSBMA-X, where X indicates the weight percentage of cross-linker to the precursor polymer. Using the preparation of PSBMA-10 as an example, polymer PSBMA-g-Furan (1.0 g) and BMD (0.1 g) were dissolved together in 8.0 mL THF in a 15 mL centrifuge tube before the solution was sonicated and centrifuged at 8000 rpm for 5 min. The supernatant was poured into a Teflon mold and dried at ambient temperature. After 48 h, the solvent was evaporated, and the mold was transferred to an oven set at 60 $^{\circ}$C and kept for 12 hr. The oven was cooled down to room temperature slowly and vacuum was applied to the oven in order to remove any remaining solvent within the film.

Measurements

300 MHz ^{1}H NMR spectra were recorded on a Varian Mercury 300 spectrometer with tetramethylsilane (TMS) as an internal reference. Molecular weight and molecular weight distribution of polymers were determined using a gel permeation chromatography

(GPC) equipped with a 2414 RI detector, a 1525 Binary Pump and three Styragel columns. The columns consist of HR 1, HR 3 and HR 5E with molecular weight in the range of 1×10^2 - 5×10^3 g/mol, 5×10^2 - 3×10^4 g/mol and 2×10^3 - 4×10^6 g/mol respectively. THF was used as eluent at 35 $^{\circ}$C with a flow rate of 1.0 mL/min. The system was calibrated with polystyrene standards obtained from Polymer Laboratories. GPC samples were prepared by dissolving the sample in THF with a concentration of 3.0 mg/mL and passing through microfilters with an average pore size of 0.2 μm.

Fourier transform infrared spectrometry (FT-IR) spectra were taken on a PerkinElmer spectrum 100 FT-IR spectrometer. The glass transition temperature (T_g) of polymers was determined through differential scanning calorimetry (DSC) conducted on a DSC 2000 instrument (TA instruments). Samples were firstly heated from -70 $^{\circ}$C to 200 $^{\circ}$C at a rate of 10 $^{\circ}$C /min. After cooling down to -70 $^{\circ}$C at the same rate, the data were collected from the second heating scan. 10 mg of each sample was used for DSC test with nitrogen gas at a flow rate of 50 mL/min. Tensile stress-strain testing was carried out with an Instron 5543A testing instrument. Dog-bone shaped specimens were cut from films with a length of 22 mm and width of 5.0 mm before testing at room temperature with the crosshead speed of 10 mm/min. The cyclic tensile test was conducted stepwise to a tensile strain of 20% (PSBA-12 & PSBA-12R) or 50% (PSBMA-10 & PSBMA-10R). In each step, once the specimen reached 20% or 50% strain, the crosshead direction was reversed and the sample strain was decreased at the same rate (1 mm/min) till stress was released to zero. The crosshead was immediately reversed when zero stress was reached and the sample was then extended again till 20% or 50% strain. The cyclic deformation was repeated for 5 times. The dynamic mechanical tests (DMA) were performed on a RAS3 DMA (TA instruments)

from -60 $^{\circ}$C to 100 $^{\circ}$C. The frequency was set to 10 Hz, and the heating rate was 3 $^{\circ}$C/min.

5.4 Results and discussion

Synthesis and crosslinking chemistry of fatty-containing polymers

Early work has shown that these polymers with pendant long fatty chains have very high chain entanglement molecular weight in the range of 100,000 g/mol.[34] It indicates that polymers below this molecular weight have low chain entanglement, thus reducing intermolecular friction. We selected two acrylic polymers with fatty side chain derived from soybean oil. Polymers with low glass transition temperature (T_g), poly(soybean acrylate) (PSBA, M_n = 19,300 g/mol, T_g = –33 $^{\circ}$C) and poly(soybean methacrylate) (PSBMA, M_n = 44,500 g/mol, T_g = –6 $^{\circ}$C) (Scheme 5.2), were prepared from high oleic soybean oil, in which one of the steps involved a base catalyzed amidation reaction with *N*-methyl ethanolamine, as reported in our early work.[26] Each repeat unit of both polymers has an average of one unsaturated double bond, which was then partially installed with a furan group by a UV-mediated thiol-ene reaction with furfuryl mercaptan (Scheme 5.2).[35-36] In comparison with ^{1}H NMR spectra of the unmodified polymers, new peaks from the furan group were clearly observed at 7.33, 6.29 and 6.12 ppm the modified polymers (PSBMA-g-Furan given in Figure 5.1A as a representative). Meanwhile, two peaks corresponding to protons next to the sulfur atom at 3.69 ppm (-C$\boldsymbol{H_2}$-S-CH-) and 2.55 ppm (-C$\boldsymbol{H}$-S-CH$_2$-) appeared after the modification. Using the methyl protons on the nitrogen atom (-NC$\boldsymbol{H_3}$) as the reference, the molar grafting ratio of furan groups per side chain for PSBMA-g-Furan and PSBA-g-Furan was calculated to be 25% and 35% respectively. It should be mentioned that both polymers still have low T_gs after the modification, as indicated by DSC (Figure 5.1B). The successful modification was further proved by FT-

95

IR characterization. In the spectrum of PSBA-g-Furan, the characteristic peak for the breathing mode of furan ring (1010 cm^{-1}) was observed (Figure 5.1C).
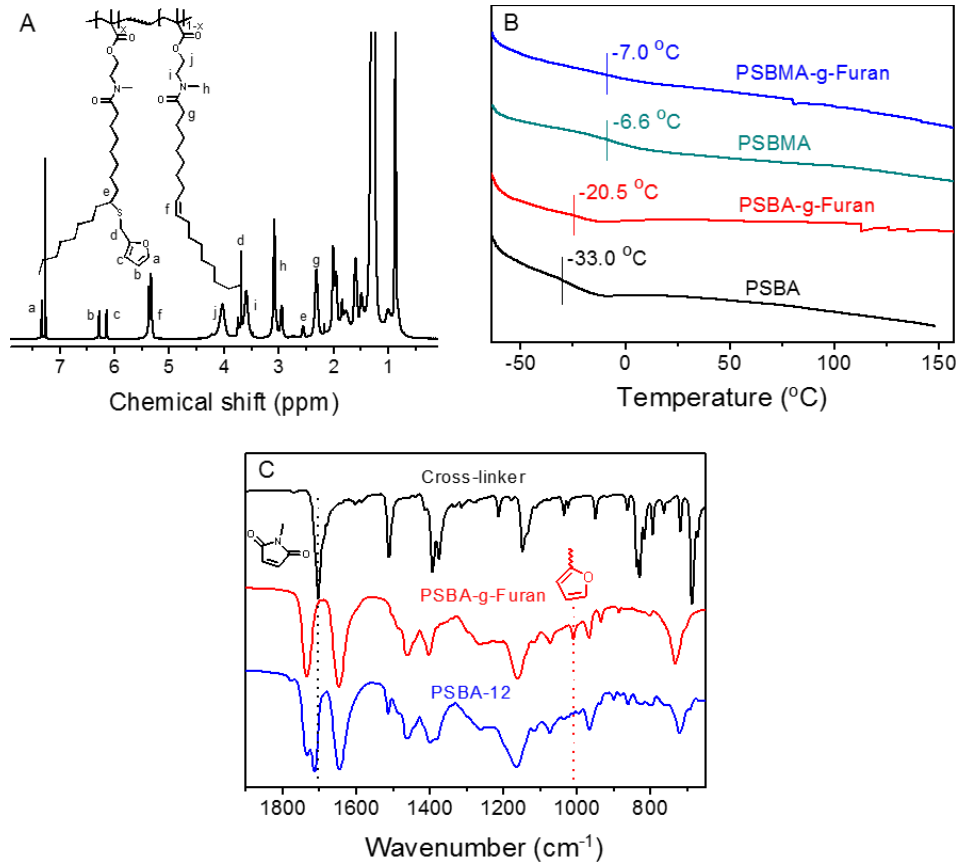

Figure 5.1 (A) ^{1}H NMR spectrum of PSBMA-g-Furan; (B) DSC curves of PSBA, PSBA-g-Furan, PSBMA and PSBMA-g-Furan; (C) FT-IR spectra of cross-linker, PSBA-g-Furan and crosslinked film PSBA-12.
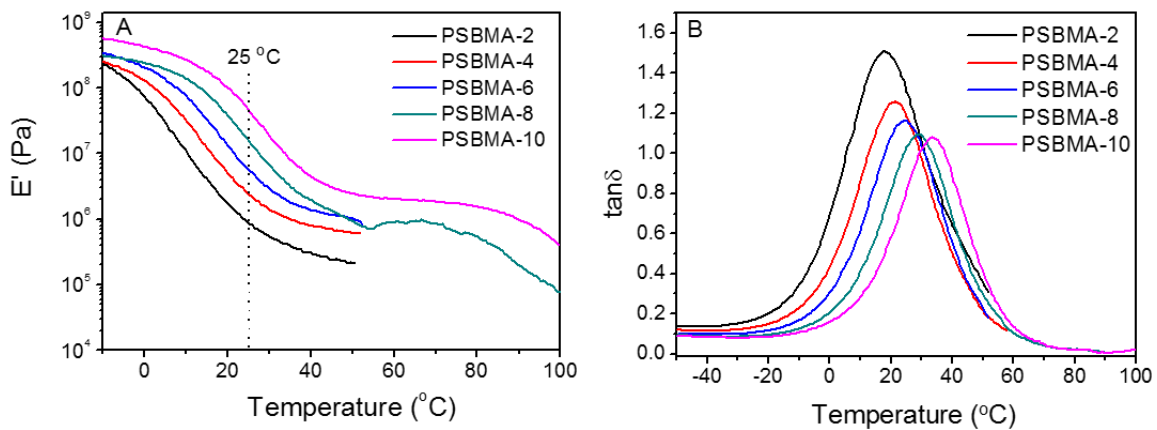

Figure 5.2 DMA curves of (A) storage modulus E′ versus temperature and (B) loss tangent tanδ versus temperature for PSBMA-g-Furan based elastomers.

Furan grafted polymers, PSBA-g-Furan and PSBMA-g-Furan, were mixed with a di-functional cross-linker, 4,4'-bismaleimido-diphenylmethane (BMD), at different weight fractions (Scheme 5.2). Following solvent evaporation, free-standing films were obtained. The crosslinked films were named as PSBA-X or PSBMA-X, where X represents weight percentage of the cross-linker compared to furan-grafted polymers. FT-IR characterization was firstly used to verify the Diels-Alder reaction between diene (furan) and dienophile (the cross-linker). Figure 5.1C presents FT-IR spectra of crosslinked film from PSBA-g-Furan. The spectrum of PSBA-12 (12 wt% cross-linker) was given together with those of the cross-linker and PSBA-g-Furan. The furan peak at 1010 cm^{-1} almost disappeared and the carbonyl group from the cross-linker at 1704 cm^{-1} shifted to 1717 cm^{-1} after the Diels-Alder reaction.[37][38] These results indicated the successful Diels-Alder reaction.

Dynamic mechanic analysis was applied to test the thermomechanical properties of films of furan grafted polymers in a tensile mode. For PSBMA-g-furan polymers, films with lower weight fractions of cross-linker (PSBMA-2, PSBMA-4 and PSBMA-6) failed at ~50 ^{o}C while films with higher level of cross-linking (PSBMA-8 and PSBMA-10) ruptured up to 100 ^{o}C. Figure 5.2 shows storage modulus and dissipation factor (tan δ) as a function of temperature for PSBMA-g-furan based films. The storage moduli at 25 ^{o}C increased with the increase of cross-linking level. A single glass transition temperature (T_g) was observed for each film, and the T_g increased gradually from 17.4 ^{o}C (PSBMA-2) to 34.0 ^{o}C (PSBMA-10). For all PSBA-g-furan polymers, the films appeared soft even with 12wt% cross-linker.

Elastic recovery and resilience of crosslinked fatty polymers

The tensile test measurement of crosslinked bioelastomers was carried out at room temperature, and the results are given in Figure 5.3. Both series of crosslinked films (PSBA-X and PSBMA-X) exhibited increasing stress-at-break and modulus with the increase of cross-linker amount. For films from PSBA-g-Furan, a linear increase of stress with strain was observed with strain-at-break between 50% - 70% (Figure 5.3A). The stress-at-break increased from 0.10 MPa to 0.88 MPa as the weight fraction of cross-linker increased from 4 wt% to 12 wt%. In comparison, films from PSBMA showed higher mechanical strength with stress-at-break around 3.29 MPa when 10 wt% of cross-linker was used (Figure 5.3B). The strain-at-break for PSBMA based films were between 80% - 200%. The dependence of strain-at-break and stress-at-break on the level of cross-linking indicated a facile control over the mechanical properties of elastomers.

Using polymers PSBA-12 and PSBMA-10, which have the highest respective level of cross-linking, repetitive cyclic tensile deformation tests were carried out to examine elastic recovery and resilience of bioelastomers. Maximum strain was set at 20% for PSBA-12 and 50% for PSBMA-10 (Figure 5.3C). A nearly full recovery was observed during each loading-unloading cycle for PSBA-12, demonstrating excellent elasticity. PSBMA-10 showed about 26% residual strain after the first cycle and close to full recovery thereafter (Figure 5.3D). The residue deformation was recovered minutes after removing the sample from the load. The elastic recovery rates from the cyclic tests are given in Figure 5.3E. The area of the hysteresis loop from each loading-unloading cycle indicates the dissipated energy from internal chain friction. The ability to recover the energy (resilience) from the cyclic test of the material is reflected by the ratio between the area under the

unloading curve and the loading curve. The experimental resilience for PSBA-12 and PSBMA-10 is summarized in Figure 5.3F. It is clearly shown that the resilience for PSBA-12 is about 93%, which is comparable to natural resilin (~92%).[17]
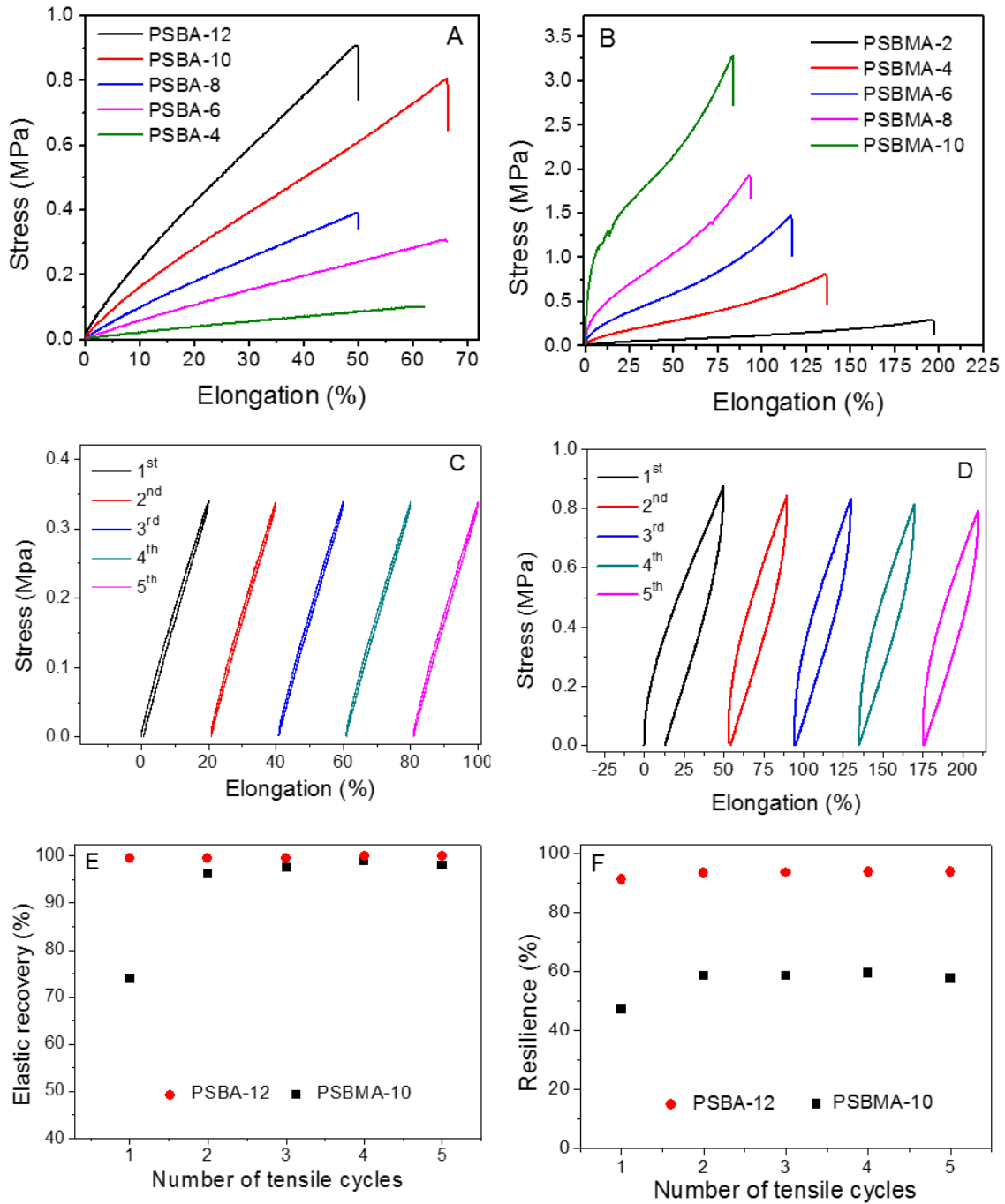

Figure 5.3 Tensile tests of films from (A) PSBA-g-Furan and (B) PSBMA-g-Furan; cyclic tensile tests of (C) PSBA-12 and (D) PSBMA-10; (E) elastic recovery and (F) resilience as a function of tensile cycles for PSBA-12 and PSBMA-10.

The high resilience could be understood by excellent chain flexibility and low chain entanglement of PSBA due to its high chain entanglement molecular weight (Scheme 5.1). In comparison, PSBMA-10 shows much lower resilience (~56%) than PSBA-12. The polymer backbone structure could help explain such difference. The presence of a methyl group on each repeat unit of PSBMA could bring more steric hindrance and thus higher rigidity on polymer chains relative to PSBA. The chains of PSBA-12 are easier to slide past each other than those of PSBMA-10 during deformation. As a result, PSBA-12 has a higher elastic recovery rate and resilience than PSBMA-10.

Dynamic Covalent Crosslinking and Mendablity of Fatty Polymers

The reversible and dynamic covalent crosslinking of both films of PSBA-12 and PSBMA-10 was examined. After immersing the films in toluene at 25 ^{o}C overnight, swelling of films was observed while the solution maintained colorless, indicating that polymers were not dissolved (representative photos of PSBA-12 in Figure 5.4A). Then solution in toluene was heated to 120 ^{o}C for 10 minutes. Complete dissolution of PSBA-12 and PSBMA-10 was observed with the formation of clear yellow solution. At high temperature (120 ^{o}C), the covalent bond resulted from the Diels-Alder reaction was cleaved via a retro-Diels-Alder process to destroy the crosslinked network in polymers. Successful precipitation of the solution in methanol further verified the decoupling reaction. ^{1}H NMR spectra of the recovered polymers of PSBA-g-furan and PSBMA-g-furan are nearly identical to their precursor polymers. The recovered polymers also exhibited elution curves and molecular weight similar to their precursor polymers, as characterized by GPC. As depicted by DSC analysis (Figure 5.4B), the recovered PSBA-g-furan exhibited a T_g around -19.8 ^{o}C, comparable to the initial PSBA-g-Furan (T_g = -20.5 ^{o}C). In comparison,

100

crosslinked PSBA-12 film has a T_g of -2.8 °C, indicating that the cross-linking process increased T_g of PSBA-g-Furan. Meanwhile, an endothermic peak was observed between 80 °C and 140 °C, originating from the decoupling of Diels-Alder adducts. Similar results were obtained for recovered PSBMA-g-furan and crosslinked PSBMA-10 (Figure 5.4C).
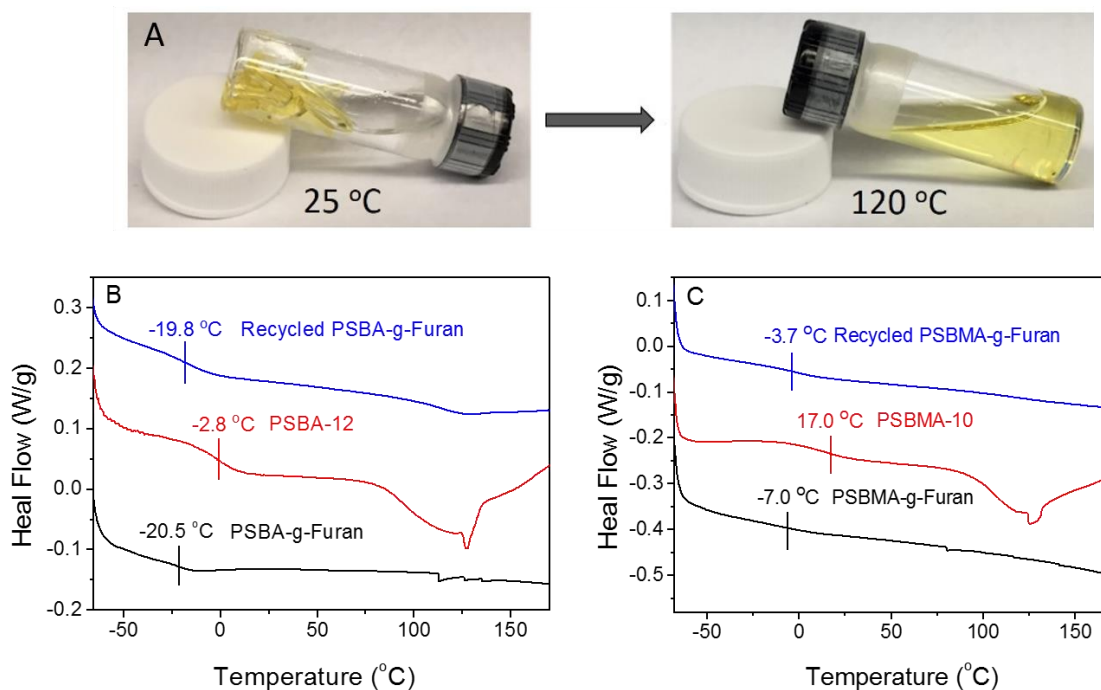

Figure 5.4 (A) Photos of PSBA-12 in toluene at 25 °C (left) and 120 °C (right); (B) DSC curves of PSBA-g-Furan (black), PSBA-12 (red) and recycled PSBA-g-Furan (blue); (C) DSC curves of PSBMA-g-Furan (black), PSBMA-10 (red) and recycled PSBMA-g-Furan (blue).

The above study indicated the possibility to re-mold the crosslinked polymers by hot compression. As shown in Figure 5.5A, pieces of crosslinked PSBA-12 were processed under a pressure of 30 MPa for 5 min at 140 °C to give a new free-standing film. Figure 5.5B shows the tensile test of the remolded bio-elastomer PSBA-12R, which exhibited similar modulus to, but somewhat higher tensile strength than PSBA-12. The same procedure was carried out for the crosslinked PSBMA-10. The newly remolded film (PSBMA-10R) exhibited elastomer properties with lower stress-at-break than PSBMA-10.

101

To confirm the integrity and resilience of the newly formed films (PSBA-12R and PSBMA-10R), repetitive cyclic tensile deformation tests were also carried out, and comparable results were observed (Figures 5.5C and 5.5D). Remolded PSBA-12R showed similar resilience (90%) and elastic recovery rate (99%) to PSBA-12, while PSBMA-10R has an inferior performance of resilience as determined by calculation.
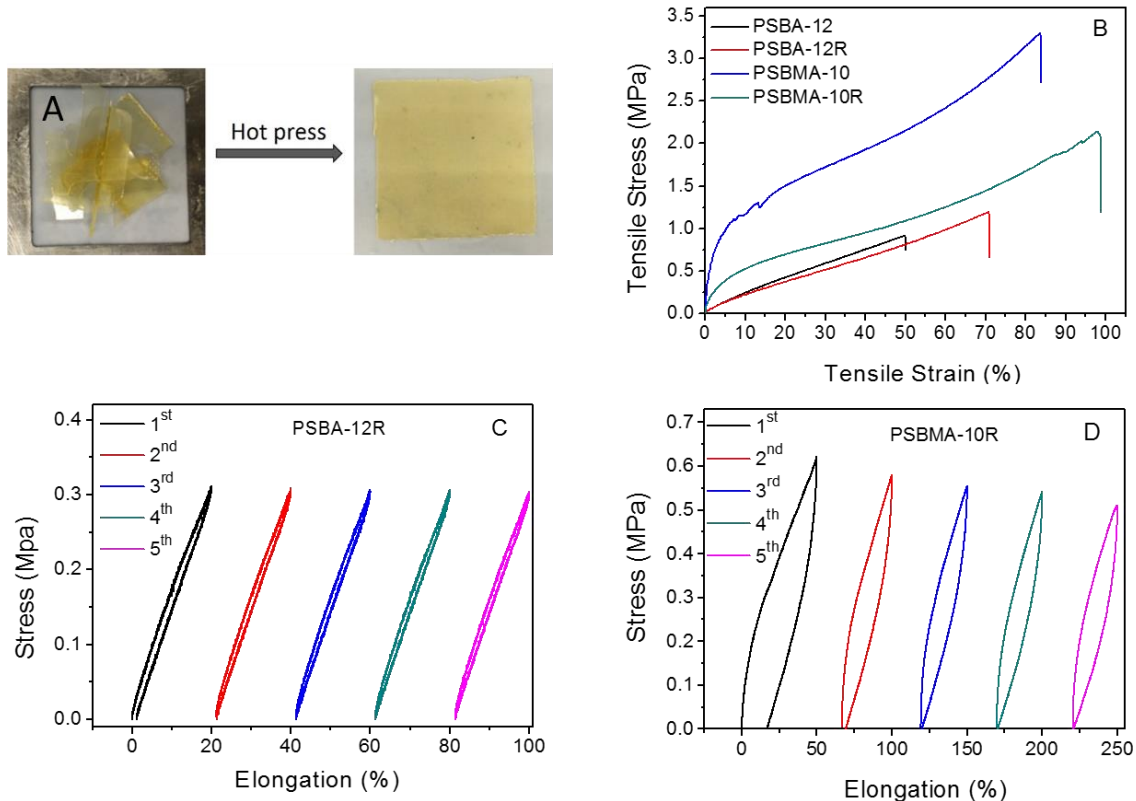
Figure 5.5 (A) Hot-compression remolding of PSBA-12; (B) tensile tests of PSBA-12, PSBA-12R, PSBMA-10 and PSBMA-10R; cyclic tensile tests for remolded films: (C) PSBA-12R and (D) PSBMA-10R.

5.5 Conclusions

We developed a new approach on the use of low chain-entanglement polymers for designing high resilient elastomers. These elastomers are based on side-chain fatty-containing acrylic polymers, which were further installed with a furan group for subsequent crosslinking via Diels-Alder reaction. Both fatty and furan groups are derived from

biomass, thus rendering sustainability on these elastomers. These bioelastomers exhibited high resilience (~93%) that is dictated by the low chain entanglement of fatty polymers and well-defined network resulted from side-chain crosslinking. The dynamic reversibility of the Diels-Alder addition provided mendability of these elastomers. Our approach provides a facile strategy for the preparation of sustainable re-processable high resilient bioelastomers from biomass.

5.6 References

(1) Elvin, C. M.; Carr, A. G.; Huson, M. G.; Maxwell, J. M.; Pearson, R. D.; Vuocolo, T.; Liyou, N. E.; Wong, D. C.; Merritt, D. J.; Dixon, N. E. *Nature* **2005,** *437*, 999-1002.

(2) Lv, S.; Dudek, D. M.; Cao, Y.; Balamurali, M.; Gosline, J.; Li, H. *Nature* **2010,** *465*, 69-73.

(3) Li, L.; Kiick, K. L. *ACS Macro Letters* **2013,** *2*, 635-640.

(4) Qin, G.; Hu, X.; Cebe, P.; Kaplan, D. L. *Nature communications* **2012,** *3*, 1003.

(5) Li, B.; Alonso, D. O. V.; Bennion, B. J.; Daggett, V. *Journal of the American Chemical Society* **2001,** *123*, 11991-11998.

(6) Truong, M. Y.; Dutta, N. K.; Choudhury, N. R.; Kim, M.; Elvin, C. M.; Nairn, K. M.; Hill, A. J. *Biomaterials* **2011,** *32*, 8462-8473.

(7) Qin, G.; Rivkin, A.; Lapidot, S.; Hu, X.; Preis, I.; Arinus, S. B.; Dgany, O.; Shoseyov, O.; Kaplan, D. L. *Biomaterials* **2011,** *32*, 9231-9243.

(8) Zhu, M.; Liu, Y.; Sun, B.; Zhang, W.; Liu, X.; Yu, H.; Zhang, Y.; Kuckling, D.; Adler, H. J. P. *Macromolecular rapid communications* **2006,** *27*, 1023-1028.

(9) Cui, J.; Lackey, M. A.; Madkour, A. E.; Saffer, E. M.; Griffin, D. M.; Bhatia, S. R.; Crosby, A. J.; Tew, G. N. *Biomacromolecules* **2012,** *13*, 584-588.

(10) Park, K.; Ha, J. U.; Xanthos, M. *Polymer Engineering & Science* **2010,** *50*, 1105-1110.

(11) Nambiar, R. R.; Blum, F. D. *Macromolecules* **2008,** *41*, 9837-9845.

(12) Belous, A.; Tchoudakov, R.; Tzur, A.; Narkis, M.; Alperstein, D. *Polymers for Advanced Technologies* **2012,** *23*, 938-945.

(13) Wang, Z.; Niu, Y.; Fredrickson, G. H.; Kramer, E. J.; Shin, Y.-W.; Shimizu, F.; Zuo, F.; Rong, L.; Hsiao, B. S.; Coates, G. W. *Macromolecules* **2010,** *43*, 6782-6788.

(14) Deplace, F.; Wang, Z.; Lynd, N. A.; Hotta, A.; Rose, J. M.; Hustad, P. D.; Tian, J.; Ohtaki, H.; Coates, G. W.; Shimizu, F. *Journal of Polymer Science Part B: Polymer Physics* **2010,** *48*, 1428-1437.

(15) Jiang, F.; Wang, Z.; Qiao, Y.; Wang, Z.; Tang, C. *Macromolecules* **2013,** *46*, 4772-4780.

(16) Wang, Z.; Jiang, F.; Zhang, Y.; You, Y.; Wang, Z.; Guan, Z. *ACS nano* **2014,** *9*, 271-278.

(17) Wang, Z.; Yuan, L.; Jiang, F.; Zhang, Y.; Wang, Z.; Tang, C. *ACS Macro Letters* **2016,** *5*, 220-223.

(18) Türünç, O.; Billiet, S.; De Bruycker, K.; Ouardad, S.; Winne, J.; Du Prez, F. E. *European Polymer Journal* **2015,** *65*, 286-297.

(19) Yu, S.; Zhang, R.; Wu, Q.; Chen, T.; Sun, P. *Advanced Materials* **2013,** *25*, 4912-4917.

(20) Imato, K.; Nishihara, M.; Kanehara, T.; Amamoto, Y.; Takahara, A.; Otsuka, H. *Angewandte Chemie International Edition* **2012,** *51*, 1138-1142.

(21) Gandini, A. *Progress in Polymer Science* **2013,** *38*, 1-29.

(22) Vilela, C.; Silvestre, A. J.; Gandini, A. *Journal of Polymer Science Part A: Polymer Chemistry* **2013,** *51*, 2260-2270.

(23) Intemann, J. J.; Huang, W.; Jin, Z.; Shi, Z.; Yang, X.; Yang, J.; Luo, J.; Jen, A. K.-Y. *ACS Macro Letters* **2013,** *2*, 256-259.

(24) Yuan, L.; Wang, Z.; Trenor, N. M.; Tang, C. *Macromolecules* **2015,** *48*, 1320-1328.

(25) Wang, Z.; Yuan, L.; Trenor, N. M.; Vlaminck, L.; Billiet, S.; Sarkar, A.; Du Prez, F. E.; Stefik, M.; Tang, C. *Green Chemistry* **2015,** *17*, 3806-3818.

(26) Yuan, L.; Wang, Z.; Trenor, N. M.; Tang, C. *Polymer Chemistry* **2016,** *7*, 2790-2798.

(27) Wang, Z.; Zhang, Y.; Yuan, L.; Hayat, J.; Trenor, N. M.; Lamm, M. E.; Vlaminck, L.; Billiet, S.; Du Prez, F. E.; Wang, Z. *ACS Macro Letters* **2016,** *5*, 602-606.

(28) Xu, Y.; Yuan, L.; Wang, Z.; Wilbon, P. A.; Wang, C.; Chu, F.; Tang, C. *Green Chemistry* **2016,** *DOI: 10.1039/C6GC00859C*.

(29) Williams, C. K.; Hillmyer, M. A. *Polymer Reviews* **2008,** *48*, 1-10.

104

(30) Yao, K.; Tang, C. *Macromolecules* **2013,** *46*, 1689-1712.

(31) Biermann, U.; Bornscheuer, U.; Meier, M. A.; Metzger, J. O.; Schäfer, H. J. *Angewandte Chemie International Edition* **2011,** *50*, 3854-3871.

(32) Quinzler, D.; Mecking, S. *Angewandte Chemie International Edition* **2010,** *49*, 4306-4308.

(33) Wang, S.; Robertson, M. L. *ACS Applied Materials & Interfaces* **2015,** *7*, 12109-12118.

(34) Wang, S.; Vajjala Kesava, S.; Gomez, E. D.; Robertson, M. L. *Macromolecules* **2013,** *46*, 7202-7212.

(35) Lowe, A. B. *Polymer Chemistry* **2014,** *5*, 4820-4870.

(36) Bai, J.; Li, H.; Shi, Z.; Yin, J. *Macromolecules* **2015,** *48*, 3539-3546.

(37) Polgar, L. M.; van Duin, M.; Broekhuis, A. A.; Picchioni, F. *Macromolecules* **2015,** *48*, 7096-7105.

(38) García‐Astrain, C.; Algar, I.; Gandini, A.; Eceiza, A.; Corcuera, M. Á.; Gabilondo, N. *Journal of Polymer Science Part A: Polymer Chemistry* **2015,** *53*, 699-708.

CHAPTER 6

Bio-Renewable Elastomers from Plant Oil Polymers and Lignin through Thermal Azide-Alkyne Cyclization

6.1 Abstract

Elastomer products from biomass resources are of great importance for a sustainable development. Azide functionalized polymers were developed from soybean oil and reacted with alkyne functionalized lignin via the thermal azide-alkyne cycloaddition reaction (TAAC) to afford elastomers with excellent elastic recovery rates. Mechanical properties of these elastomers could be tuned via controlling the azide content in the soy-based polymers and the ratio of cross-linker. Model study was carried out to prove the TAAC reaction between the soy-based polymer and the cross-linker.

6.2 Introduction

Elastomers are important materials in our daily life, with a forecasted global revenue of US\$56 billion in 2020. Petroleum based synthetic rubbers, such as styrene butadiene rubber (SBR), polybutadiene rubber (BR) and acrylonitrile butadiene rubber (NBR), are sharing two-thirds of the world rubber market.[1-3] For a sustainable development, great efforts have been made to replace petrochemical-based elastomer products with natural ones.[4-10] Besides natural rubber, polymers showing elastomer properties have been presented from a variety of renewable biomass, like plant oils, terpene, menthol, etc.[11-17]

Thermoplastic elastomer (TPE) is an important type of elastomers. One universal approach is to develop low glass transition temperature (T_g) polymers from biomass and incorporate such polymers as the elastic component within TPEs.[18-21] For example, poly(menthide) with T_g=-22 ^{o}C and poly(δ-decalactone) with T_g=-51 ^{o}C have been used as the soft component for constructing ABA triblock structured TPEs.[22-23] On the other hand, thermoset elastomers from bio-derived reactive precursors are receiving increasing attention due to the facile processing procedures.[24-27] These precursors could be small

107

molecules or polymers. For example, Zhang et al. reported bio-elastomers through the cross-linking of soybean oil based polymeric precursors with T_g between -30 °C to -17 °C.[24] We envisaged that further exploration of reactive bio-based precursors and applicable cross-linking methods could bring about novel elastomer products.

Cross-linking procedures could undergo either a non-selective or a selective bond formation process. Non-selective bond formation procedures are uncontrolled with ill-defined networks, while cross-linking through a selective bond formation mechanism offers control over the cross-linking degree and the formed networks.[28-32] Strategies for controlled cross-linking include in-situ ketene generation & coupling,[33-35] Diels-Alder coupling[36-38], triazolinedione-ene coupling[39-40] and the azide-alkyne Huisgen cycloaddition.[41-45]

Recently, we reported the preparation of polymers with low glass transition temperatures from soybean oil.[21] Cross-linking by auto-oxidation of polymers with similar structure resulted in brittle product due to an uncontrolled procedure.[46] Herein, we report the cross-linking of soybean oil based polymers in a controlled manner by thermal azide-alkyne cycloaddition (TAAC). As shown in Scheme 6.1, azide modified polymers, prepared from two soybean oil based monomers (Scheme 6.2), were mixed with alkyne functionalized lignin and thermally treated to get the thermoset bio-elastomers. The TAAC coupling reaction between the azide group on the plant oil polymers and the alkyne group on the modified lignin was further proved through a model study.

Scheme 6.1 Elastomers from the thermal azide-alkyne cycloaddition (TAAC) of soy-based reactive elastomers and lignin-based cross-linker.
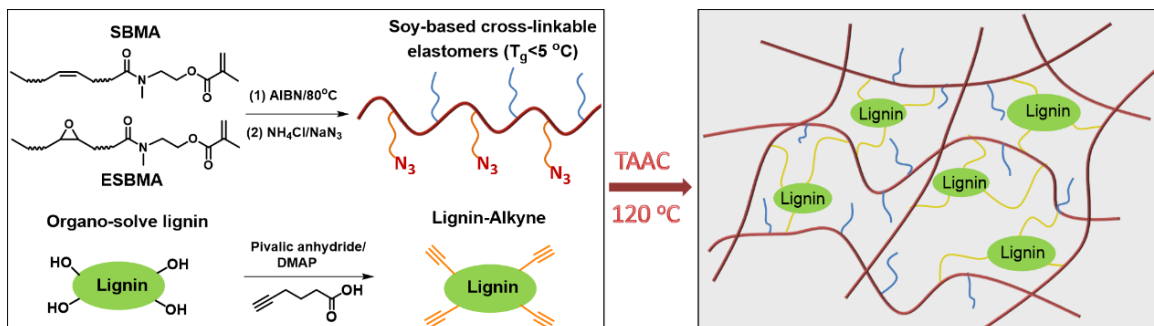
Scheme 6.2 Soybean oil based methacrylate monomers SBMA and ESBMA.
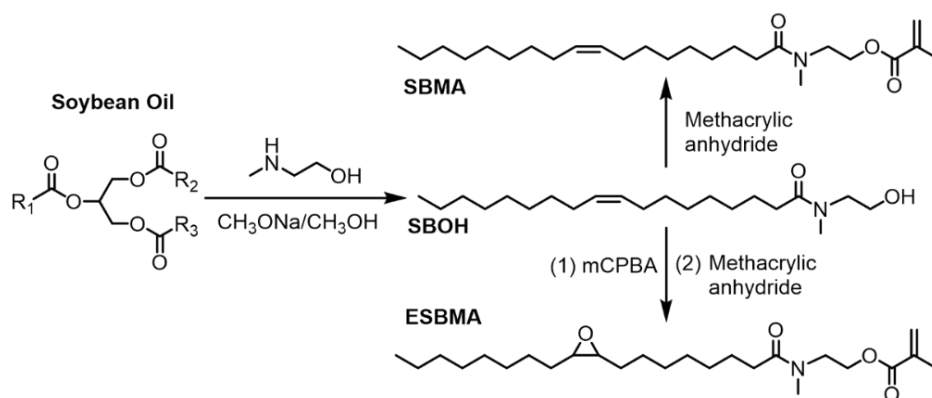
6.3 Experimental section

Materials

Plenish high oleic soybean oil was provided by DuPont. Organo-solve lignin (Lignol corporation), methacrylic anhydride (94%, Aldrich), 4-dimethylaminopyridine (DMAP, 99%, Aldrich), sodium azide (Sigma Aldrich), ammonium chloride (Sigma Aldrich), trimethylacetic anhydride (99%, Aldrich) and 5-hexynoic acid (97%, Alfa Aesar) were used as received. Azobisisobutyronitrile (AIBN, 98%, Aldrich) was recrystallized from methanol. Soybean oil derived monomer SBMA was prepared according to the method in Chapter 1. All other reagents were from commercial resources and used as received unless otherwise mentioned.

www.manaraa.com

Monomer ESBMA

Epoxidation of the amidation product (SBOH in Scheme 6.2) between high oleic soybean oil and N-methylethanolamine was done by mCPBA. Monomer **2** was obtained by methacrylation of the epoxidized product. Specifically, the epoxidized product (38 g, 0.107 mol), methacrylic anhydride (16.5 g. 0.107 mol), and DMAP (0.12 g, 0.001 mol) were mixed in a 100 mL round bottle flask. After stirring at 60 ^{o}C for 18 hours, 5.0 ml THF and 5.0 ml water were added to quench the excess anhydride. NaHCO$_3$ solution was added to neutralize the mixture before the product was extracted by DCM. After washing by brine solution, the product was dried over anhydrous MgSO$_4$ and concentrated as a light yellow liquid.

Random copolymers P30 and P10

Free radical copolymerization of monomers SBMA and ESBMA were initiated by AIBN. The epoxide group in the final polymer could be controlled by their feed ratio. Specifically, for a copolymer with 30 mol% of ESBMA, SBMA (9.36 g, 0.023 mol) and ESBMA (4.23 g, 0.01 mol) and AIBN (54 mg, 0.33 mmol) were dissolved in 20 ml toluene and purged with N$_2$ for 15 mins. The polymerization was started by putting the flask into a pre-heated 80 ^{o}C oil bath and stopped after 24 hours by cooling down in an ice-water bath. After precipitation from cold methanol and dried in vacuum oven, the polymer was obtained and named as P30. Similarly, polymer P10 containing 10 mol% of ESBMA was prepared.

Azide containing polymers PA30 and PA10

The pendant oxirane group in P30 and P10 were opened by sodium azide. Specifically, polymer P30 (7.8 g, 5.7 mmol oxirane group) was dissolved in 20 ml THF

and 20 ml DMF. Ammonium chloride (3.8 g, 71 mmol) and sodium azide (1.4 g, 22 mmol) were added to the solution. After refluxing at 80 °C for 12 hours, DCM (100 ml) was added to the cooled solution, which was later washed by brine solution for 3 times. The organic phase was dried over anhydrous MgSO$_4$, concentrated and precipitated into cold methanol to get the final product, labeled as PA30. The product from the azidation of P10 leaded to polymer PA10.

Lignin based multi-functional cross-linker Lignin-Alkyne

Lignin (2.0 g, 11.2 mmol hydroxyl group), 5-hexynoic acid (1.5 g, 13 mmol), trimethylacetic anhydride (2.4 g, 13 mmol) and DMAP (16 mg, 0.13 mmol) were mixed in 10 ml dry THF and stirred at 60 °C for 48 hours. The product was purified by precipitating from methanol. The solid product was washed with methanol for three times and dried under vacuum to get alkyne group modified lignin as a brittle brown powder, referred as Lignin-Alkyne.

Preparation of thermoset elastomers through TAAC

Soy-based azide containing elastomer (1.0 g, PA10 or PA30) was dissolved in 10 ml dry THF. A certain amount of Lignin-Alkyne was added and stirred for 2 hours to make a homogeneous solution. After degassing and centrifuging, the solution was poured into a Teflon mold. The solution was slowly evaporated for 2 days and dried at 50 °C for 12 hours. Then, the film was dried under vacuum for 2 hours at room temperature before increasing the temperature step-by-step to 40 °C, 60 °C, 80 °C. Each temperature was maintained for 2 hours. Finally, the temperature was increased to 120 °C and kept for another 16 hours under vacuum. The films were recognized as PA(X)-L(Y), number X indicates the percentage of azide containing side chains, and Y indicates the weight percentage of

111

Lignin-Alkyne to the polymer. For example, PA30-L1 means the film was cured using PA30 (1.0 g) and 1.0 wt% of Lignin-Alkyne (10 mg).

Polymer film extraction

The cured polymer films (around 0.4 g, measured to the exactness of 1.0 mg) was wrapped in a stapled filter paper and extracted in a Soxhlet extractor for 24 hours with 300 mL dichloromethane refluxed at 65 ^{o}C. Light yellow colored solution was observed in the Soxhlet extractor in the beginning and turned to be colorless after several hours. The sample was dried completely under vacuum and measured to the exactness of 1.0 mg.

Instrumental methods

^{1}H NMR and ^{13}C NMR spectra were recorded on a Varian Mercury 300 spectrometer with tetramethylsilane (TMS) as an internal reference. Gel permeation chromatography (GPC) was used to determine molecular weight and molecular weight distribution of polymers. The system was equipped with a 2414 RI detector, a 1525 Binary Pump and three Styragel columns. The columns consist of HR 1, HR 3 and HR 5E with molecular weight in the range of 1×10^2 - 5×10^3 g/mol, 5×10^2 - 3×10^4 g/mol and 2×10^3 - 4×10^6 g/mol respectively. The eluent was tetrahydrofuran (THF) at 35 °C with a flow rate of 1.0 mL/min. Polystyrene standards from Polymer laboratories were used for calibration. GPC samples were prepared by filtering a 3.0 mg/mL solution in THF through microfilters with an average pore size of 200 nm.

Fourier transform infrared spectrometry (FT-IR) spectra were taken on a PerkinElmer spectrum 100 FT-IR spectrometer. The glass transition temperature (T_g) of polymers was tested through differential scanning calorimetry (DSC) conducted Ion a DSC 2000 instrument (TA instruments). Samples were firstly heated from -70 ^{o}C to 200 ^{o}C at a

112

rate of 10 ºC /min. After cooling down to -70 ºC at the same rate, the data were collected from the second heating scan. 10 mg of each sample was used for DSC test with nitrogen gas at a flow rate of 50 mL/min. Thermogravimetric analysis (TGA) was conducted on a Q5000 TGA system (TA instruments), ramping from 25 ºC to 700 ºC with a rate of 10 ºC /min. Each test cost around 10 mg of the sample.

Tensile stress-strain testing was carried out with an Instron 5543A testing instrument. Dog-bone shaped specimens were cut from the film with a length of 22 mm and width of 5.0 mm before tested at room temperature with the crosshead speed of 10 mm/min. The cyclic tensile test was conducted stepwise to a tensile strain of 50%. In each step, once the specimen reached 50% strain, the crosshead direction was reversed and the sample strain was decreased at the same rate (1 mm/min) till stress was released to zero. The crosshead was immediate reversed when zero stress was reached and the sample was then extended again till 50% strain. The cyclic deformation was repeated for 5 times.

6.4 Results and discussion

Preparation of azide immobilized polymers from soybean oil

With a T_g of -6 ºC, PSBMA was found to be viscoelastic at room temperature. A cross-linking processing could achieve property improvement. Due to sluggish reactivity of the unsaturation, introduction of more reactive groups to PSBMA was firstly attempted as given in Scheme 6.1 & 6.2. Monomer ESBMA with an epoxy group was firstly prepared from soybean oil and confirmed by ^{1}H NMR (Figure 6.1A). Peak for the protons of -CH_2OH shifted completely from 3.75 ppm to 4.28 ppm after the methacrylation. New peaks at 6.09 ppm, 5.56 ppm and 1.93 ppm are attributed to the methacrylate end group.
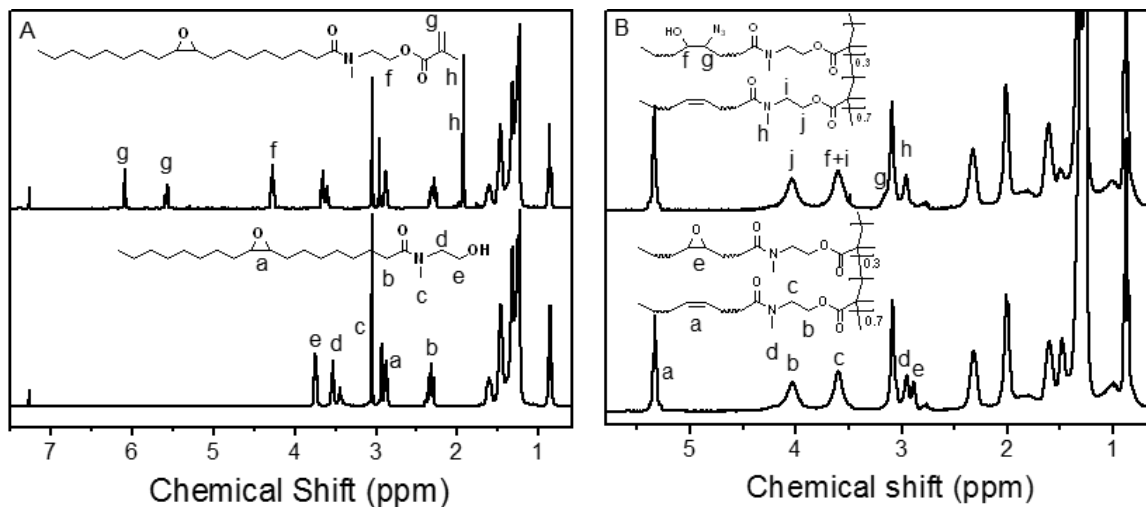
Figure 6.1 ^{1}H NMR spectra of (A) ESBMA and its epoxy fatty hydroxyl amide precursor (B) soybean oil derived polymers P30 and PA30.

Following the copolymerization of SBMA and ESBMA, nucleophilic ring opening reaction of the oxirane group by sodium azide was carried out to afford azide functionalized polymers. Two copolymers (P30 & P10), containing 30 mol% and 10 mol% monomer ESBMA respectively, were firstly prepared. The oxirane ring was opened by NaN_3 to get PA30 and PA10. ^{1}H NMR spectra for P30 and PA30 were given in Figure 6.1. Protons on the oxirane ring were observed at 2.88 ppm for P30. In the spectrum of PA30, new peaks at 3.08 ppm (-C*H*N$_3$-) and 1.48 ppm (-C*H$_2$*-CHOH-) were observed after the complete disappearance of the peak at 2.88 ppm. FT-IR spectra (Figure 6.2A) proved the presence of azide moieties in PA30, with a sharp peak at around 2104 cm^{-1}.

The polymers are also characterized by GPC and DSC (Figure 6.2B) with the characteristic parameters summarized in Table 6.1. The molecular weights of the polymers were in the range of 17k-28k. The synthesized polymer shows elastomer property with glass transition temperatures below 5 ^{o}C.
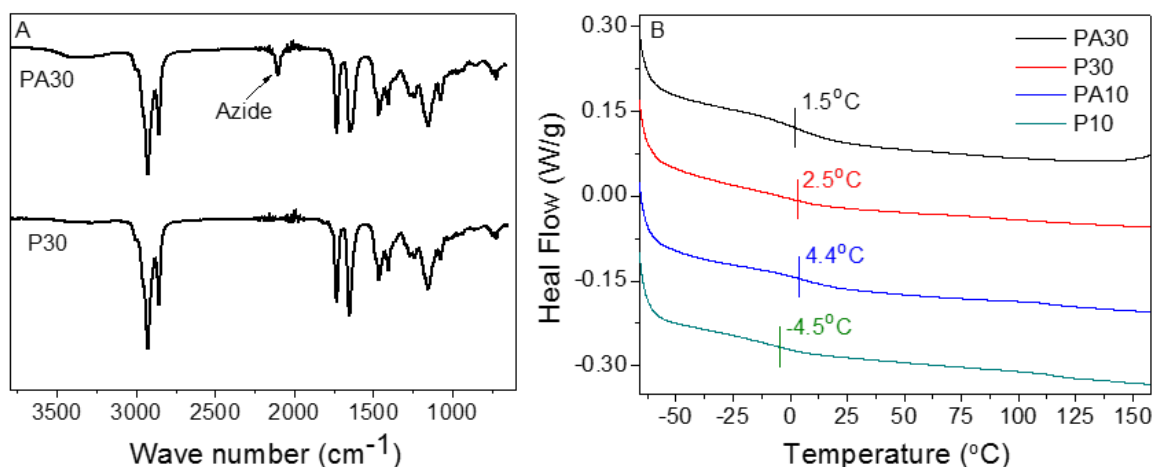
Figure 6.2 (A) FT-IR spectra of soybean oil derived polymers P30 and PA30, (B) DSC curves of soybean oil derived copolymers.

Table 6.1 Characteristic parameters of soybean oil derived copolymers.

Entry	M_n (g/mol)	$Đ$	T_g (°C)
P30	27,800	1.78	2.5
PA30	23,000	1.55	1.5
P10	23,500	1.60	-4.5
PA10	17,400	1.57	4.4

Multi-functional Cross-linker from Lignin

As a multi-functional biopolymer from the secondary cell walls of plants, lignin has been widely used as a filler/crosslinker in varied polymer products, such as epoxy resins, PLA, silicone elastomers and polyurethanes.[47-51] Recently, we reported the functionalization of lignin with azide or alkyne groups for making thermoset polymers via the TAAC strategy.[52] Thus, alkyne modified lignin could serve as the cross-linker for soy-based reactive elastomers via TAAC. As shown in Scheme 6.3, multi-functional cross-linker Lignin-Alkyne was prepared by direct esterification coupling between the hydroxyl groups on lignin and 5-hexynoic acid. ^{1}H NMR spectrum (Figure 6.3A) proved the presence of 5-hexynoic acid group in the modified lignin. FT-IR spectra show a strong ester

115

group (1749 cm^{-1}), terminal alkyne group (3289 cm^{-1}) and an apparent decrease of the broad peak (3200-3500 cm^{-1}) from the hydroxyl groups after the modification (Figure 6.3B). T_g of Lignin-Alkyne is 89 °C from DSC characterization (Figure 6.3C). The alkyne content is 3.81 mmol/g by ^{1}H NMR quantification using 1,3,5-trioxane as the reference. The molecular weight of Lignin-Alkyne is 5.5k with Đ=2.1 as calculated from GPC analysis (Figure 6.3D).

Scheme 6.3 Preparation of Lignin-Alkyne.
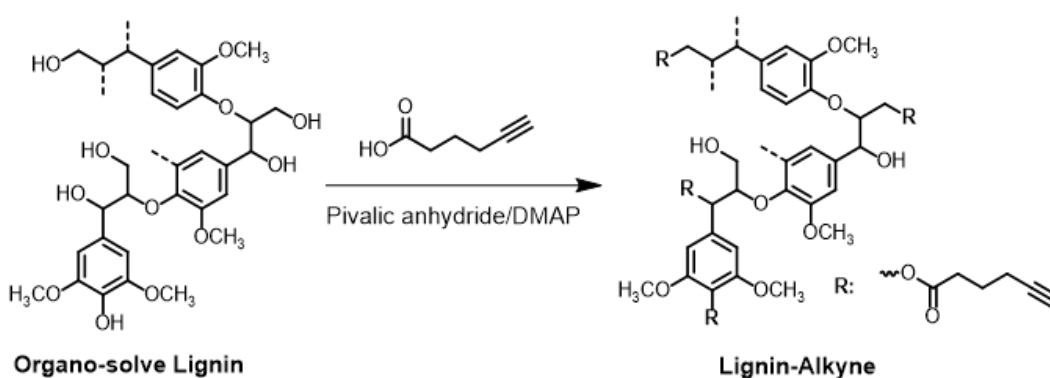
Renewable elastomers from soy-based azide polymers and Lignin-Alkyne

Different percentages of Lignin-Alkyne were firstly mixed with PA30 and thermally cured at 120 °C. Cured films with high Lignin-Alkyne content (12 wt%, 15 wt%, 20 wt%) turned out to have uneven surfaces possibly due to compatibility issues. Films with lower Lignin-Alkyne content (1 wt%, 2 wt%, 5 wt%, 8 wt%, 10 wt%) gave smooth and uniform surfaces after TAAC curing (Figure 6.4A). Light yellow to dark color was observed due to the presence of lignin. For cured films from PA30, constant increase in stress with strain was shown until failure without yielding (Figure 6.4B). Moreover, the elongation-at-break and stress-at-break values displayed an apparent dependence on the cross-linker content (Table 6.2). The stress-at-break increased gradually from 0.84 MPa to 2.12 MPa when the cross-linker content increased from 1 wt% to 10 wt%, while the strain-

116

at-break values decreased slightly from 127 % to 112 %. The elongations from these elastomers were higher than those cross-linked resins from plant oils or their derivatives.[44]
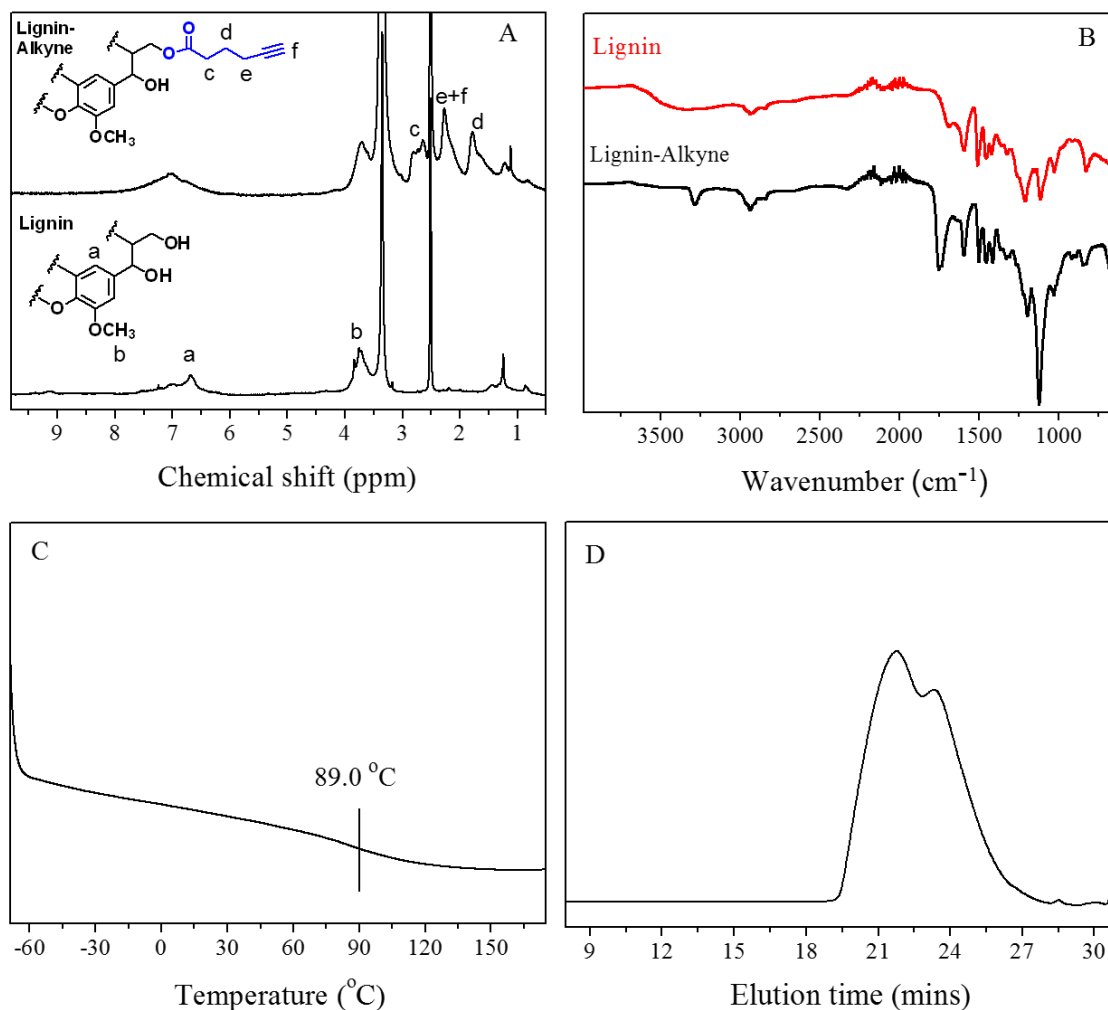

Figure 6.3 (A) ^{1}H NMR spectra of lignin and Lignin-Alkyne, (B) FT-IR spectra of the lignin and Lignin-Alkyne, (C) DSC curve and (D) GPC curve of Lignin-Alkyne.

Table 6.2 Tensile tests and solvent extraction results of elastomers from TAAC.

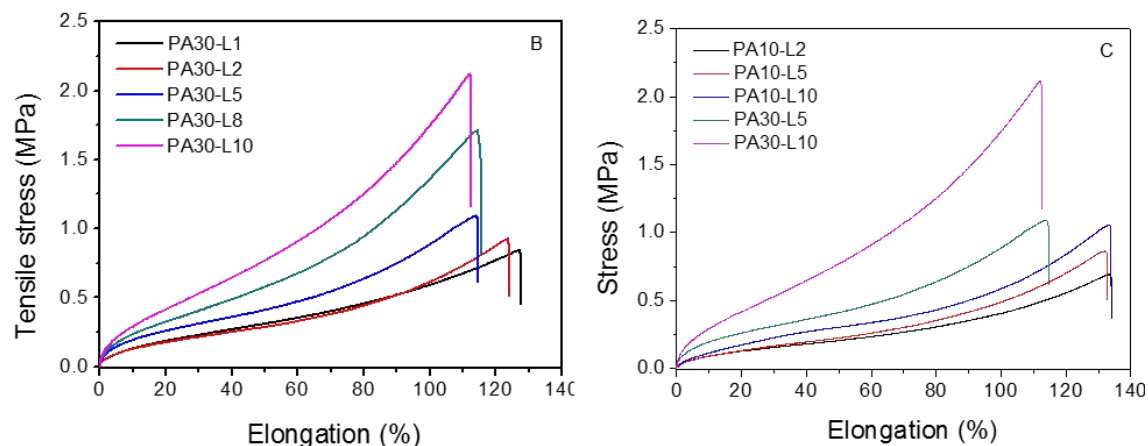| Composites	Tensile strain (%)	Tensile stress (MPa)	Solid content
PA30-L1	127	0.84	94.5%
PA30-L2	124	0.92	92.7%
PA30-L5	114	1.09	92.4%
PA30-L8	115	1.66	93.0%
PA30-L10	112	2.12	94.4%
PA10-L2	134	0.69	88.0%
PA10-L5	132	0.86	88.6%
PA10-L10	133	1.06	88.5%

117

Figure 6.4 (A) a photo of the dog-bone shaped samples from PA30 based elastomers, (B) stress-strain curves of elastomers from PA30, (C) stress-strain curves of films from PA10 (PA10-L2, PA10-L5, PA10-L10) with comparison to films from PA30 (PA30-L5, PA30-L10).

The influence of azide content was elucidated using PA10, which had a lower content of azide groups than PA30. Three films with 2 wt%, 5 wt% and 10 wt% of Lignin-Alkyne were prepared and exhibited similar mechanical properties as those from PA30. However, the films from PA10 were more elastic than films from PA30, as their strain-at-breaks were above 130%. Their stress-at-breaks were lower than cured PA30 films, given that the cross-linker content was the same (Figure 6.4C). With lower azide content, cross-linker Lignin-Alkyne has a less possibility to react with azide, leading to a lower content of cross-linking sites inside the film.

The elasticity of PA30-L10 was examined by repetitive cyclic tensile deformation at a strain of 50 % (Figure 6.5). About 35 % residual strain with a large hysteresis loop was

118

observed in the first cycle, while close to complete strain recovery (96-100%) and smaller hysteresis loop were observed after the first cycle. Additional recovery occurred after unloading and the original size was recovered. Similar result was observed from bio-elastomer PA30-L8.
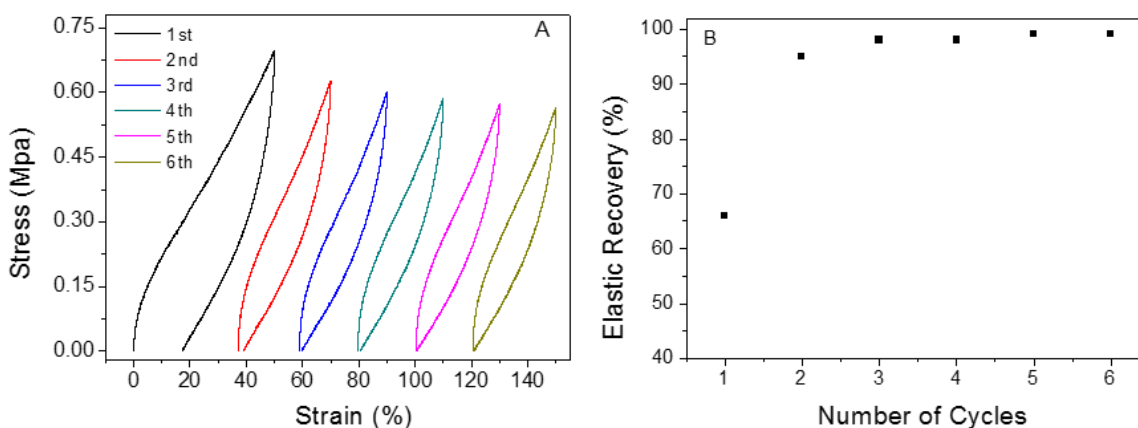

Figure 6.5 (A) Cyclic tensile test and (B) elastic recovery rate for PA30-L10.

FT-IR Characterization and Model Study for the Curing Process

The curing mechanism for the soy-based azide polymers (PA30 and PA10) and Lignin-Alkyne is supposed to be the thermal azide-alkyne cycloaddition (TAAC). The applied temperature (120 °C) is far above the $T_g s$ of PA30 and PA10. FT-IR spectra of the uncured blend and the cured sample PA30-L10 were given in Figure 6.6, normalized by the peak at 2925 cm⁻¹ from the C-H symmetric stretching vibration. The intensity of the azide peak at 2104 cm⁻¹ was dramatically decreased after curing. Residual peak from the unreacted azide group was observed, which was also reported from other TAAC cured systems.[44]

A model study was also used to prove the reactivity of the azide soy-based polymers and Lignin-Alkyne. Azide-SBOAC, structurally similar to the azide containing side chains in PA-30, was prepared from soybean oil (Scheme 6.4). Azide-SBOAC and Lignin-Alkyne were mixed together and heated under vacuum at 120 °C for 16 hours. Figure 6.7 presents

119

the ^{1}H NMR spectrum of the purified product. The proton on the tri-azole ring at around 7.5 ppm (peak c) and the proton from the -C*H*- at 4.4 ppm (peak d) were clearly shown. The model study directly proved the reactivity between the azide group on the soy-based polymers and the alkyne group from Lignin-Alkyne.
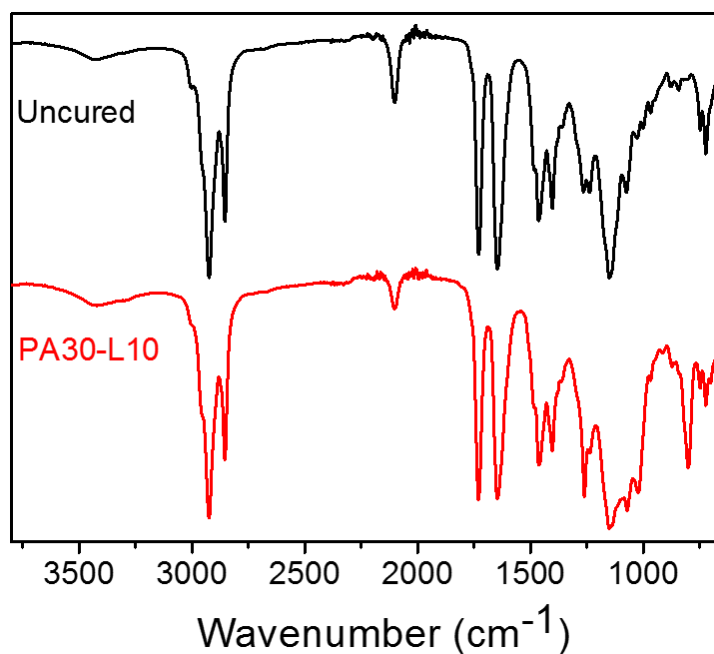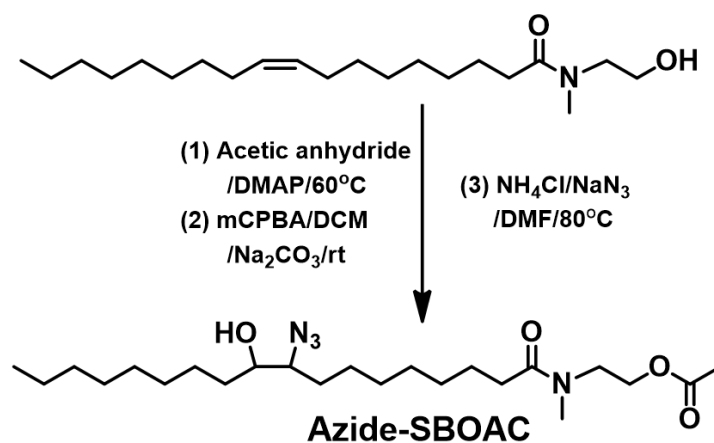

Figure 6.6 FT-IR spectra of the film PA30-L10 before and after the cross-linking.

Scheme 6.4 Preparation of soy-derived azide containing compound Azide-SBOAC.
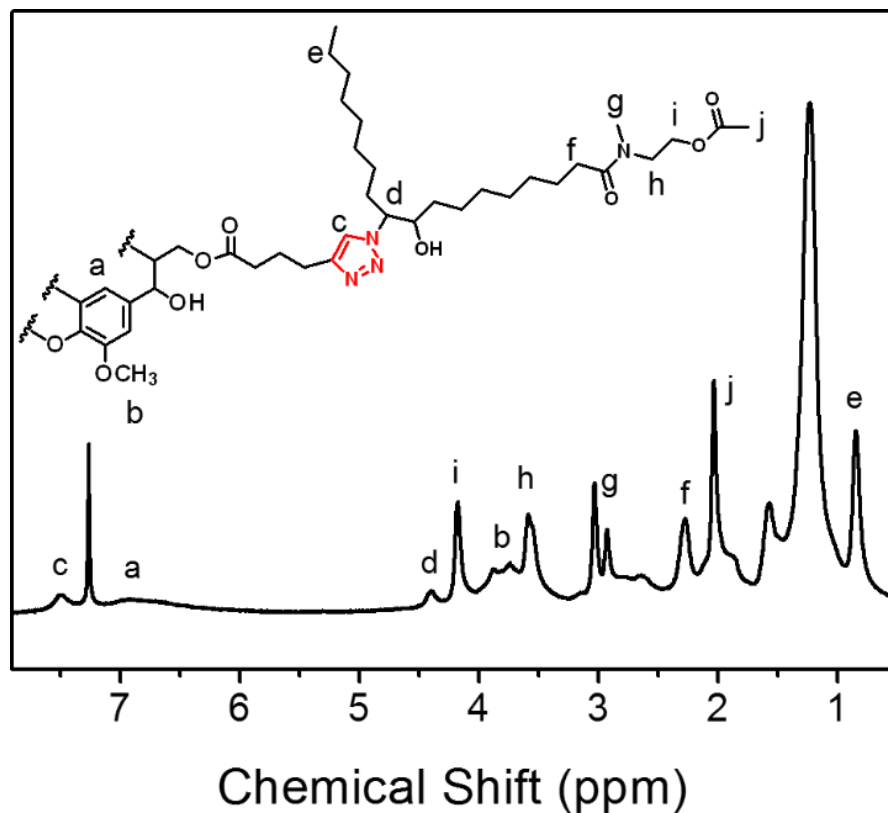
120

Figure 6.7 ^{1}H NMR spectrum of the product from TAAC reaction between Lignin-Alkyne and Azide-SBOAC.

Extraction and thermal stability of the bio-elastomer

Soxhlet extraction was done for the cured polymers. The extracted soluble part ranged from 5.2 wt% to 12.0 wt% as shown in Table 6.2. Films from PA30 had higher insoluble content than films from PA10, due to the higher degree of cross-linking in PA30 films. Thermal gravimetric analysis (TGA) was done to the cured samples from PA30. Similar decomposition behavior was observed for films with varied content of Lignin-Alkyne (Figure 6.8). The onset temperature of decomposition was around 280 $^{\circ}$C. As given in Table 6.3, the 5 % and 50 % weight loss temperatures increased with the content of Lignin-Alkyne.
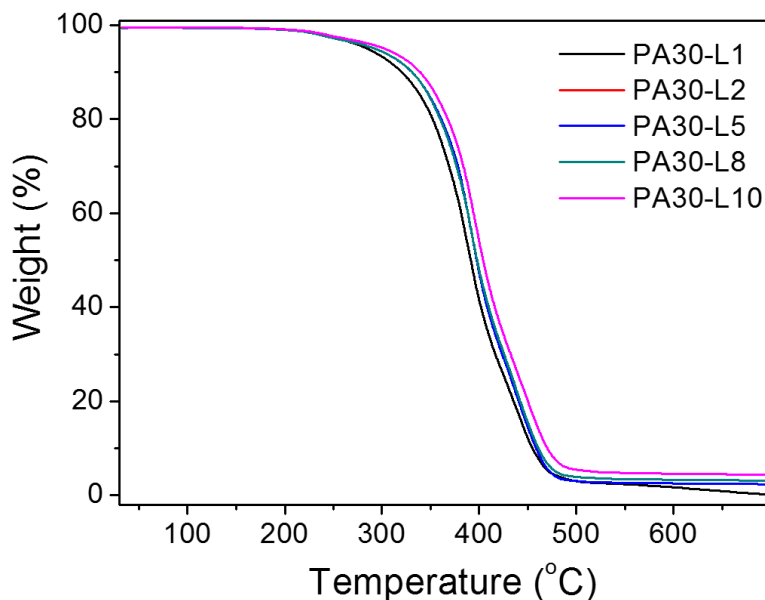
121

Figure 6.8 TGA curves of thermally cured films from PA30.

Table 6.3 TGA results of thermally cured samples from PA30 and Lignin-Alkyne.

Composites	T_5 (^{o}C)[a]	T_{50} (^{o}C)[b]	Decom. at 500 ^{o}C (%)
PA30-L1	284.3	391.4	97.0
PA30-L2	292.7	397.4	96.9
PA30-L5	292.7	397.9	96.1
PA30-L8	302.7	404.1	94.7
PA30-L10	302.3	403.1	93.4

[a] Five percent weight loss temperature. [b] Fifty percent weight loss temperature.

6.5 Conclusions

Azide functionalized polymers with T_g<5°C were prepared from soybean oil based monomers. After cross-linking with alkyne functionalized lignin via the thermal azide-alkyne cycloaddition reaction (TAAC), elastomers with high solid content (88%-95%) and excellent elastic recovery rate (96%-100% after the first cycle) were obtained. Higher azide content in the soy-based polymers and higher content of cross-linker can help to increase the tensile stress of the obtained elastomers. FT-IR and a model study proved the reactivity of the azide moieties in the polymers toward the alkyne group in the cross-linker. This research may help to establish a new strategy for bio-renewable elastomers.

122

6.6 References

(1) Song, J.-S.; Huang, B.-C.; Yu, D.-S. *Journal of Applied Polymer Science* **2001,** *82*, 81-89.

(2) Essawy, H.; El-Nashar, D. *Polymer Testing* **2004,** *23*, 803-807.

(3) Rahiman, K. H.; Unnikrishnan, G.; Sujith, A.; Radhakrishnan, C. *Materials Letters* **2005,** *59*, 633-639.

(4) Meier, M. A.; Metzger, J. O.; Schubert, U. S. *Chemical Society Reviews* **2007,** *36*, 1788-1802.

(5) Gandini, A. *Macromolecules* **2008,** *41*, 9491-9504.

(6) Coates, G. W.; Hillmyer, M. A. *Macromolecules* **2009,** *42*, 7987-7989.

(7) Yao, K.; Tang, C. *Macromolecules* **2013,** *46*, 1689-1712.

(8) Lligadas, G.; Ronda, J. C.; Galia, M.; Cádiz, V. *Biomacromolecules* **2010,** *11*, 2825-2835.

(9) Hillmyer, M. A.; Tolman, W. B. *Accounts of chemical research* **2014,** *47*, 2390-2396.

(10) Liu, Q.; Jiang, L.; Shi, R.; Zhang, L. *Progress in polymer science* **2012,** *37*, 715-765.

(11) Xia, Y.; Larock, R. C. *Green Chemistry* **2010,** *12*, 1893-1909.

(12) Liu, Z.; Xu, Y.; Cao, L.; Bao, C.; Sun, H.; Wang, L.; Dai, K.; Zhu, L. *Soft Matter* **2012,** *8*, 5888-5895.

(13) Wang, S.; Vajjala Kesava, S.; Gomez, E. D.; Robertson, M. L. *Macromolecules* **2013,** *46*, 7202-7212.

(14) Bolton, J. M.; Hillmyer, M. A.; Hoye, T. R. *ACS Macro Letters* **2014,** *3*, 717-720.

(15) Liu, Y.; Yao, K.; Chen, X.; Wang, J.; Wang, Z.; Ploehn, H. J.; Wang, C.; Chu, F.; Tang, C. *Polymer Chemistry* **2014,** *5*, 3170-3181.

(16) Wang, Z.; Yuan, L.; Trenor, N. M.; Vlaminck, L.; Billiet, S.; Sarkar, A.; Du Prez, F. E.; Stefik, M.; Tang, C. *Green Chemistry* **2015,** *17*, 3806-3818.

(17) Yu, J.; Wang, J.; Wang, C.; Liu, Y.; Xu, Y.; Tang, C.; Chu, F. *Macromolecular rapid communications* **2015,** *36*, 398-404.

(18) Hoogenboom, R.; Schubert, U. S. *Green Chemistry* **2006,** *8*, 895-899.

(19) Chernykh, A.; Alam, S.; Jayasooriya, A.; Bahr, J.; Chisholm, B. J. *Green Chemistry* **2013,** *15*, 1834-1838.

(20) Tarnavchyk, I.; Popadyuk, A.; Popadyuk, N.; Voronov, A. *ACS Sustainable Chemistry & Engineering* **2015,** *3*, 1618-1622.

(21) Yuan, L.; Wang, Z.; Trenor, N. M.; Tang, C. *Macromolecules* **2015,** *48*, 1320-1328.

(22) Shin, J.; Lee, Y.; Tolman, W. B.; Hillmyer, M. A. *Biomacromolecules* **2012,** *13*, 3833-3840.

(23) Martello, M. T.; Schneiderman, D. K.; Hillmyer, M. A. *ACS Sustainable Chemistry & Engineering* **2014,** *2*, 2519-2526.

(24) Wang, Z.; Zhang, X.; Wang, R.; Kang, H.; Qiao, B.; Ma, J.; Zhang, L.; Wang, H. *Macromolecules* **2012,** *45*, 9010-9019.

(25) Wang, R.; Ma, J.; Zhou, X.; Wang, Z.; Kang, H.; Zhang, L.; Hua, K.-c.; Kulig, J. *Macromolecules* **2012,** *45*, 6830-6839.

(26) Amsden, B. G.; Misra, G.; Gu, F.; Younes, H. M. *Biomacromolecules* **2004,** *5*, 2479-2486.

(27) Tsujimoto, T.; Uyama, H.; Kobayashi, S. *Biomacromolecules* **2001,** *2*, 29-31.

(28) Canalle, L. A.; van Berkel, S. S.; de Haan, L. T.; van Hest, J. *Advanced Functional Materials* **2009,** *19*, 3464-3470.

(29) Hoyle, C. E.; Bowman, C. N. *Angewandte Chemie International Edition* **2010,** *49*, 1540-1573.

(30) Madsen, F. B.; Dimitrov, I.; Daugaard, A. E.; Hvilsted, S.; Skov, A. L. *Polymer Chemistry* **2013,** *4*, 1700-1707.

(31) Golas, P. L.; Matyjaszewski, K. *Chemical Society Reviews* **2010,** *39*, 1338-1354.

(32) Spruell, J. M.; Wolffs, M.; Leibfarth, F. A.; Stahl, B. C.; Heo, J.; Connal, L. A.; Hu, J.; Hawker, C. J. *Journal of the American Chemical Society* **2011,** *133*, 16698-16706.

(33) Leibfarth, F. A.; Kang, M.; Ham, M.; Kim, J.; Campos, L. M.; Gupta, N.; Moon, B.; Hawker, C. J. *Nature chemistry* **2010,** *2*, 207-212.

(34) Leibfarth, F. A.; Schneider, Y.; Lynd, N. A.; Schultz, A.; Moon, B.; Kramer, E. J.; Bazan, G. C.; Hawker, C. J. *Journal of the American Chemical Society* **2010,** *132*, 14706-14709.

(35) Leibfarth, F. A.; Hawker, C. J. *Journal of Polymer Science Part A: Polymer Chemistry* **2013,** *51*, 3769-3782.

(36) Zhang, Y.; Broekhuis, A. A.; Picchioni, F. *Macromolecules* **2009,** *42*, 1906-1912.

124

(37) Gandini, A. *Progress in Polymer Science* **2013,** *38*, 1-29.

(38) Zhang, J.; Niu, Y.; Huang, C.; Xiao, L.; Chen, Z.; Yang, K.; Wang, Y. *Polymer Chemistry* **2012,** *3*, 1390-1393.

(39) Billiet, S.; De Bruycker, K.; Driessen, F.; Goossens, H.; Van Speybroeck, V.; Winne, J. M.; Du Prez, F. E. *Nature chemistry* **2014,** *6*, 815-821.

(40) De Bruycker, K.; Billiet, S.; Houck, H. A.; Chattopadhyay, S.; Winne, J. M.; Du Prez, F. E. *Chemical reviews* **2016**.

(41) Gonzaga, F.; Yu, G.; Brook, M. A. *Macromolecules* **2009,** *42*, 9220-9224.

(42) Rambarran, T.; Gonzaga, F.; Brook, M. A. *Macromolecules* **2012,** *45*, 2276-2285.

(43) Hong, J.; Luo, Q.; Shah, B. K. *Biomacromolecules* **2010,** *11*, 2960-2965.

(44) Hong, J.; Luo, Q.; Wan, X.; Petrović, Z. S.; Shah, B. K. *Biomacromolecules* **2012,** *13*, 261-266.

(45) Hong, J.; Shah, B. K.; Petrović, Z. S. *European Journal of Lipid Science and Technology* **2013,** *115*, 55-60.

(46) Alam, S.; Chisholm, B. J. *Journal of coatings technology and research* **2011,** *8*, 671-683.

(47) Chung, Y.-L.; Olsson, J. V.; Li, R. J.; Frank, C. W.; Waymouth, R. M.; Billington, S. L.; Sattely, E. S. *ACS Sustainable Chemistry & Engineering* **2013,** *1*, 1231-1238.

(48) Ismail, T. N. M. T.; Hassan, H. A.; Hirose, S.; Taguchi, Y.; Hatakeyama, T.; Hatakeyama, H. *Polymer International* **2010,** *59*, 181-186.

(49) Laurichesse, S.; Avérous, L. *Progress in Polymer Science* **2014,** *39*, 1266-1290.

(50) Zhang, J.; Chen, Y.; Sewell, P.; Brook, M. A. *Green Chem.* **2015,** *17*, 1811-1819.

(51) Chung, H.; Washburn, N. R. *ACS Applied Materials & Interfaces* **2012,** *4*, 2840-2846.

(52) Han, Y.; Yuan, L.; Li, G.; Huang, L.; Qin, T.; Chu, F.; Tang, C. *Polymer* **2016,** *83*, 92-100.

CHAPTER 7

SUMMARY AND OUTLOOK

In this dissertation, two major research goals were achieved. First, a facile strategy was developed for preparing mono-functional monomers from soybean oil. These monomers can be easily polymerized to obtained homopolymers with a wide range of properties. Three hydroxyl fatty amides from the amidation reactions between amino alcohols and soybean oil were converted to 3 methacrylate monomers, 3 norbornene monomers and 2 cyclic imino ethers. The homopolymers from free radical polymerization of methacrylate monomers and ROMP of norbornene monomers show tunable thermal property depending on the monomer structure. The amidation reaction of soybean oil with a library of amino alcohols was later systematically studied to afford seventeen mono-hydroxyl fatty amides products, which were further modified to sixteen (meth)acrylate monomers. Homopolymers from their free radical polymerizations were characterized through DSC and mechanical studies for understanding the structure-property relationship of soybean oil based thermoplastic polymers. Hydrogenation of selected homopolymers was carried out to examine the influence of saturation on thermal properties.

The second research objective is to develop elastomers from soybean oil derived monomers and homopolymers. First A-B-A triblock copolymer TPEs were prepared by ATRP with a soybean oil based acrylate monomer (SBA) forming the middle block and styrene forming the outside blocks. The mechanical properties can be tuned by the chemical composition, block length and quantitative cross-linking of the middle block. Multi-graft copolymer TPEs were prepared from ROMP copolymerization of a soybean oil based norbornene monomer (SBN) and a norbornene-capped PLA. The multi-graft copolymer TPEs exhibited improved elastomer properties from A-B-A triblock copolymers. Elastomers with cross-linked structures were further developed through Diels-

127

Alder reaction and thermally promoted azide-alkyne cyclization. Furan group was incorporated onto soybean oil based homopolymers and subsequently cross-linked via Diels-Alder reaction with a di-functional maleimide cross-linker. The structure of the precursor polymers and the cross-linking density have direct influence on the mechanical properties of the cross-linked elastomers. The elastomers could be reprocessed at elevated temperatures. Azide group was incorporated onto PSBMA through the copolymerization with an epoxy functionalized monomer (ESBMA) and subsequent ring opening reaction with sodium azide. Lignin was modified with alkyne groups. Under elevated temperatures, elastomers were obtained from the azide containing polymer and alkyne modified lignin, which was used as a cross-linker and reinforcement filler.

Research on renewable bio-based polymer materials has drawn a lot of interest and will keep growing in the future. Plant oils have the advantages of worldwide availability, low prices and relatively well-defined chemical structures. Traditionally, they were used as oil-based coating and painting products. Recent applications are observed in the oelochemical industry (fatty acids, fatty alcohol, biodiesel, etc.) and thermoset polymeric materials. The underdeveloped situation of thermoplastic polymers from plant oils is due to the lack of efficient conversion technologies and limited material properties. New synthetic routes and material developments are essential in the future. The work in this dissertation provides an efficiency method to get (meth)acrylate monomers and thermoplastic polymers from soybean oil. However, procedure optimization to eliminate the use of organic solvent and to reduce the production cost has to be realized first. For example, emulsion polymerization or precipitation polymerization of these monomers can be attempted. The homopolymers only exhibits limited mechanical strength or elastic

properties as a result of their comb-shaped structures, which leads to extremely high chain entanglement molecular weights (M_e), unachievable from current polymerization strategies. Copolymerization with monomers to reduce M_e and increase molecular weights can be a simple strategy to improve the mechanical properties (tensile strength, elasticity, etc.). Combination with natural polymers (cellulose, lignin, chitosan, etc.) would be another interesting direction to maximize the use of soybean oil based monomers and thermoplastic polymers

APPENDIX A – PERMISSION TO REPRINT

ACS Publications
Most Trusted. Most Cited. Most Read.

Title: Robust Amidation Transformation of Plant Oils into Fatty Derivatives for Sustainable Monomers and Polymers

Author: Liang Yuan, Zhongkai Wang, Nathan M. Trenor, et al

Publication: Macromolecules

Publisher: American Chemical Society

Date: Mar 1, 2015

Copyright © 2015, American Chemical Society

PERMISSION/LICENSE IS GRANTED FOR YOUR ORDER AT NO CHARGE

131

www.manaraa.com

RSC | Advancing the
Chemical Sciences

Royal Society of Chemistry
Thomas Graham House
Science Park
Milton Road
Cambridge
CB4 0WF

Tel: +44 (0)1223 420 066
Fax: +44 (0)1223 423 623
Email: contracts-copyright@rsc.org

www.rsc.org

Acknowledgements to be used by RSC authors

Authors of RSC books and journal articles can reproduce material (for example a figure) from the RSC publication in a non-RSC publication, including theses, without formally requesting permission providing that the correct acknowledgement is given to the RSC publication. This permission extends to reproduction of large portions of text or the whole article or book chapter when being reproduced in a thesis.

The acknowledgement to be used depends on the RSC publication in which the material was published and the form of the acknowledgements is as follows:

- For material being reproduced from an article in *New Journal of Chemistry* the acknowledgement should be in the form:

    o [Original citation] - Reproduced by permission of The Royal Society of Chemistry (RSC) on behalf of the Centre National de la Recherche Scientifique (CNRS) and the RSC

- For material being reproduced from an article *Photochemical & Photobiological Sciences* the acknowledgement should be in the form:

    o [Original citation] - Reproduced by permission of The Royal Society of Chemistry (RSC) on behalf of the European Society for Photobiology, the European Photochemistry Association, and RSC

- For material being reproduced from an article in *Physical Chemistry Chemical Physics* the acknowledgement should be in the form:

    o [Original citation] - Reproduced by permission of the PCCP Owner Societies

- For material reproduced from books and any other journal the acknowledgement should be in the form:

    o [Original citation] - Reproduced by permission of The Royal Society of Chemistry

The acknowledgement should also include a hyperlink to the article on the RSC website.

The form of the acknowledgement is also specified in the RSC agreement/licence signed by the corresponding author.

Except in cases of republication in a thesis, this express permission does not cover the reproduction of large portions of text from the RSC publication or reproduction of the whole article or book chapter.

A publisher of a non-RSC publication can use this document as proof that permission is granted to use the material in the non-RSC publication.

VAT Registration Number: GB 342 1764 71   Registered Charity Number: 207890

132

www.manaraa.com